The petrography and geochemistry of the Platreef on the farm Townlands, near Potgietersrus, northern Bushveld Complex

By

Tawanda Darlington Manyeruke

Submitted in partial fulfillment of the requirements for the degree
MASTER IN SCIENCE
In the Faculty of Natural & Agricultural Science
Geology Department
University of Pretoria
Pretoria

Supervisor:	Prof. W.D. Maier
Co-supervisor:	Prof. S.A. de Waal

August 2003

TABLE OF CONTENTS

ABSTRACT

The Platreef is a platinum group element (PGE) and base metal enriched mafic/ ultramafic layer situated along the base of the northern (Potgietersrus) limb of the Bushveld Complex. It represents an important resource of PGE which is only in its early stages of exploitation. The present study contains a detailed petrographic and geochemical investigation of a borehole core drilled on the farm Townlands. At this locality, the Platreef rests on metasedimentary rocks of the Silverton Formation of the Transvaal Supergroup, and is comprised of three medium grained units of gabbronorite/feldspathic pyroxenite that are separated by hornfels interlayers. I refer to the three platiniferous layers as the Lower, Middle and Upper Platreef. The Middle Platreef is the main mineralised layer, with total PGE contents up to 4 ppm. The Lower and Upper Platreefs are less well mineralised (up to 1.5 ppm).

Trace element and S-isotope data show compositional breaks between the different platiniferous layers suggesting that they represent distinct sill-like intrusions. The study also reveals a reversed differentiation trend of more primitive rocks towards the top of the succession. For example, pyroxene shows an increase in Cr_2O_3 with height coupled with a decrease in TiO_2. Olivine from the Upper Platreef has Fo contents between 80-83 (averaging Fo_{81}) and those from the Middle Platreef have Fo from 78-83 (averaging Fo_{79}).

The Upper and Lower Platreefs have $\delta^{34}S$ values averaging 8 ‰ while the Middle Platreef has $\delta^{34}S$ values averaging 4 ‰. All three Platreef layers have elevated $\delta^{34}S$ values, indicating addition of ^{34}S-enriched crustal sulphur. The model of contamination is supported by elevated K, Ca, Zr and Y contents in the Platreef relative to Critical Zone rocks from elsewhere in the Bushveld Complex, and by high Zr/Y ratios.

Well defined correlations between concentrations of the individual PGE, and between the PGE and S suggest that the concentration of the PGE was controlled by segregating sulphide melt. Alteration of the rocks, possibly due to infiltration by fluids derived from the floor rocks, caused localized redistribution of Cu and, to a lesser degree, the PGE.

A model is proposed whereby the Platreef magma assimilated calcsilicate and hornfels from the country rocks. The hornfels and calcsilicate of the Silverton Formation that forms the floor rocks to the Platreef on the farm Townlands constitute a possible source of the crustal sulphur. Release of S from the floor rocks caused S-supersaturation in the magma, followed by segregation of an immiscible sulphide melt. The sulphide melt scavenged the PGE from the silicate magma. The sulphides and the xenoliths were entrained by successive, metal-undepleted magma flows, causing high metal tenors in the sulphides and undepleted Ni contents in associated olivine.

CHAPTER ONE: INTRODUCTION

1.1 Introduction and Aims

The Platreef is a platinum group element (PGE) and base metal enriched mafic ultramafic layer situated along the base of the northern (Potgietersrus) limb of the Bushveld Complex (Fig. 1.1). It represents an important resource of PGE, estimated by Vermaak (1995) to contain 6581 tonnes of PGE to a depth of 1200 m, which is only in its early stages of exploitation.

In addition to the northern limb, basal PGE mineralisation of a similar type to that found in the Platreef has recently been described from the Mineral Range (Sharpe et al. 2002). In the remainder of the Complex, basal PGE mineralisation appears to be absent. Past workers have proposed that this is due to the fact that the floor rocks to most of the eastern and western limbs of the Bushveld Complex are constituted by relatively refractory quartzites. In contrast, in the northern limb, the floor rocks show more lithological variation, including shale, ironstone, dolomite, and granite gneiss. These lithologies are believed to be more reactive when in contact with magma (e.g. de Waal, 1977). The assimilation of country rock material by the magma is generally thought to be important in the formation of magmatic sulphides (e.g. Gain and Mostert, 1982; Buchanan and Rouse, 1984; Barton et al. 1986; Buchanan, 1988). However, the precise mechanism that may have triggered the sulphide segregation remains unclear. For example, de Waal (1977) proposed that devolatization of the dolomite may increase the O fugacity of the magma, thereby decreasing the activity of Fe^{2+} and decreasing S solubility. Alternatively, sulphide segregation could have been triggered by assimilation of S from the floor rocks.

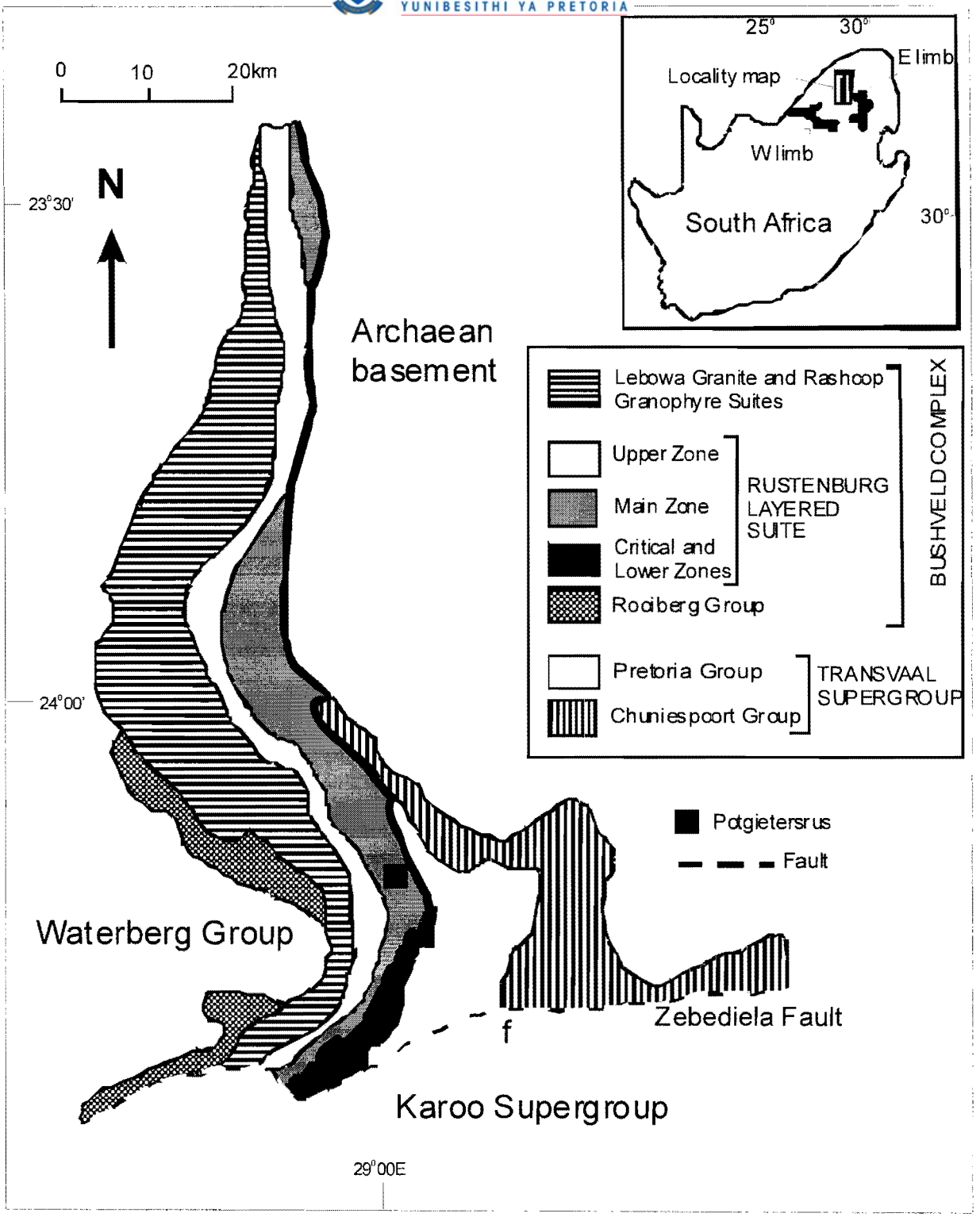

Figure 1.1: Geological map of the Potgietersrus limb of the Bushveld Complex. Thick black line, running north from Potgietersrus, represents the trace of the Platreef. Insert shows the outcrop of the Rustenburg Layered Suite in Southern Africa (modified after Harris and Chaumba, 2001).

Some authors (Lee, 1996) proposed that the Platreef sulphides segregated in a staging chamber at depth and were entrained by the ascending Critical Zone silicate magma.

One of the main problems in constraining the mechanism of mineralization is that there have been few quantitative studies of noble metal concentrations in the Platreef rocks. The most comprehensive description of the mineralization so far has been published by Viljoen and Schurmann (1998). Maier (2003; submitted) presented Pt, Pd, Cu and Ni contents of the Platreef on the farm Townlands (Fig. 1.2). Armitage et al. (2002) published more complete noble metal data from 13 Platreef samples at Sandsloot, some 30km to the north of Potgietersrus. The scarcity of data make it difficult to judge whether there is any regional variation in metal tenors and whether such variation, if present, can be correlated to lithological and chemical variation of the floor rocks. The present study was initiated to address this scarcity of data, and to thereby constrain the genesis of the mineralization. In particular, I provide

i) a detailed lithological and petrographical description of the Platreef as exposed in a 200 m borehole core intersection on the farm Townlands (Fig. 1.2),
ii) new major and trace element data, including concentrations of the noble metals.

1.2 General geology

The Platreef consists of an up to 250 m thick package of texturally heterogeneous pyroxenite, norite and gabbro, containing numerous xenoliths of metadolomite, calcsilicate and shale derived from the floor rocks. The xenoliths range from several

cm to 100 m in diameter. The reef is overlain by a thick (up to 2000 m) package of gabbro, magnetite gabbro and diorite belonging to the Rustenburg Layered Suite. Buchanan et al. (1981) correlated the Platreef with the Critical Zone, the overlying gabbro with the Main Zone, and the magnetite gabbro and diorite that may contain up to ca. 20 layers of massive magnetitite with the Upper Zone (Fig. 1.3). The intrusion transgresses the floor rocks of the Transvaal Supergroup, to the south of Potgietersrus, the reef overlies the Magaliesberg Quartzite Formation, but towards the north, it rests on progressively lower portions of the Pretoria Group and finally on the Achaean granite-gneiss basement.

Detailed descriptions of the lateral extension of the Platreef are lacking. Viljoen and Schurmann (1998) and White (1994) report that the well mineralised sectors of the Platreef extend about 35 km northwards from the farm Townlands to the farm Drenthe, but unconfirmed reports from various exploration companies suggest that the Platreef is developed along most of the base of the northern limb of the Complex, albeit in variable thickness. The average dip of the Platreef is ~ 40^0 to the southwest.

The Platreef has been interpreted as the local equivalent of the Merensky reef (Wagner 1929, White 1994). Significant differences, however, exist between the Platreef and the Merensky reef as exposed in the western and eastern lobes of the Complex (e.g. Van der Merwe, 1976; Buchanan et al., 1981; Cawthorn et al., 1985; Eales & Cawthorn, 1996). Firstly, the Merensky reef tends to occur within the layered sequence, in many instances some 2 km above the floor of the Bushveld Complex, whereas the Platreef overlies the floor of the complex (Fig. 1.3). Secondly, the mineralized interval is much thicker in the Platreef than in the Merensky reef (up to

200m versus ca 1m). Thirdly, there are signs of compositional differences between the two layers, e.g. a relatively higher crustal signature and lower metal tenors (e.g. Buchanan et al. 1981, Barnes and Maier, 2002) in the Platreef relative to the Merensky reef.

1.3 Methodology

Fourty samples of quarter borehole core, 10-30 cm in length, from borehole TL01-3 (Fig. 1.2) were selected for detailed study. Polished thin sections were prepared for all 40 samples. The modal proportions of mineral phases were estimated by point counting, where samples were relatively unaltered. Thirty two samples were pulverised using a C-steel jaw-crusher and a C-steel milling vessel. The samples were analysed for major and trace elements by X-ray fluorescence spectroscopy (XRF) at the University of Pretoria. The PGE concentrations were determined at the University of Quebec at Chicoutimi, Canada by Ni-sulphide fire assay followed by INAA. The compositions of selected minerals were determined by electron microprobe at Rhodes University, South Africa. Sulphur isotope analyses on selected samples were done at the University of Indiana, U.S.A. All analytical details are given in Appendix 1.

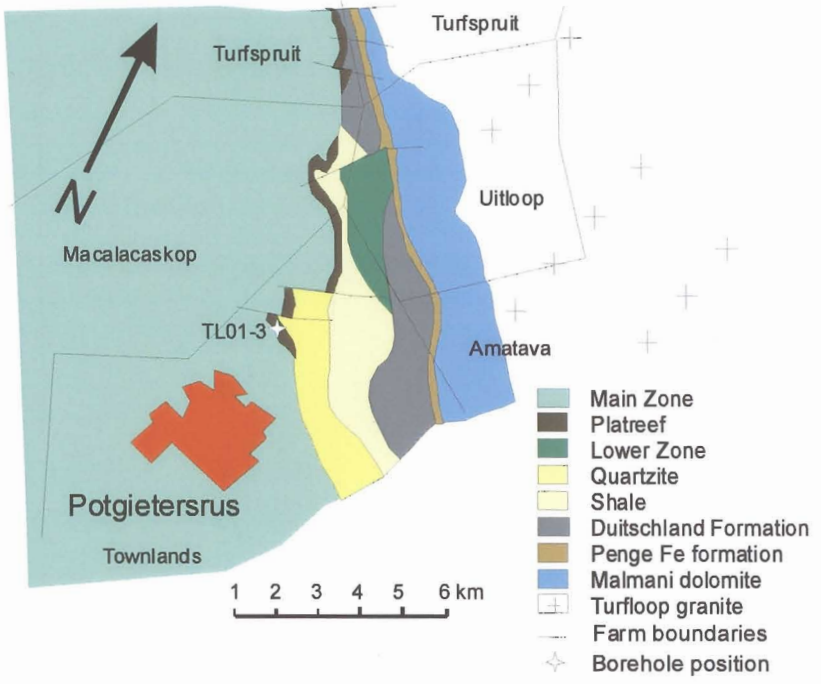

Fig. 1.2: Geological map of the Platreef on the farm Townlands and the position of the borehole TL01-3.

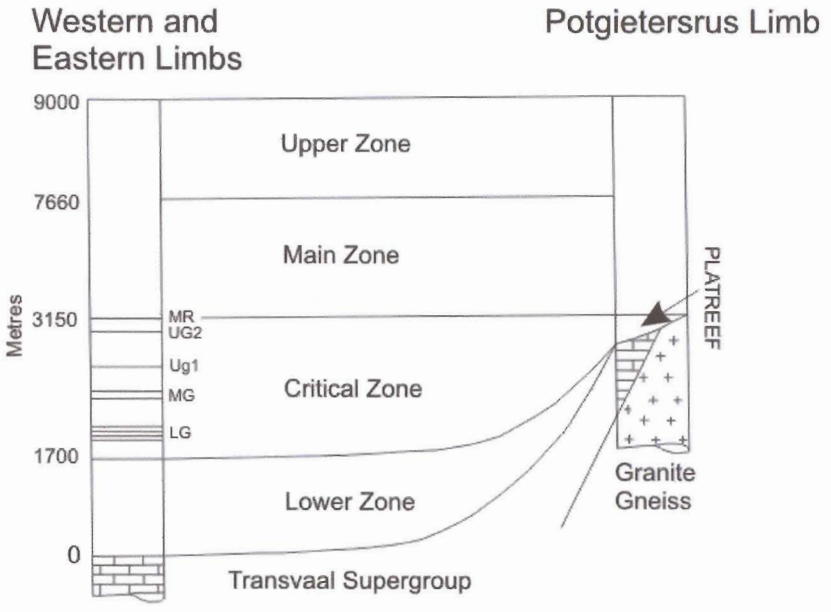

Fig. 1.3: Schematic section through the Rustenburg Layered Suite in different limbs of the Bushveld Complex (from Cawthorn et al. 2002). Lateral correlation after Buchanan et al. (1981).

1.4 Previous work

The first report on the occurrence of platinum in the northern limb was made in 1923 by a prospector named A. Erasmus, referring to a farm 31 km southwest of Potgietersrus (White, 1994). Wagner (1929) provided the first descriptions of the Platreef during platinum-mining operations in the 1920s. He correlated the variably sulphide mineralised, composite rocks forming the floor rocks of the Bushveld Complex in the northern limb with the Merensky reef. Wagner described three distinct layers, which Buchanan (1979) later referred to as the A, B and C units (or reefs), from the base to the top, based on texture and mineral mode. The 'A' reef may contain finely disseminated sulphides and, commonly, larger blebs (up to 3 cm) of composite base metal sulphides (BMS) (Buchanan and Rouse, 1984; Buchanan, 1988; White, 1994). The 'B' reef generally has the largest amount of disseminated base metal sulphides (White, 1994), whilst the 'C' reef is usually barren of PGE mineralisation.

Other studies of the Platreef have emphasized the abundance of xenoliths of metasediments and dolomite in the rocks. Buchanan et al. (1981) proposed that the Platreef sequence on Tweefontein reflects the assimilation of anhydrite-bearing Malmani dolomite, banded ironstone, argillaceous sediments, and micronoritic sills by Bushveld magma. They conducted S isotopic studies on sulphides from the Platreef and suggested that the anhydrite-bearing dolomite reacted with the Platreef magma releasing sulphur which resulted in the precipitation of an immiscible sulphide liquid. In contrast, de Waal (1977) and Gain and Mostert (1982), the latter authors working on the farm Drenthe, north of Potgietersrus, prefer a mechanism whereby the

Bushveld magma was oxidized in response to devolatization of the dolomite. The devolatisation released H_2O, CO_2 and S into the magma thereby changing the physicochemical parameters of the magma leading to a decrease in sulphur solubility and triggering sulphide supersaturation.

Regional trends in the platinum-group mineralogy of the Critical Zone of the Bushveld Complex (hosting the Platreef) where investigated by Kinloch (1982). The author reported that unlike the Merensky reef and UG-2 chromitite, the Platreef on the farm Zwartfontein is depleted in laurite (RuS_2). This was attributed to the metamorphism of dolomite floor rocks and xenoliths by the Platreef magma releasing CO_2 which volatilises Ru.

Cawthorn et al. (1985) presented major element, trace element and Sr isotope data of the Platreef on the farm Overysel. Here, the immediate floor rocks consist of a suite of highly metamorphosed, banded tonalitic gneisses with leucotonalitic veins. Through isotope and trace element modeling, the workers suggested that the immediate floor rocks cannot be the source of contamination. Instead, the contaminant was the partial melt derived from granites that intruded the metamorphosed floor rocks of the Transvaal Sequence to the south.

White (1994) provided a description of the Platreef at several localities. He reported that the pyroxenite of the B reef has virtually no olivine and that the PGE grades in the Platreef are dependent on the floor rocks. PGE grades are relatively higher where the floor rocks consist of dolomite, but relatively lower where they consist of granite,

iron-formation or shale. A chromitite layer was intersected by drilling on the northern portion of Tweefontein, where floor rocks are banded iron formation and hornfels. The sulphides were thought to have segregated due to a decrease in S solubility in response to a decrease in FeO content of the silicate magma as a result of chromite formation.

In situ formation of the Platreef sulphides was rejected by Lee (1996) who instead proposed that the sulphides segregated in a staging chamber at depth and were entrained by the ascending Platreef magma.

Viljoen and Schurmann (1998) produced a detailed summary of the available data on the Platreef, including information on geology, mineralogy and theories of ore genesis.

Harris and Chaumba (2001) conducted a detailed major and trace element investigation as well as S and O isotopic study of the Platreef at Sandsloot. They found evidence for local contamination of Bushveld magma by dolomite, but in addition they suggest a component of contamination that occurred in a staging chamber.

Armitage et al. (2002) studied the PGE mineralisation in the Platreef at Sandsloot platinum mine and provided an account of the PGE and Au concentrations, and the nature of the PGM. Notably, at this locality, disseminated and vein-type PGE mineralisation is found up to several meters within the sedimentary floor rocks, below

the basal contact of the intrusion. From SEM studies of four polished samples, the authors report the complete absence of PGE sulphides and the existence of low-temperature semi-metallides and alloys and their high-temperature equivalents. The authors also report that PGE signatures in the intrusion and its footwall are broadly similar pointing to similar processes controlling or influencing the final PGE distribution in the two packages. Based on the above and the widespread evidence for fluid activity, the authors favour hydrothermal activity as the major process that influenced the final distribution of the PGE in the rocks.

CHAPTER TWO: OVERVIEW OF THE BUSHVELD COMPLEX

2.1 General

The Bushveld Complex is the largest known layered intrusion on Earth, with an outcrop area of over 29450 km^2 and further sub-outcrops of 36550 km^2 (Fig. 1.1, Von Gruenewaldt, 1977). It lies almost entirely within the bounds of the Transvaal sedimentary basin with both the intrusion and the sedimentary rocks possibly forming in response to intracratonic rifting (Eriksson et al. 1991). The Bushveld Complex contains approximately 80% of the world's resource of PGE (Morrissey, 1988), as well as the bulk of resources in Cr and V.

The Complex consists of three suites of plutonic rocks, namely the mafic-ultramafic Rustenburg Layered Suite (South African Committee for Stratigraphy, 1980), the Rashoop Granophyre Suite and the Lebowa Granite Suite (Von Gruenewaldt et al., 1985). The Rustenburg Layered Suite is an approximately 8 km thick succession of layered mafic and ultramafic rocks, exposed in 5 major lobes, i.e., the eastern-, western-, and far-western lobes, the northern or Potgietersrus - Villa Nora lobe, and the Bethal lobe. The latter, hidden below younger sedimentary cover, was identified on the basis of a gravity high and is only known from borehole core. The individual lobes differ in aerial extent, thickness and degree of exposure. There is still controversy as to whether the limbs are joined at depth. Connectivity of the lobes at depth was first proposed by Hall (1932). Later interpretations of the Bouger anomalies suggested that the mafic rocks were not continuous at depth (Cousins, 1959). Drilling

established extensions of the western limb at its northern end beneath the Bushveld granite, and of the eastern limb beneath the Karoo sedimentary cover to the west of the Wonderkop fault (Eales and Cawthorn, 1996). Cawthorn and Webb (2001) proposed that Hall's initial model was correct, in that the eastern and the western limb of the Bushveld Complex are linked and formed within a single lopolithic intrusion. Their proposition is largely based on the lithological and compositional similarity between the different lobes, and by considering the isostatic response of the crust after emplacement of the Bushveld magma.

The Complex intruded the 2550 – 2060 Ma (Nelson et al., 1999) Transvaal Supergroup largely along an unconformity between the Magaliesberg quartzite of the Pretoria Group and the overlying Rooiberg felsites (Cheney and Twist, 1992). The exceptions are (i) the eastern lobe south of the Steelpoort fault, where the Complex transgressed upwards through more than 2 km of sediments and (ii) the Potgietersrus limb where intrusion occurred at the level of the Magaliesberg quartzite in the south, but transgressing downwards towards the north, until the mafic rocks abut Achaean granitic gneiss (Eales and Cawthorn, 1996).

The Transvaal Supergroup is a supracrustal volcanosedimentary sequence which consists, from the base to the top, of (a) the protobasinal Wolkberg and Buffelsfontein Groups, (b) the carbonaceous Chuniespoort Group, and (c) the largely pelitic Pretoria Group. U/Pb dating of titanite yielded an age of 2058 ± 0.8 Ma for the Bushveld Complex (Buick et al., 2001), and this age is virtually identical to the age of the Rooiberg volcanics at the top of the Transvaal Supergroup (Walraven et al., 1990).

The last magmatic event of the Bushveld Complex is dated at 2052 ± 48 m.y (Rb-Sr whole rock age) (Walraven et al., 1990) and is represented by the Lebowa Granite, which was emplaced at, or close to, the contact between the Rustenburg Layered Suite and the acid roof rocks (Von Gruenewaldt et al., 1985).

The mode of emplacement of the layered suite was one of repeated injections of magma. This is suggested by distinct reversals in the initial Sr – isotopic ratio and in differentiation indexes such as Mg number and Cr contents, as well as textural evidence such as resorbed plagioclase inclusions in olivine and pyroxene (Eales et al. 1986).

2.2 The Rustenburg Layered Suite

The Rustenburg Layered Suite is generally sub-divided into five zones (Hall, 1932): at the base is the Marginal Zone which is overlain by the Lower Zone, Critical Zone, Main Zone, and the Upper Zone. A simplified stratigraphic column representative of the Bushveld Complex is shown in Fig. 2.1.

The basal Marginal Zone consists of unlayered fine- to medium grained heterogeneous gabbronoritic rocks and varies in thickness between 0 and 250 m (western Bushveld Complex, Coertze, 1974). The rocks of the Marginal Zone are generally

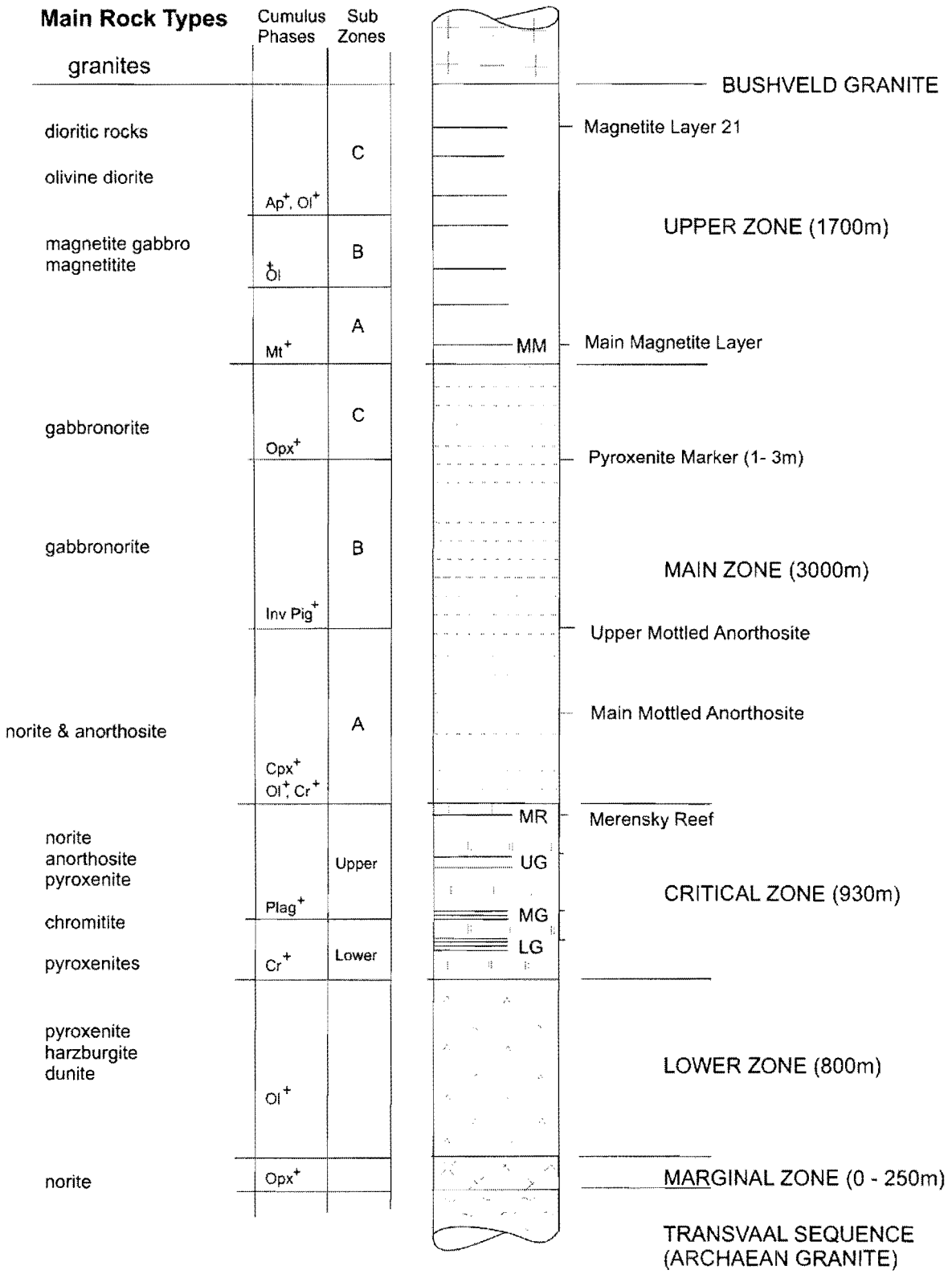

Fig. 2.1: Stratigraphy of the Rustenburg Layered Suite, Bushveld Complex (from Mitchell 1990).

established extensions of the western limb at its northern end beneath the Bushveld granite, and of the eastern limb beneath the Karoo sedimentary cover to the west of the Wonderkop fault (Eales and Cawthorn, 1996). Cawthorn and Webb (2001) proposed that Hall's initial model was correct, in that the eastern and the western limb of the Bushveld Complex are linked and formed within a single lopolithic intrusion. Their proposition is largely based on the lithological and compositional similarity between the different lobes, and by considering the isostatic response of the crust after emplacement of the Bushveld magma.

The Complex intruded the 2550 – 2060 Ma (Nelson et al., 1999) Transvaal Supergroup largely along an unconformity between the Magaliesberg quartzite of the Pretoria Group and the overlying Rooiberg felsites (Cheney and Twist, 1992). The exceptions are (i) the eastern lobe south of the Steelpoort fault, where the Complex transgressed upwards through more than 2 km of sediments and (ii) the Potgietersrus limb where intrusion occurred at the level of the Magaliesberg quartzite in the south, but transgressing downwards towards the north, until the mafic rocks abut Achaean granitic gneiss (Eales and Cawthorn, 1996).

The Transvaal Supergroup is a supracrustal volcanosedimentary sequence which consists, from the base to the top, of (a) the protobasinal Wolkberg and Buffelsfontein Groups, (b) the carbonaceous Chuniespoort Group, and (c) the largely pelitic Pretoria Group. U/Pb dating of titanite yielded an age of 2058 ± 0.8 Ma for the Bushveld Complex (Buick et al., 2001), and this age is virtually identical to the age of the Rooiberg volcanics at the top of the Transvaal Supergroup (Walraven et al., 1990).

resources of chromite within the Middle Group and Upper Group chromitite layers (Hatton and Von Gruenewaldt, 1987).

According to the most widely accepted subdivision, the base of the Main Zone may be placed at the top of the Bastard unit, although the exact position is somewhat controversial (Kruger, 1990; Mitchell and Scoon, 1991). The Main Zone is a ca. 3000 m thick sequence consisting mainly of norite in the basal and uppermost portions, but gabbronorite in the intervening central portion (Mitchell, 1990). Anorthosite constitutes some 5 % of the rocks, while pyroxenite is rare. The Main Zone is characterised by the absence of olivine and chromian spinel, coupled with the general lack of the fine scale layering that is typical of the Critical Zone.

Also a subject of debate is the position of the Main Zone – Upper Zone boundary. Based on a reversal in Sr isotopic ratio and in the trend of iron enrichment (Von Gruenewaldt, 1973; Klemm et al., 1985), Kruger (1990) placed the boundary at the level of the Pyroxenite Marker, a prominent pyroxenite layer some 2.5 km above the base of the Main Zone. The more commonly used subdivision is by Wager and Brown (1968) who defined the base of the Upper Zone by the first occurrence of cumulus magnetite, some 660 m above the Pyroxenite Marker.

2.3 PGE Mineralisation

The PGE mineralisation in the Rustenburg Layered Suite occurs as:

a) stratiform sulphide bearing horizons including the Merensky reef (Lee, 1983; Naldrett et al., 1986; Barnes and Maier, 2002), Platreef (Gain and Mostert,

1982; Van der Merwe, 1976), Bastard Reef (Lee, 1983), Pseudo Reef and Tarentaal layers (Naldrett et al., 1986), and the footwall of the Lower Magnetite Layer 2 (Von Gruenewaldt, 1976).

b) chromitites (Gain, 1985; Von Gruenewaldt et al., 1986; Hiemstra, 1986; Lee and Parry, 1988; Teigler, 1990 a, b; Scoon and Teigler, 1994) and

c) discordant PGE-enriched pipes of mafic-ultramafic pegmatite and magnesian dunite in the Critical Zone of the eastern Bushveld Complex, at Mooihoek, Onverwacht and Driekop (Scoon and Mitchell, 1994)

For the sulphide bearing layers, two main genetic models are generally considered. Most workers believe that the PGE were concentrated by a sulphide liquid that segregated from the silicate magma after S supersaturation was achieved. In the past, it was widely believed that sulphide supersaturation can be achieved by mixing of compositionally contrasting magmas, one being primitive, the other being more evolved (Naldrett and von Gruenewaldt, 1989; Irvine, 1986; Li et al., 2001a). It has recently been shown (Li et al., 2001b; Cawthorn, 2002) that this model is probably incorrect and that magma mixing cannot trigger S supersaturation. Therefore, other mechanisms to cause S supersaturation have to be considered, such as contamination of the silicate magma with the country rocks. Mechanical concentration of sulphides after initial precipitation appears to be a further pre-requisite to produce economic sulphide deposits.

An alternative model (Boudreau et al. 1986) proposes that the PGE are concentrated by percolating late-magmatic fluids, but this model has been criticized by several

authors, based, in part, on the occurrence of PGE-rich sulphide near the base of the Complex in the Platreef.

For the S-poor chromitites, some workers have in the past proposed that the PGE were initially concentrated by sulphides, but that much of the S was subsequently lost, with the PGE remaining behind (e.g. Naldrett and Lehmann, 1988; von Gruenewaldt et al., 1989). More recently, it is also considered whether PGM can precipitate directly from the silicate magma, perhaps in response to destabilization of atomic metal clusters (Tredoux et al. 1995).

The PGE mineralised discordant pipes contain a very unusual PGE assemblage, dominated by Pt, suggesting that the mineralisation is not of primary magmatic origin. Stumpfl (1993) has suggested that the PGE are instead the result of hydrothermal remobilization from cumulates. The origin of the pipes and the mineralisation remain enigmatic.

CHAPTER THREE: STRATIGRAPHY

The first detailed description of the geology of the Platreef was provided by Buchanan (1979). Based on compositional and modal variation at Sandsloot, Buchanan (1979) and White (1994) distinguished three layers, the A, B, and C-reefs from base to top. Subsequent workers studied the reef on the farms Tweefontein (Buchanan et al., 1981), Zwartfontein (Kinloch, 1982), Drenthe (Gain and Mostert, 1982), Overysel (Cawthorn et al. 1985), Sandsloot (Harris and Chaumba, 2001 and Armitage et al., 2002) and Townlands (Maier, 2003; submitted) (see Fig. 3.1 for localities). Maier (2003; submitted) suggested that on the farm Townlands, several km to the south of Sandsloot, the three reef zones can equally be identified, but that they are separated by shale interlayers.

At Sandsloot open pit mine, the mine geologists describe the A-reef as a feldspathic, pegmatoidal, pyroxenitic to noritic unit with a heterogeneous texture containing low-grade disseminated mineralisation and commonly some large blebs of composite base metal sulphides. The B-reef is a coarse grained feldspathic pyroxenite. The pyroxenite locally contains some chromite and visible disseminated base metal sulphide mineralisation (mainly pyrrhotite and chalcopyrite). The unit also hosts barren noritic bodies, up to 10's of meters in width that tend to be fine-grained in the centre and coarser grained (occasionally pegmatoidal) at the margins. These rocks are termed hybrid norite by the mine geologists. It is not yet clear whether this 'hybrid norite' is a distinct intrusive phase or represents metasomatised xenoliths. The C-reef

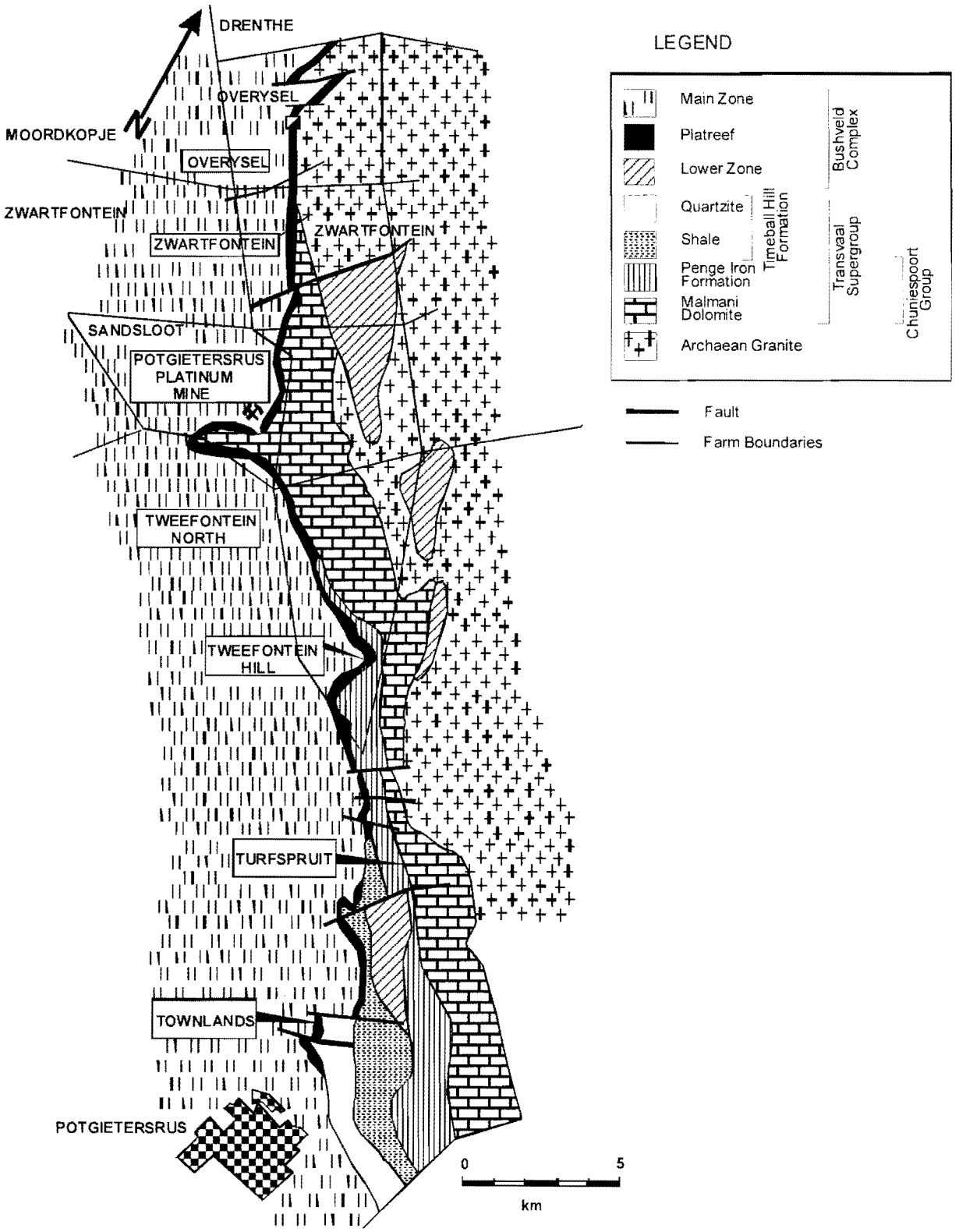

Fig 3.1: Regional geological map of the Potgietersrus limb indicating the location of mineralised sections. (modified after White, 1994).

is a fine grained feldspathic pyroxenite with a 'brown sugar texture' and is normally barren. It is overlain, usually with a relatively sharp contact, by the Main Zone gabbronorites.

On the farm Townlands, the platiniferous rocks show less lithological variation, and the pegmatoidal pyroxenite classified as A-reef on Sandsloot is not developed here. Instead there are three packages of medium-grained feldspathic pyroxenite -to gabbronorite separated by hornfels interlayers. Therefore, if the modal and textural classification applied at Sandsloot is to be followed, it appears that at Townlands, the A- and the C-reefs are not developed.

The three pyroxenite/gabbronorite horizons identified at Townlands are somewhat similar in texture and composition to the B-reef at Sandsloot. However they display a different mineral and whole rock chemistry, including PGE concentration patterns, as will be discussed in chapter 5 and 6. Therefore, the terminology of the Platreef as applied at Sandsloot will not be applied in this work. Instead, the three platiniferous pyroxenite/gabbronorite layers will be referred to as the Lower, Middle and Upper Platreef units, from the bottom to the top, respectively.

A simplified stratigraphic column of the Platreef lithologies and their floor rocks on the farm Townlands is given in Fig. 3.2. The TL1-03 borehole log is given in Appendix VII. The floor rocks of the Platreef consist of hornfels, quartzite and calcsilicates probably belonging to the early Proterozoic Silverton Formation of the Pretoria Group. The immediate floor to the Platreef is formed by a 10 m quartzite. The hornfels may

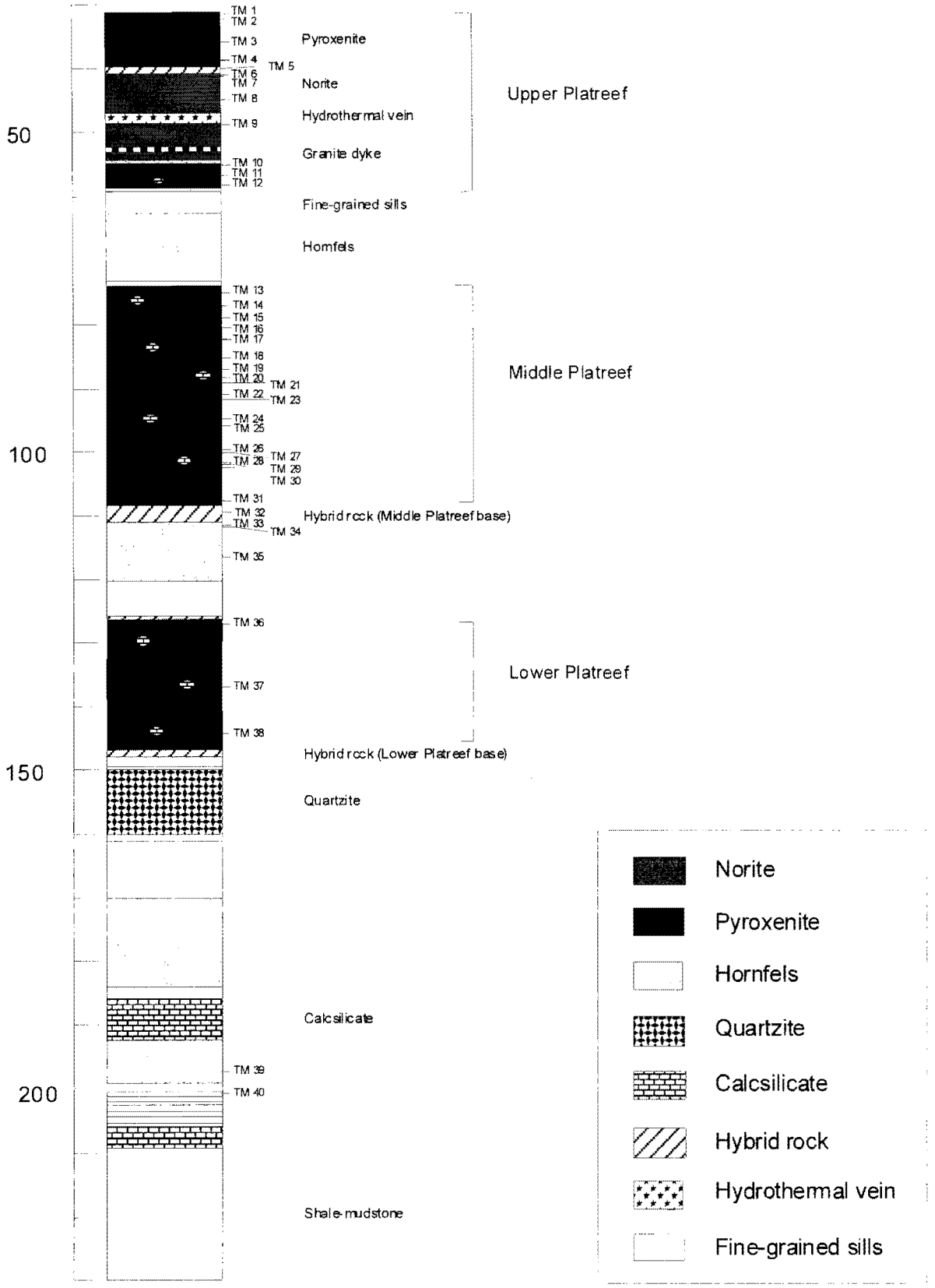

Fig. 3.2: Generalised stratigraphic column through the Platreef on the farm Townlands (scale in meters).

contain fragments of quartzite up to 3 cm in size. Occasionally, the hornfels contains abundant fine mica. The calcsilicates are fine to medium-grained rocks with a light greenish gray to light gray colour. They are locally layered on a centimeter scale with layering defined by thin (1-2mm), dark, olivine bearing layers. The sedimentary rocks are intruded by numerous sill-like bodies of pyroxenite which show internal variation in grain size, from fine-grained at the margins to medium-grained at the centre. The width of the bodies ranges from a few centimeters to several meters. The medium grained pyroxenite bodies have chilled margins at the top and bottom, up to 3 mm in thickness. Thin reaction rims (≤ 2mm) are present between the hornfels and the pyroxenites, but apart from that, the contacts between the intrusions and the sedimentary rocks are sharp.

The Lower Platreef is largely noritic in composition, with less abundant pyroxenites. The contact between the Lower Platreef and the quartzitic floor rocks is formed by a hybrid zone which consists of metasedimentary rocks apparently injected by pyroxenite. Alternatively, the package may represent pyroxenite containing a dense load of sedimentary xenoliths. A clear distinction between the two possibilities is not possible in the core.

A ca ~9 m interlayer of ferruginous hornfels separates the Lower Platreef from the Middle Platreef. The hornfels contains a fine-grained, greenish-gray, pyroxenite (116.68 – 121.00 m) containing hornfels xenoliths generally 5-18 cm in size (i.e. at 116.80 – 118.86, 117.85 – 117.95, 118.70 – 118.77 and 119.81 – 119.98 m). The contacts between the hornfels xenoliths and the fine-grained pyroxenite are sharp. A

thin whitish reaction rim (1-2 mm) composed of quartz and feldspar occurs between the fine-grained pyroxenite and the hornfels xenoliths. Towards the top of the hornfels interlayer, the sedimentary rock displays layering defined by 2-5 cm serpentinised dolomite bands alternating with light-green, fine to medium grained, diopside-rich zones developed at 108.22 – 108.34 and 108.58 -108.63 m.

The Middle Platreef is approximately 35 m thick and consists mainly of a medium grained, olivine bearing, feldspathic pyroxenite/gabbronorite with a heterogeneous texture. Pegmatoidal patches are abundant and are due to a local increase in modal proportion and grain size of feldspars intergrown with dark, grayish-green, altered, olivine and pyroxene. Coarse sulphides of up to 3 cm in size are preferably associated with the felsic pegmatoidal domains, whereas fine-grained sulphides are found in the more even-textured pyroxenite/gabbronorite. Xenoliths of metadolomite are abundant. The xenoliths have gradational contacts with the igneous rocks marked by a progressive increase in modal olivine in the latter. Interaction between the xenoliths and the intrusive rocks is also evident by means of coarse-grained to pegmatoidal textures around the xenoliths.

A ca. 10 m hornfels interlayer (similar to the one described earlier) overlain by a 3 m fine-grained pyroxenite sill (59.55 – 62.83m) separates the Middle Platreef from the Upper Platreef. The hornfels is fine- to medium grained and dark coloured. Layering is locally developed in the hornfels and defined by thin (1-2 mm) leucocratic quartzofeldspathic layers about 4 cm apart alternating with dark-coloured magnetite-rich portions. Massive magnetite is also locally present especially towards the base of

the hornfels interlayer. It occurs as narrow (< 2 cm wide) zones and blebs. Also towards the base, the hornfels becomes mottled as a manifestation of an increase in quartz and feldspar content relative to the upper portions. Finely disseminated interstitial sulphides, mostly pyrite and minor pyrrhotite, are present in minor proportions. The pyroxenite sills are fine-grained and contain traces of fine-grained sulphides (mostly pyrrhotite).

Overlying the fine-grained pyroxenite sill is a 75 cm hybrid zone similar to the one described earlier. This is in turn overlain by a medium-grained feldspathic pyroxenite/gabbronorite belonging to the Upper Platreef, similar in appearance to the Middle Platreef. The pyroxenite/gabbronorite has about 12 % interstitial plagioclase in the upper portions decreasing to about 3 % in the lower portions. Sulphides are present in the form of fine interstitial pyrrhotite and minor chalcopyrite, but locally massive sulphides form (i.e. in an 8 cm zone between 57.63 – 57.71 m).This is overlain by a 45 cm hornfels and a medium grained norite (153.04 – 41.44 m). A granite dyke occurs at 53.05-53.61 m.

The norite has a markedly different appearance to the Platreef pyroxenite/gabbronorite. It contains 50 – 60 % plagioclase and 40-50 % orthopyroxene. Minor (< 1 %) sulphides (chalcopyrite and pyrrhotite) occur as fine disseminations within the norite.

The granite dyke contains two types of feldspars, an orange-coloured variety (K-feldspar), with subhedral crystals averaging 2 mm in size, and a whitish lath-shaped

plagioclase feldspar with crystals ranging from 1 – 5 mm in size. The dyke has sharp contacts with the different rocks below and on top. No chilled zone is evident.

The norite is also cut by a 60 cm hydrothermal vein between 47.6-48.10 m. The hydrothermal vein is pegmatoidal and highly altered. It has an 8 cm light-green coloured epidote enriched zone that altered the rock on either side.

A fine-to medium grained hornfels layer grading into a hybrid zone separates the norite and the overlying part of the Upper Platreef. The hornfels is highly magnetic with magnetite reaching up to 50 modal %. The thickness of the Upper Platreef in the present intersection is not known as the core was collared in overburden overlying the pyroxenite. The upper part of the Upper Platreef (from ~40 m) is a medium grained greenish grey orthopyroxenite with about 10 % intercumulus plagioclase. Minor disseminated sulphides, reaching ca. 2-3 vol. %, are present as blebby intercumulus phases.

CHAPTER FOUR: PETROGRAPHY

4.1 Sedimentary Rocks

The sedimentary rocks of the Silverton Formation that form the floor rocks to the Platreef on the farm Townlands consist of shales (hornfelsed when in contact with the intrusion), quartzites and calcsilicates.

The hornfels are ferruginous and mostly consist of fine grained quartz, plagioclase, and magnetite as the major phases with minor cordierite, spinel, hornblende, orthopyroxene and biotite. They display a non foliated fine grained texture typical of hornfels. Plagioclase ranges from 30-40 modal %, quartz from 15-25 modal % and magnetite from 30-40 modal %. Plagioclase is anhedral with grain sizes generally < 1 mm. Slight alteration of plagioclase to sericite is common and the grains often show evidence of deformation expressed by bent lamellae. Quartz is fine-grained (< 1mm) and anhedral with serrated grain boundaries suggesting recrystallisation. Magnetite is anhedral and has a poorly developed skeletal texture. Cordierite is fine grained (≤ 1mm) and anhedral. The crystals are altered along cracks. Spinel is fine-grained (< 0.2mm), transluscent and is found associated with magnetite grain boundaries. Biotite occurs as alteration product of plagioclase and magnetite, and is found mostly surrounding magnetite. Orthopyroxene is mostly elongate (1-3 mm in size) and encloses tiny plagioclase crystals.

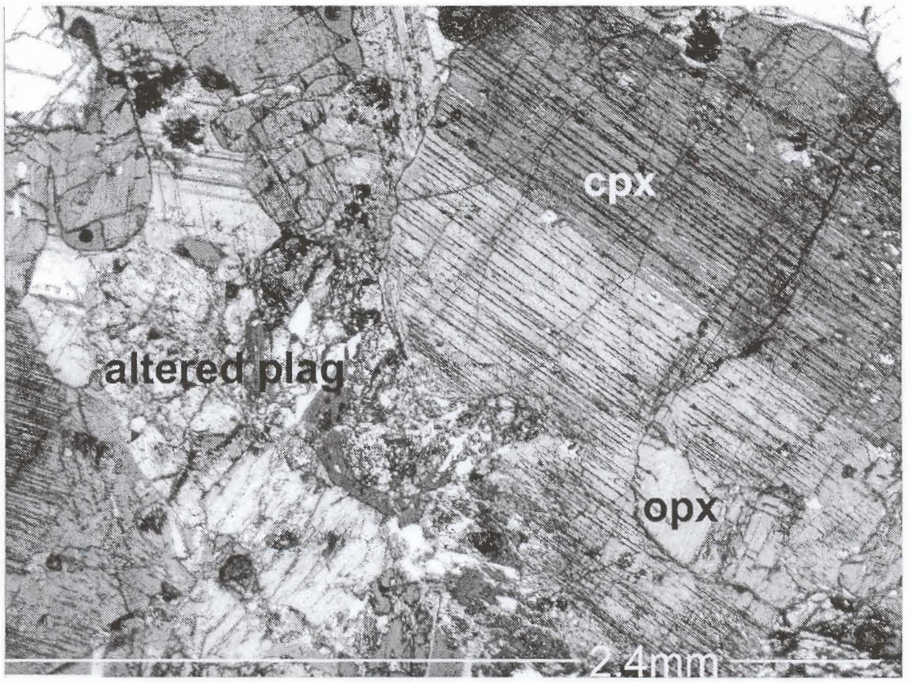

Fig. 4.13: Poikilitic, twinned clinopyroxene (cpx), with orthopyroxene exsolution lamellae enclosing orthopyroxene (opx). Sample TM 1. Transmitted light.

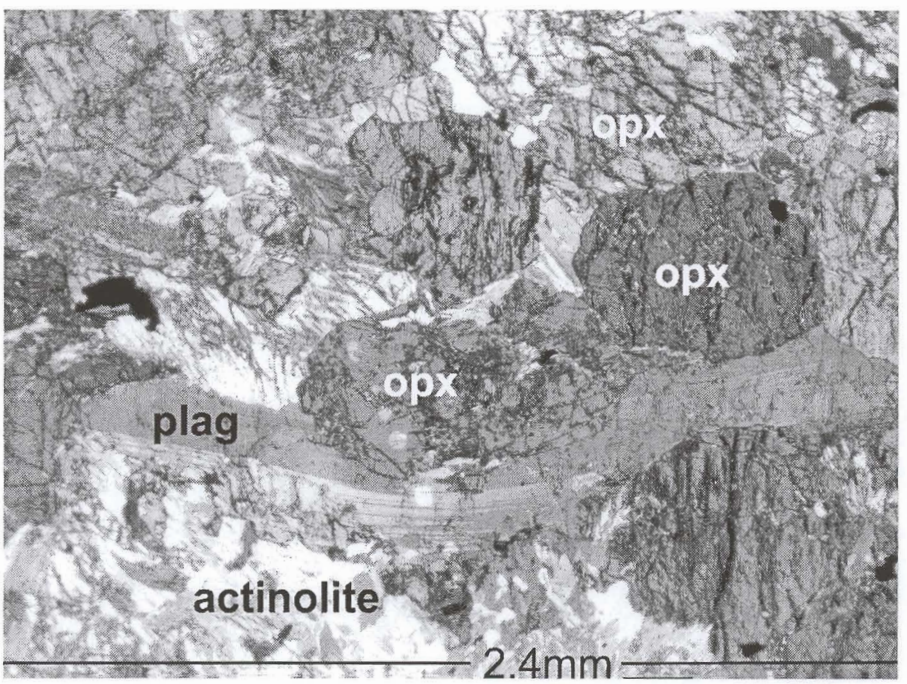

Fig. 4.14: Deformed plagioclase (plag) lamellae in feldspathic pyroxenite. Sample TM 9. Transmitted light.

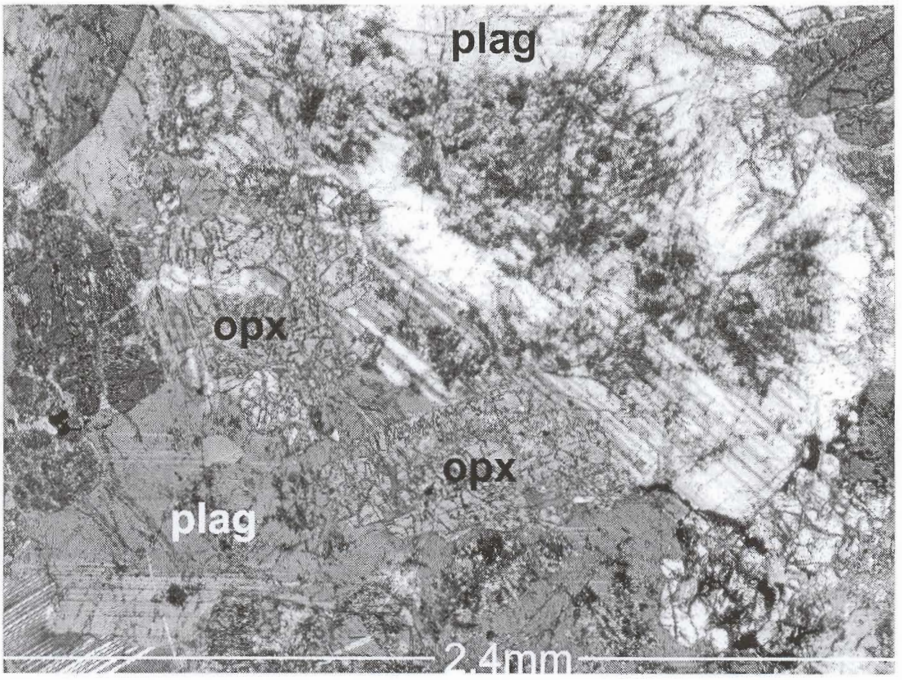

Fig. 4.15: Plagioclase (plag) showing saussuritization beginning at the core. Also note the partially altered orthopyroxene (opx). Sample TM 7. Transmitted light.

The calcsilicates are composed of interlocking calcite (70-85 %) and olivine (15-30 %) crystals. Calcite is subhedral with grain sizes ≤ 1 mm. Olivine crystals (<0.3 mm in size) may also be euhedral, partly when they are locally enclosed in calcite. Otherwise, olivine is subhedral

4.2 Platreef

Modal mineral abundances in the three Platreef horizons are given in Table 4.1. Orthopyroxene increases in abundance whereas feldspar decreases in abundance with height. The grain size of feldspar and orthopyroxene generally increases with height (not shown in Table 4.1). Sulphide is most abundant in the Middle Platreef and less so in the Upper Platreef, whereas the Lower Platreef is relatively sulphide-poor. The amount of olivine is locally variable within the Middle and Upper Platreef, while no olivine was found in the Lower Platreef.

	Lower Platreef	**Middle Platreef**	**Upper Platreef**
Orthopyroxene	55-75	65-80	75-85
Clinopyroxene	0-20	10-15	0-10
Plagioclase	20-40	10-25	5-10
Olivine	-	0-20	0-10
Quartz	-	-	0-3
Sulphides	1-2	0-10 with massive veins up to 3 cm in width	0-3
Secondary minerals after primary silicates	-biotite -amphibole -sericite -epidote -chlorite -magnetite	-biotite -amphibole -sericite -epidote -calcsilicate -magnetite	-biotite -amphibole -sericite -epidote -magnetite
Lithology	Norite and gabbronorite	Gabbronorite /feldspathic pyroxenite and norite	Gabbronorite/feldspathic pyroxenite and norite

Table 4.1. Phase abundances (in modal %) in the Platreef

4.2.1 Lower Platreef

Orthopyroxene and plagioclase are the major silicate minerals in the Lower Platreef. Clinopyroxene may locally reach major status. Minor phases are magnetite, sulphides, biotite and amphibole (Table 4.1). The rocks are mainly medium grained, but fine grained in places and have a granular texture. The size of the crystals ranges from 0.2 mm to 2 mm and averages 1 mm.

Orthopyroxene is subhedral or anhedral. Most grains are subrounded but elongate crystals are common. Towards the top of the Lower Platreef, 120^0 dihedral angles between orthopyroxene crystals are common, bearing evidence of textural equilibrium. Also towards the top of the reef, orthopyroxene crystals are sometimes enclosed in oikocrystic interstitial clinopyroxene.

Plagioclase forms lath shaped crystals averaging 1 mm in length but locally reaching 4 mm in length. Rare clinopyroxene occurs as subhedral, mainly elongate crystals ranging in size from 1 mm to 4 mm and averaging 2 mm. The crystals are twinned and have parting planes filled with magnetite. Additionally, clinopyroxene may form inclusions in plagioclase.

Sulphide (pyrrhotite and chalcopyrite) occurs mainly interstitial to the primary silicates, forming fine disseminations and veins. Fine grained pyrite, with minor chalcopyrite, may also be included in orthopyroxene and, in places, in plagioclase. Near the base of the reef, the amount of sulphides may locally increase to about 30 modal percent, but in general it amounts to less than 2 %.

Alteration

Plagioclase is slightly to heavily saussuritised resulting in the formation of sericite, epidote and sometimes chlorite. Biotite and amphibole are present as alteration products of plagioclase and orthopyroxene, especially where in contact with sulphide. The hydrous phases are usually found associated with each other and form fringes around the sulphide, orthopyroxene and plagioclase. Amphibole may also form large euhedral crystals about 4 mm in size, or fibrous masses.

4.2.2 Middle Platreef

The rocks of the Middle Platreef layer are predominantly composed of orthopyroxene, clinopyroxene and plagioclase. In addition, variable amounts of olivine may occur. Minor phases are biotite, sulphide, magnetite and amphibole (Table 4.1). According to IUGS terminology, the rock is a gabbronorite, but locally pyroxenite may occur.

Orthopyroxene crystals are mostly subhedral or euhedral. They may be elongate and up to 4 mm in length by 1 mm in width, usually showing a weak preferred horizontal orientation. The equigranular crystals average 2-3 mm in size. Exsolution lamellae of clinopyroxene are common (Fig. 4.1). Orthopyroxene sometimes shows granular textures with 120^0 dihedral angles (Fig. 4.2), indicating textural re-equilibration during cooling or re-crystallization. In some thin sections, clinopyroxene chadacrysts may be found enclosed in orthopyroxene. Some crystals are pervasively altered with associated development of magnetite filling the alteration cracks.

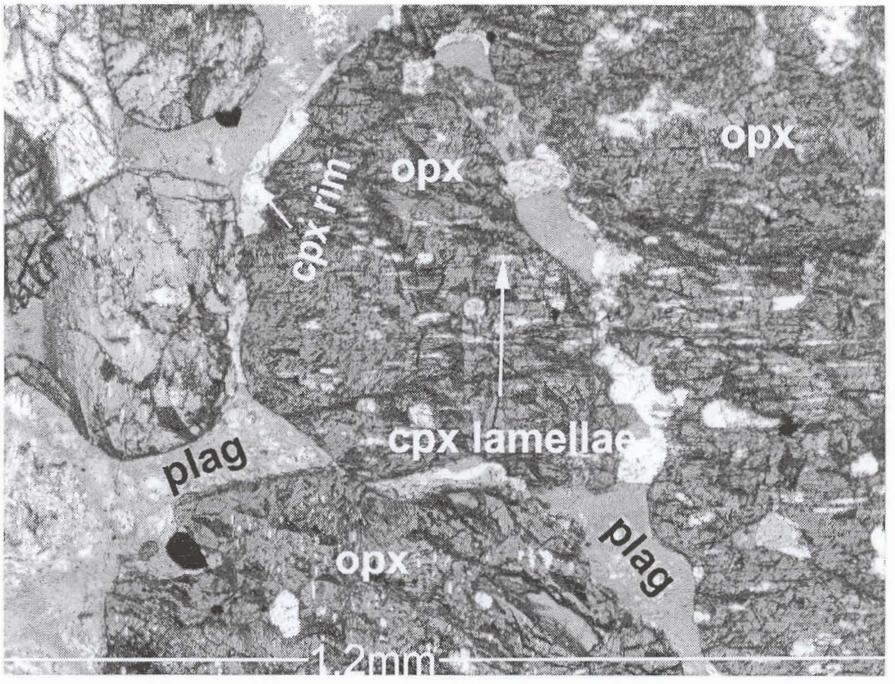

Fig. 4.1: Subhedral orthopyroxene (opx) with clinopyroxene exsolution lamellae, in sericitised interstitial plagioclase (plag). Note the secondary clinopyroxene rim (cpx rim) around opx. Sample TM 14. Transmitted light.

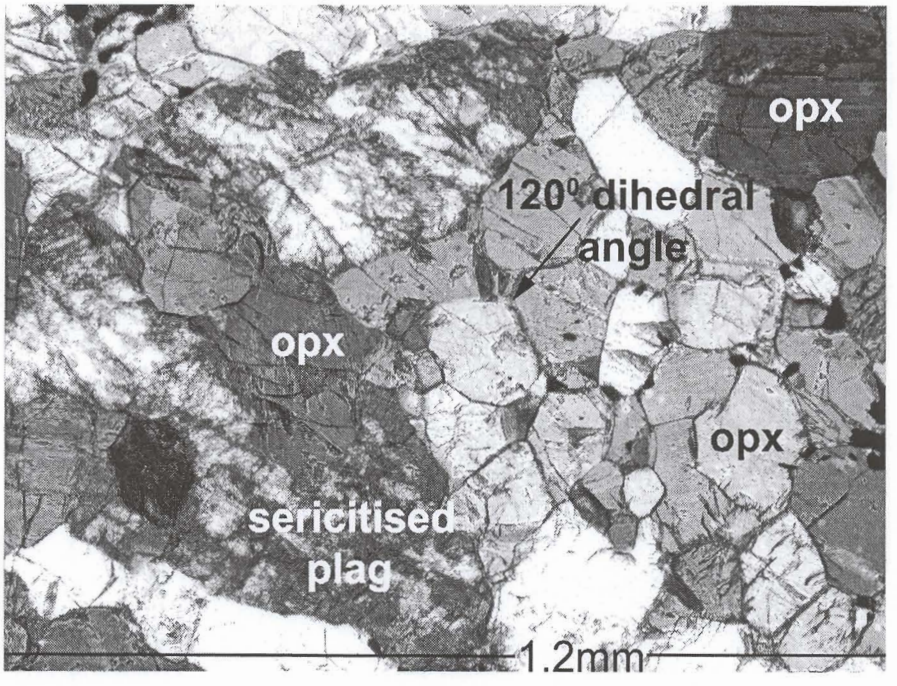

Fig. 4.2: Subhedral orthopyroxene (opx) crystals in a mixture of altered plagioclase (plag). Opx show 120^0 dihedral angles. Sample TM 29. Transmitted light.

Clinopyroxene is mostly anhedral, filling interstices between orthopyroxene and olivine. Large subhedral or euhedral cumulus crystals are less abundant. Interstitial grains average 2 mm in size while cumulus grains range from 2 to 8 mm in size (Fig. 4.3 and 4.4). The cumulus crystals have a high relief and contain slightly pleochroic, blebby to wormlike inclusions believed to consist of actinolite. The inclusions cut across clinopyroxene grain boundaries suggesting they formed after the clinopyroxene. The inclusions are altered (see Fig. 4.5 and 4.6) and sometimes show a fibrous texture. Some of the clinopyroxenes are partially altered to hornblende. Secondary clinopyroxene is sometimes present surrounding orthopyroxene and separating it from altered plagioclase. This may suggest that the secondary clinopyroxene is a reaction product of the two phases it separates.

Plagioclase is interstitial to the orthopyroxene and olivine (where present) and is slightly to pervasively saussuritised, giving a brownish appearance to the matrix. Small rounded olivine crystals may be included in the interstitial plagioclase.

Olivine occurs in varying proportions in the reef and displays a varied grain size distribution ranging from about 0.2 to 2 mm in diameter. The crystals are subhedral and occur enclosed in orthopyroxene, poikilitic interstitial plagioclase and sometimes clinopyroxene. Accordingly, olivine appears to have crystallised before the phases enclosing it. Most olivines are pervasively serpentinised. Secondary orthopyroxene is developed as thin rims between some of the olivines that are enclosed in altered plagioclase (Fig. 4.7 and 4.8).

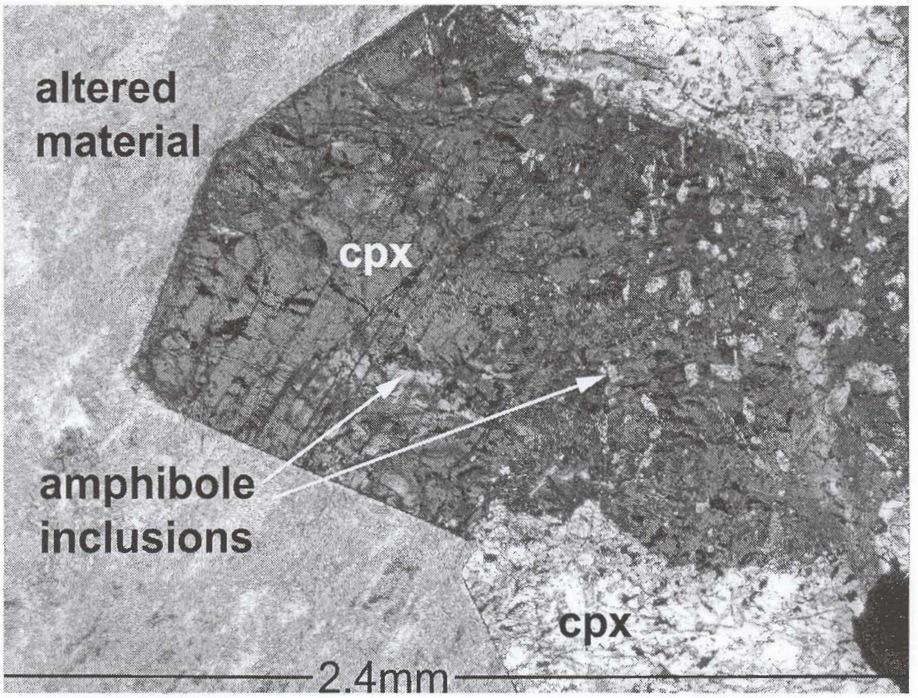

Fig. 4.3: Subhedral clinopyroxene (cpx) (with amphibole inclusions) growing into altered material. Sample TM 19. Transmitted light.

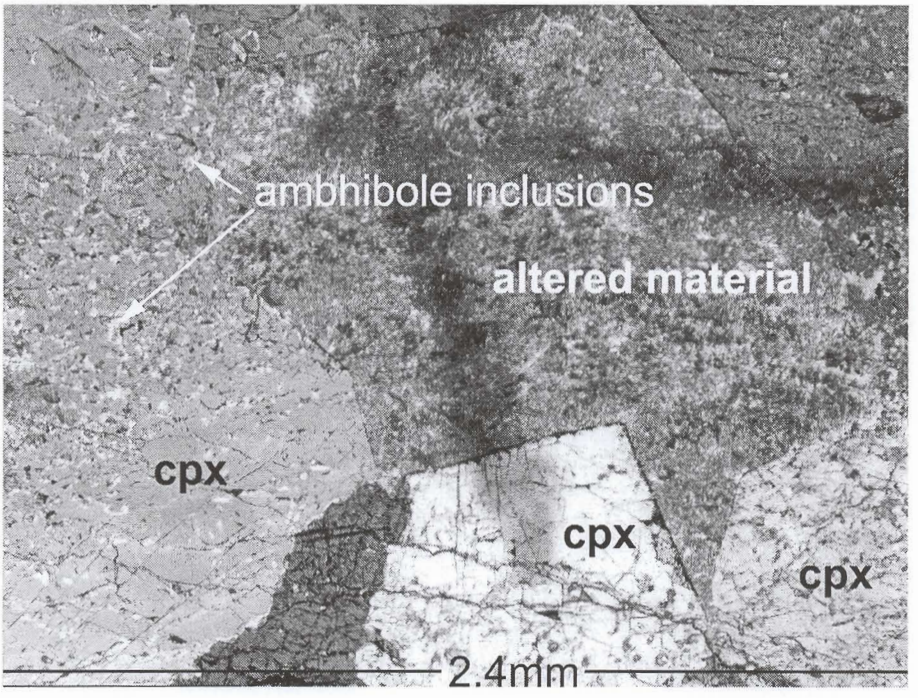

Fig. 4.4: Subhedral clinopyroxene (cpx) (with amphibole inclusions) growing into altered material. Sample TM 24. Transmitted light.

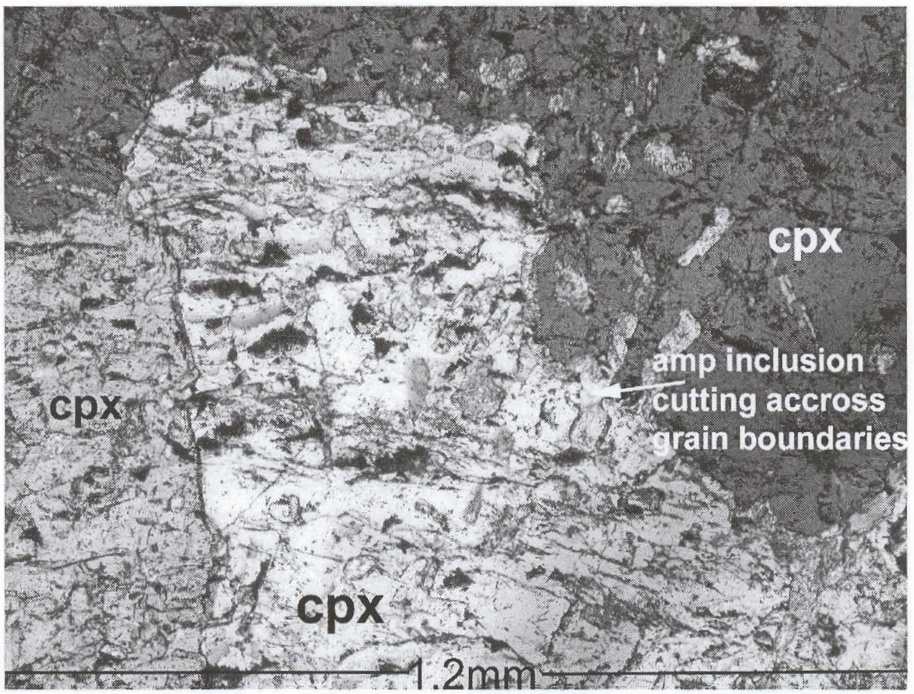

Fig. 4.5: Clinopyroxene (cpx) with amphibole and orthopyroxene (opx) inclusions, some cutting across clinopyroxene grain boundaries. Sample TM 19. Transmitted light.

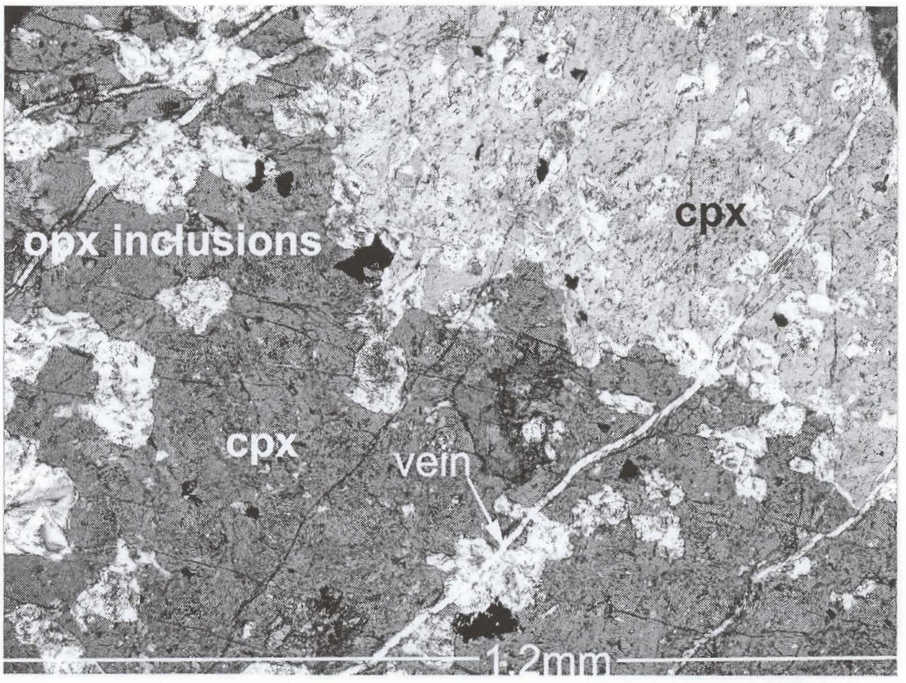

Fig. 4.6: Orthopyroxene (opx) inclusions in clinopyroxene (cpx). Note that the inclusions are altered to amphibole. Sample TM 22. Transmitted light.

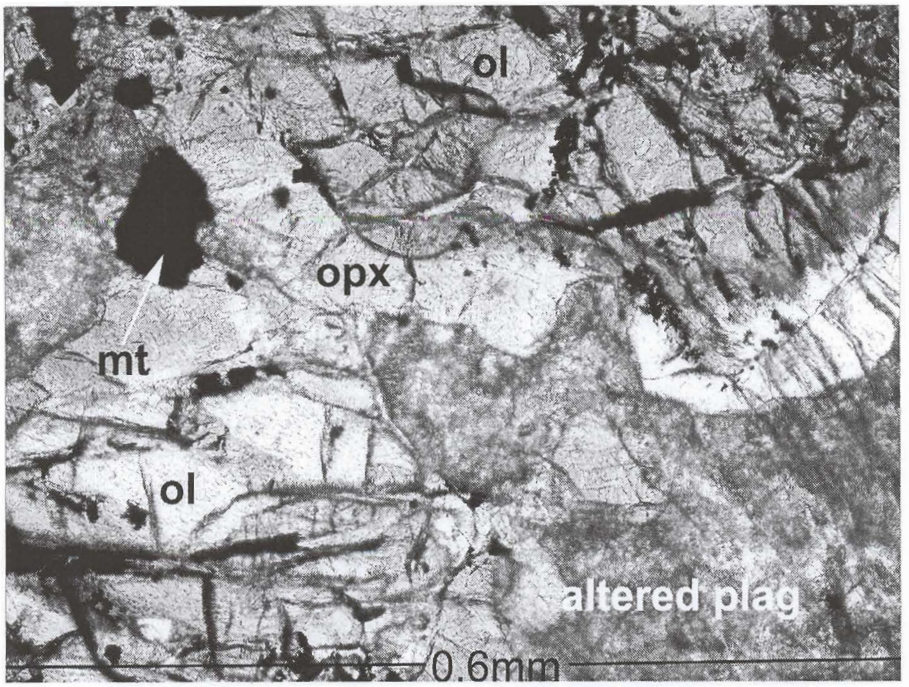

Fig. 4.7: Orthopyroxene (opx) rim around olivine (ol). Note the magnetite (mt) and altered plagioclase (plag). Sample TM 11. Transmitted light.

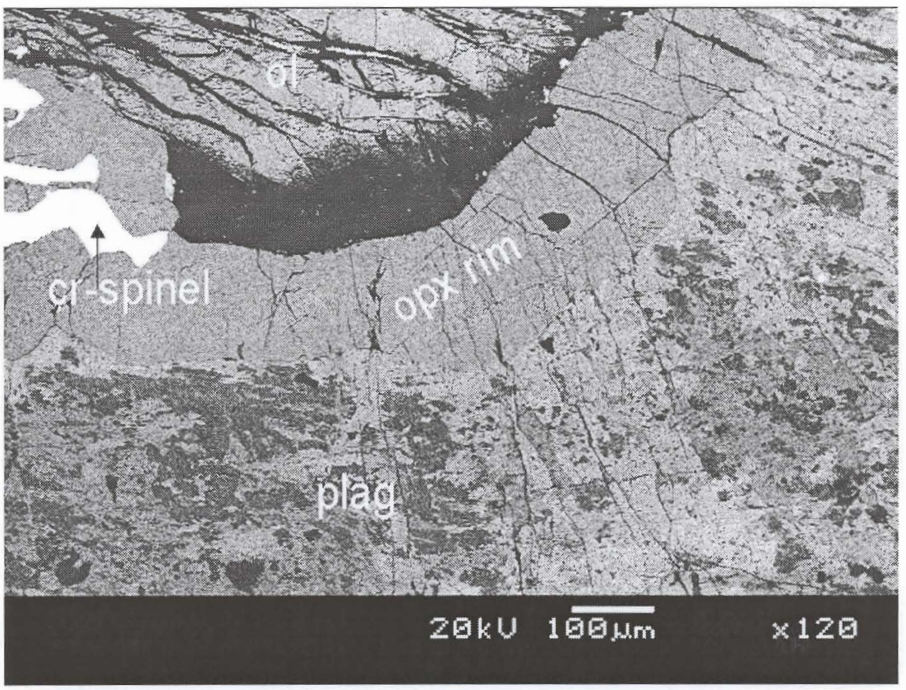

Fig. 4.8: Orthopyroxene (opx) rim around olivine (ol). Note the cr-spinel. BSE image. Sample TM 11.

Coronas consisting of orthopyroxene and a symplectic intergrowth of spinel around olivine are common in ultramafic and gabbroic rocks, for example in the Sulitjelma troctolite where they were considered (Mason, 1967) to be a result of diffusion of the appropriate ions in solution in an aqueous medium across the olivine-plagioclase.

Deer, Howie and Zussman (1978) provide the following chemical equation for the above reaction.

$$(6\text{-}4x)(Mg,Fe)_2SiO_4 + 3CaAl_2Si_2O_8 = (6\text{-}4x)(Mg,Fe)SiO_3 + 2x(Mg,Fe)Al_2SiO_6$$
olivine anorthite Al-orthopyroxene

$$+(3\text{-}2x)Ca(Mg,Fe)Si_2O_6 + 2xCaAl_2SiO_6 + (3\text{-}4x)(Mg,Fe)Al_2O_4$$
Al-clinopyroxene spinel

Where $0 < x < 0.75$

N.B: Clinopyroxene was not identified in the present corona assemblages, possibly due to its fine grain size.

An alternative explanation could be reaction between olivine and silica-rich magma to produce the orthopyroxene coronas, but this model fails to explain the presence of spinel.

Some portions of the Middle Platreef have a pegmatoidal texture, due to the presence of large intercumulus plagioclase crystals. The pegmatoidal portions are more altered, with plagioclase being heavily sericitised and orthopyroxene being altered to amphibole and biotite possibly suggesting enhanced fluid activity. Serpentinised olivine is common and gives the rock a heterogeneous texture.

Alteration

Minor biotite and amphibole are present as secondary alteration minerals formed by reaction of orthopyroxene and plagioclase. Biotite occurs as platy crystals, about 1mm in size, and is associated with orthopyroxene and sulphides. Amphibole occurs either as unaltered euhedral diamond shaped hornblende crystals (Fig. 4.9) or as fibrous actinolite (Fig. 4.10 and 4.11). The actinolite may have formed in response to reaction of calcsilicate with silica-rich hydrous magmatic fluids. Amphibole is found mostly associated with sulphides and saussuritised feldspars. Olivine is commonly partially or completely altered to serpentine and iron magnetite. At Sandsloot, due to the prevalence of serpentinite, the pyroxenite is referred to as parapyroxenite by the mine geologists, but at Townlands, the platiniferous rocks are less altered. Some olivine crystals show embayment textures (Fig. 4.12).

Calcsilicate xenoliths are common in the Middle Platreef and have been metamorphosed to skarns. Skarns are metamorphic rocks surrounding an igneous intrusive where the later has come in contact with limestone or dolomite rocks. The skarns have a heterogeneous mineral assemblage. Skarn assemblages resulting from xenoliths completely engulfed by silicate magma comprise of lizardite, magnetite, talc, calcite, hematite, biotite and minor quartz. Close to the contact with the intrusive rocks, the mineral assemblage comprises of lizardite, magnetite, hematite, andradite garnet, brucite, monticellite and fosterite as determined by X-ray diffraction. Lizardite, hematite and brucite are probably not primary skarn minerals, but of secondary origin after alteration primary silicate minerals.

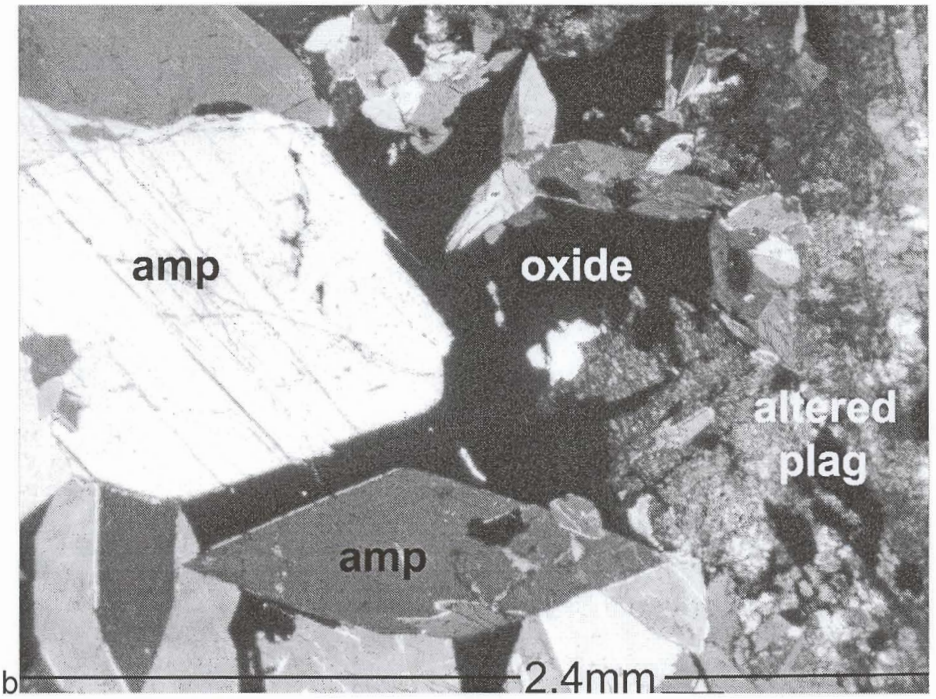

Fig. 4.9: Euhedral amphibole (amp) in magnetite next to altered plagioclase (plag). Sample TM 19. Transmitted light.

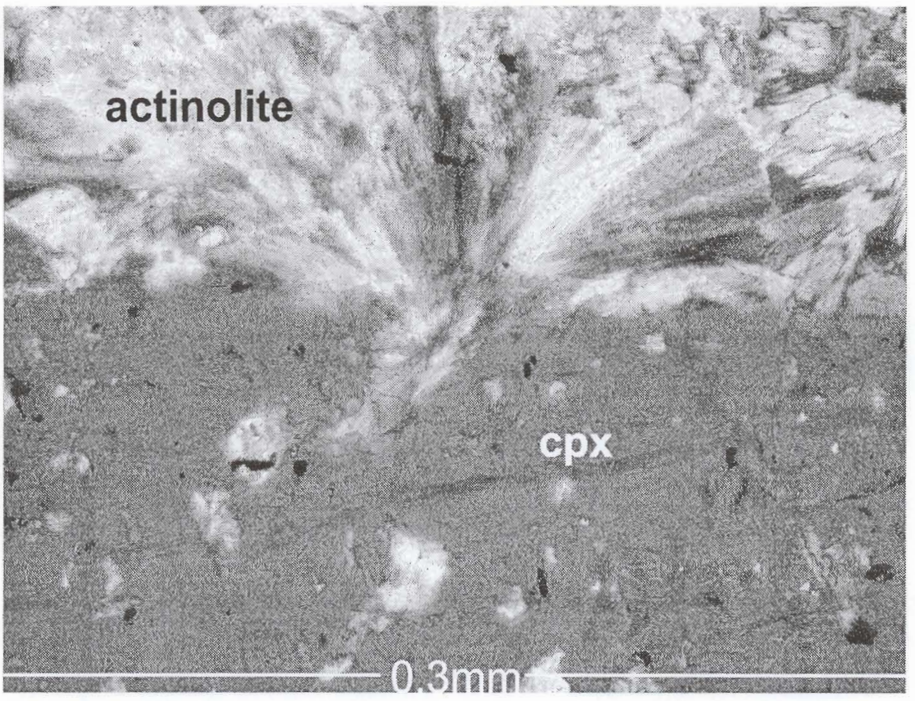

Fig. 4.10: Actinolite apparently growing on clinopyroxene (cpx). Sample TM 24. Transmitted light

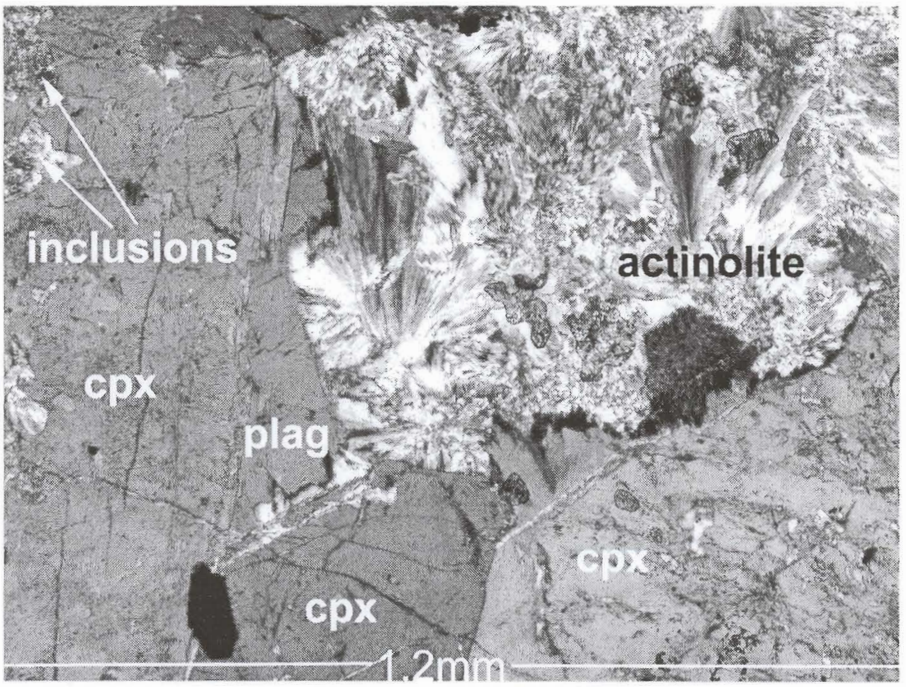

Fig. 4.11: Actinolite apparently growing on clinopyroxene (cpx) and plagioclase (plag). Sample TM 24. Transmitted light.

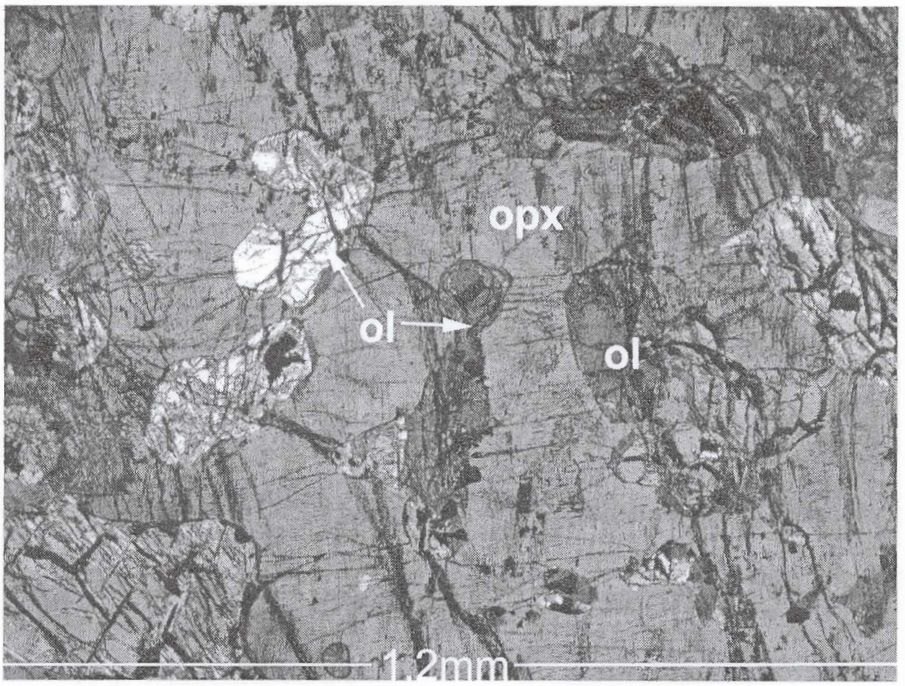

Fig. 4.12: Olivine (ol) enclosed in orthopyroxene (opx). Note the embayment texture. Sample TM 16. Transmitted light.

4.2.3 Upper Platreef

The Upper Platreef consists predominantly of orthopyroxene, with subordinate clinopyroxene and plagioclase. According to IUGS terminology, most of the rocks are gabbronorites. Olivine, quartz, biotite, magnetite, sulphide and amphibole are minor phases (Table 4.1). Quartz occurs as an accessory interstitial mineral (<1.5 mm in size) and sometimes encloses small anhedral orthopyroxene crystals. Orthopyroxene crystals are subhedral, being subrounded to prismatic in shape and averaging 2-4 mm in size. Most grains show bleb-like exsolution lamellae of clinopyroxene along the 110 direction.

Clinopyroxene occurs as large, 3-7 mm, prismatic, subhedral, poikilitic crystals enclosing small orthopyroxene crystals, and locally as interstitial material between orthopyroxene. The clinopyroxene crystals show twinning and exsolution lamellae of orthopyroxene (Fig. 4.13). Clinopyroxene locally contains inclusions of orthopyroxene and minor plagioclase.

Plagioclase is interstitial to orthopyroxene and almost always pervasively altered. It infrequently encloses small anhedral orthopyroxene crystals. In places, e.g. below the norite sill at 48.70m, plagioclase shows evidence of deformation in the form of bent lamellae (Fig. 4.14). The deformation could be related to intrusion of the norite sill or it may reflect a phenocrystic origin of the plagioclase.

Olivine may reach about 30 % in modal abundance. The portions with olivine are highly altered and olivine replaces clinopyroxene. The crystals are subrounded in shape and have variable sizes ranging from 0.3 mm to 2 mm in diameter. The olivine always occurs included in orthopyroxene or plagioclase but is more commonly associated with plagioclase-rich domains.

Alteration

Plagioclase is generally altered to sericite and epidote. The process of saussuritisation begins at the core of individual plagioclase grains, as shown by some relatively fresh plagioclase crystals (Fig. 4.15). This may point to zoning in plagioclase since An-rich parts of plagioclase are more readily sericitised by the exchange of Ca^{2+} for K^{+}. When adjacent to calcsilicate xenoliths, the orthopyroxenes tend to be serpentinised. Serpentinisation is accompanied by the occurrence of fine-grained magnetite and sulphides which are intergrown with the secondary silicates. The sulphides and magnetite increase in abundance with an increase in alteration suggesting some S mobility. Amphibole may replace clinopyroxene, orthopyroxene, magnetite and sulphides. Actinolite needles sometimes penetrate into the sulphides. Near the granite dyke, (at 53.55 – 53.25m) the rocks are cut by numerous veins rich in sericite and quartz and K-feldspar. Magnetite and biotite are present as alteration products of orthopyroxene and tend to occur along its grain boundaries. Olivine is generally partially altered to serpentine with the cores remaining unaltered. Secondary orthopyroxene is developed as thin rims between some of the altered crystals of serpentinised olivine embedded in altered plagioclase (as in the Middle Platreef).

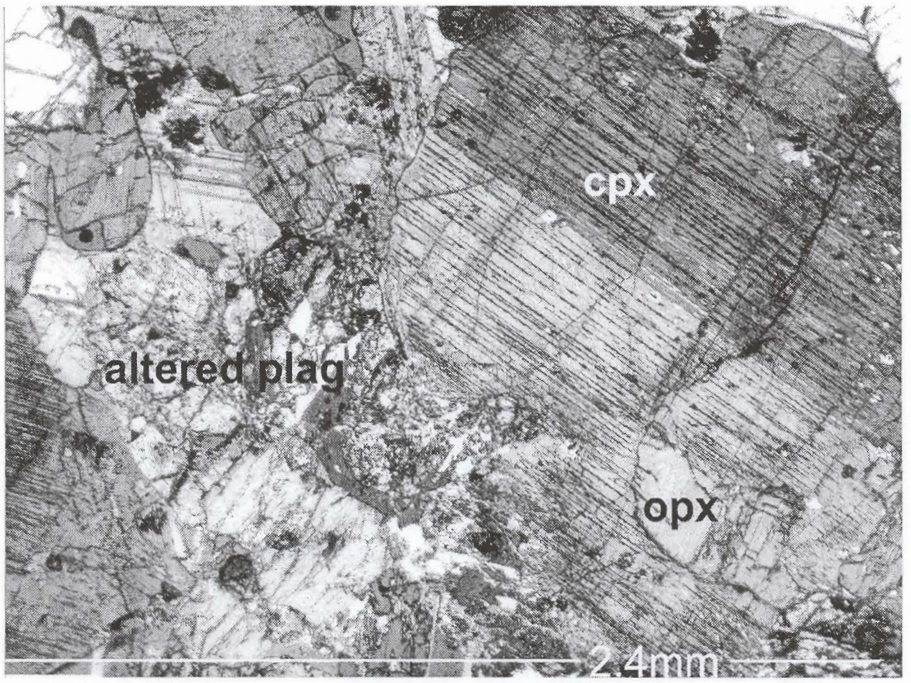

Fig. 4.13: Poikilitic, twinned clinopyroxene (cpx), with orthopyroxene exsolution lamellae enclosing orthopyroxene (opx). Sample TM 1. Transmitted light.

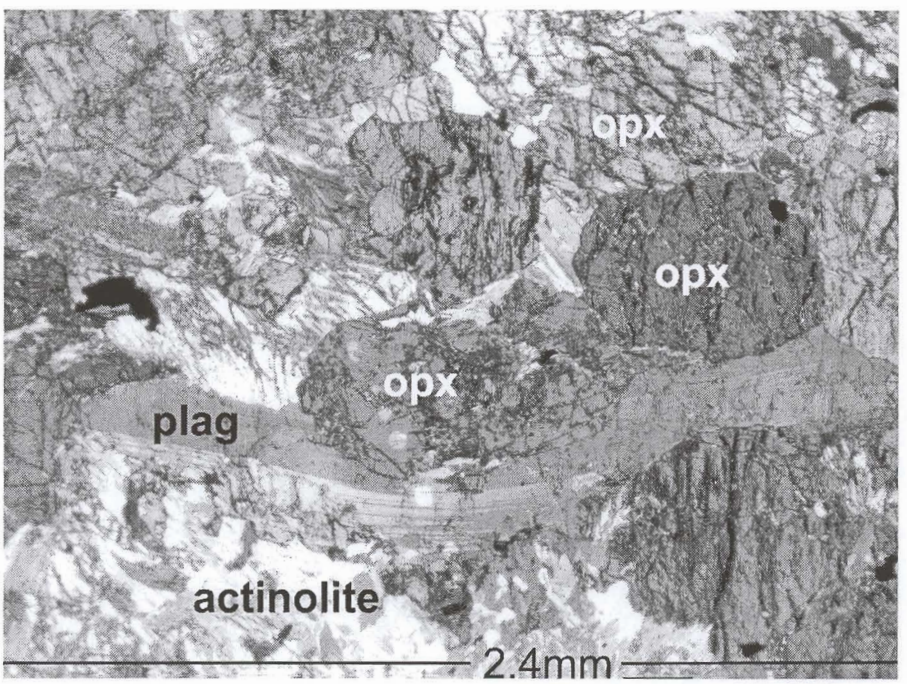

Fig. 4.14: Deformed plagioclase (plag) lamellae in feldspathic pyroxenite. Sample TM 9. Transmitted light.

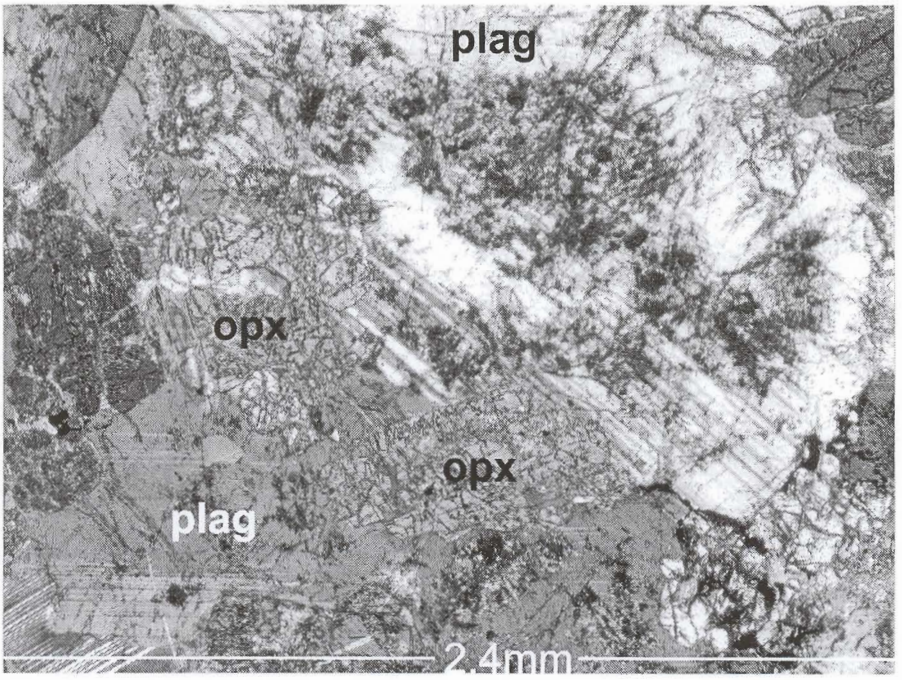

Fig. 4.15: Plagioclase (plag) showing saussuritization beginning at the core. Also note the partially altered orthopyroxene (opx). Sample TM 7. Transmitted light.

4.3 Other Intrusive Rocks

Fine to medium grained norites with a sub-ophitic texture that are interpreted as sills occur at 41.44 to 53.04 m. They contain subhedral orthopyroxene and plagioclase set in a matrix of anhedral plagioclase and quartz. Other minor phases present are magnetite and hornblende.

The norite shows a granular texture of interlocking orthopyroxene and plagioclase crystals. The orthopyroxene crystals have an average size of 3 mm and show minor exsolution lamellae of clinopyroxene. Plagioclase forms laths and oikocrysts. Crystal sizes average 2 to 3 mm. Alteration to sericite and epidote is common. Orthopyroxene and magnetite are locally included in the plagioclase. Quartz, magnetite and hornblende occur as post cumulus phases. Quartz occurs mainly interstitial to orthopyroxene, along parting planes in orthopyroxene and along orthopyroxene grain boundaries. It may sometimes enclose small orthopyroxene grains. Fibrous hornblende has grown on orthopyroxene and altered plagioclase, probably after the reaction between the two phases. Magnetite is interstitial or is included in orthopyroxene and plagioclase.

4.4 Sulphides

The sulphide assemblage in all three layers consists dominantly of pyrrhotite and chalcopyrite with minor pentlandite and pyrite. The sulphide minerals average 2-5 wt. % in abundance in the three layers. They are fine-grained and are mostly located in the interstitial spaces between the silicates (olivine, plagioclase and pyroxene) which tend to be altered along their contacts with the sulphide phase to form reaction rims of

hornblende and biotite. Fine grained pyrite with minor chalcopyrite is locally included in orthopyroxene and plagioclase. Sparsely developed larger blebs of sulphides, up to 2 cm, may occur particularly in the more felsic, pegmatoidal patches within the Middle Platreef. Near the base of the Middle Platreef, the sulphides locally increase in abundance to about 10 wt. %, and the texture changes to large blebs of composite base metal sulphides sometimes reaching 2 cm in size. Zones of massive sulphide (mostly containing pyrrhotite) occur at 101.43 – 101.49 m, 102.46–102.51 m and 102.67–102.72 m. The coarse sulphides, including the massive zones mentioned above, are associated with the relatively more felsic and pegmatoidal parts of the core. Some portions of the reef (99.81–100.54 m) are barren or have only trace amounts of sulphides.

The hornfels may have fine-grained disseminated interstitial pyrite and pyrrhotite usually in amounts < 1 %. The pyroxenite sills are mostly barren but may contain traces of pyrrhotite. Minor (<1 modal %) chalcopyrite and pyrrhotite are found disseminated in the norite sills where they occur interstitial to the silicates. The pyroxenite sills tend to be barren of sulphides.

CHAPTER FIVE: MINERAL CHEMISTRY

5.1 Introduction

The chemical composition of the most important rock forming minerals was determined with a Jeol CXA – 733 Superprobe at Rhodes University. Representative analyses are given in Table 5.1. The remainder of the analytical data and details of analytical procedures are given in Appendices IV and I, respectively. In this chapter, Fo will be used to denote 100 x cationic ratio of Mg ÷ (Mg + Fe) in olivine, An to denote 100 x cationic ratio of Ca / (Ca + Na) in plagioclase, and Mg# to denote 100 x cationic ratio of Mg ÷ (Mg + Fe) in orthopyroxene and clinopyroxene.

5.2 Orthopyroxene

Orthopyroxene compositions cluster in the enstatite field of the pyroxene quadrilateral (Fig. 5.1) and show a range of Mg# between 68 and 82 (Fig. 5.2).

Orthopyroxene from the three Platreef layers shows a wide compositional variation in terms of Al_2O_3. In comparison, orthopyroxene from rocks of the Upper Critical Zone (UCZ) in the western Bushveld (Maier and Eales, 1997) have Al_2O_3 contents between 0.7 and 1.7 wt. %, at broadly similar Mg# as the Platreef orthopyroxenes. TiO_2 and MnO contents are similar in the UCZ and the Platreef but Cr_2O_3 and NiO contents, for corresponding Mg#, are markedly lower in the Platreef than in the UCZ (0.1-0.4 versus 0.1-0.55 in the UCZ of the western Bushveld Complex). Of further note is that Al_2O_3, TiO_2, Cr_2O_3, NiO, and MnO show a poor correlation with Mg# (Fig 5.2), when compared with e.g. the UCZ (Maier and Eales, 1997).

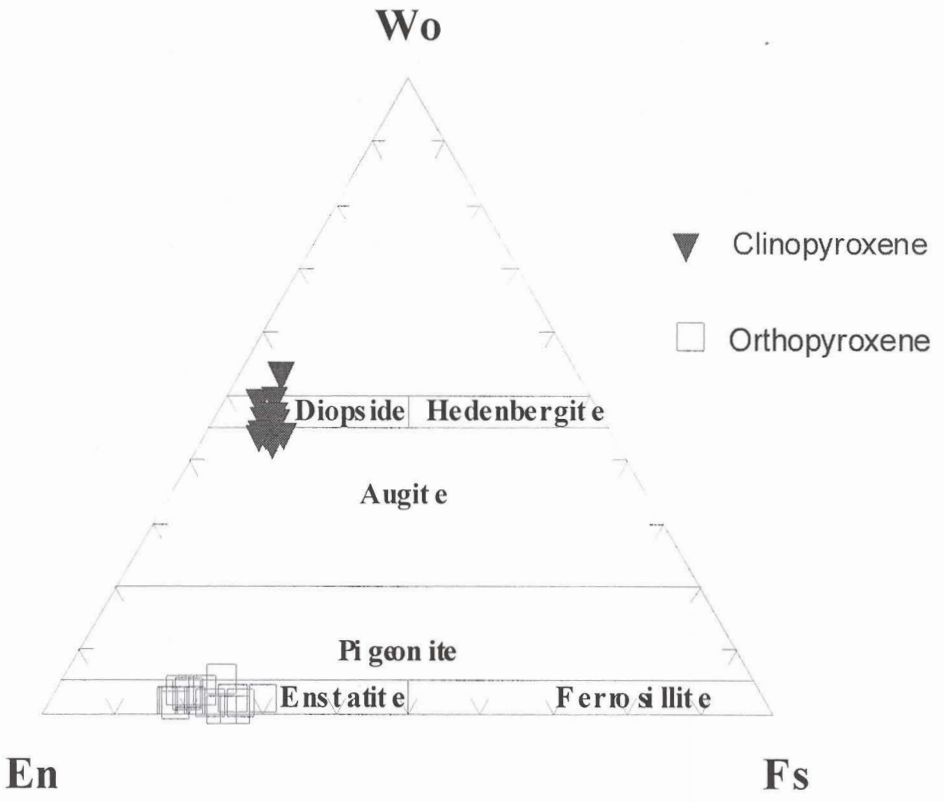

Fig. 5.1: Average pyroxene composition from the Platreef, plotted in the conventional pyroxene triangle.

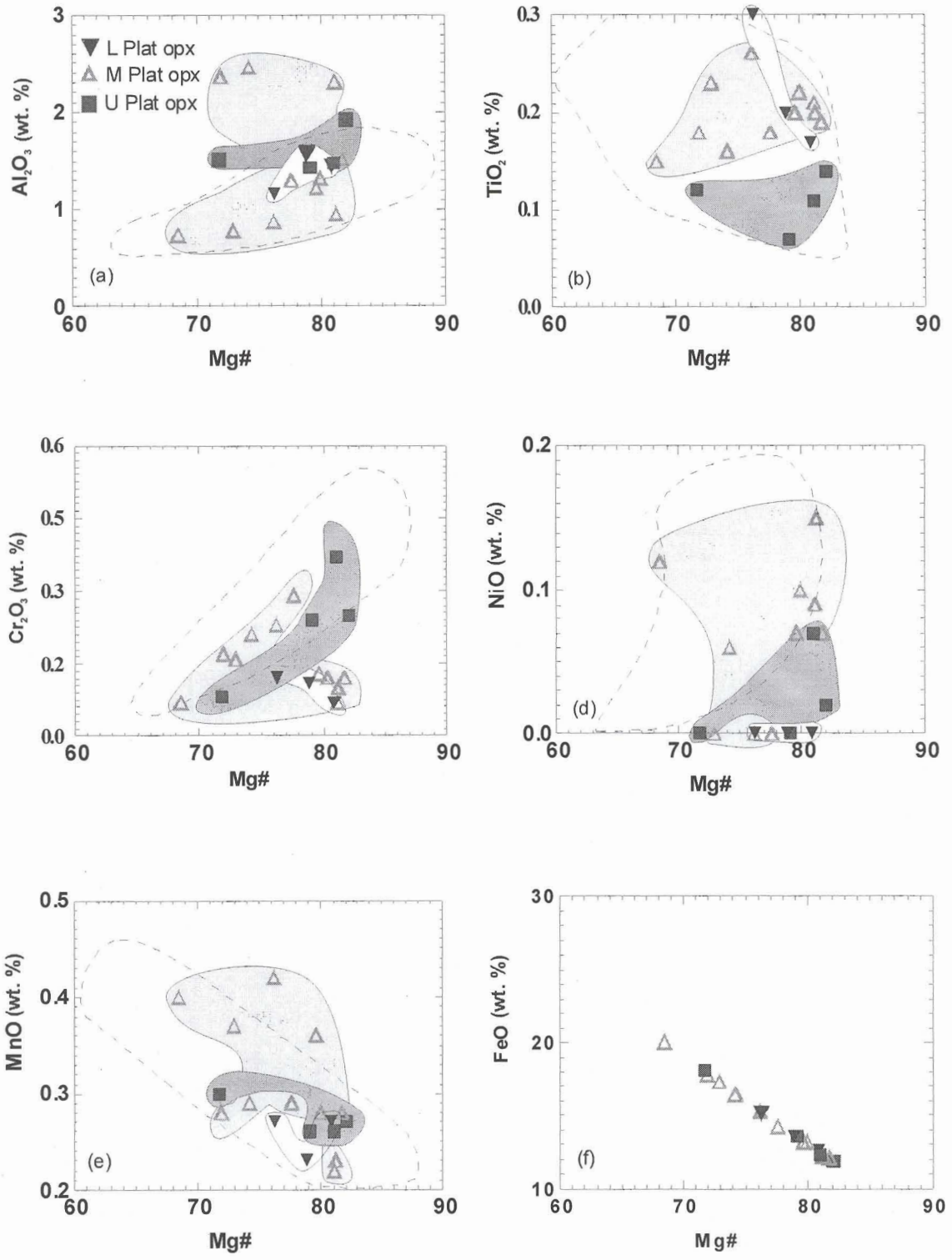

Fig. 5.2: Plot of Al_2O_3, TiO_2, Cr_2O_3, NiO, MnO and FeO in orthopyroxene (opx) versus Mg# of orthopyroxenes. Stippled area represents the field of Merensky-UG2 interval of the Bushveld Complex (Maier and Eales, 1997). U Plat = Upper Platreef, M Plat = Middle Platreef and L Plat = Lower Platreef.

Table 5.1: Compositions of selected minerals

	Orthopyroxene						Clinopyroxene				Olivine		Plagioclase				
sample:	TM2opx2	TM4opx3	TM13opx1	TM20opx5	TM36opx1	TM37opx4	TM2cpx1	TM4cpx1	TM13cpx1	TM22cpx3	TMol4	TMol3	TM4 pl1	TM9 pl1	TM16 pl2	TM 30 pl2	TM37pl1
Type:	UP	UP	MP	MP	LP	LP	UP	UP	MP	MP	UP	MP	UP	UP	MP	MP	LP
SiO2	51.73	53.11	53.07	52.82	53.93	53.45	49.98	50.70	51.33	54.73	37.79	38.68	45.39	52.47	45.72	47.93	49.52
Al2O3	1.57	1.62	0.65	1.79	1.40	1.19	2.21	2.65	1.40	0.76	0.00	0.00	32.77	28.60	33.46	33.15	34.12
Na2O	nd	nd	nd	nd	0.03	0.19	0.31	0.24	0.10	nd	nd	nd	1.99	4.98	1.78	2.43	3.24
MgO	29.12	29.09	25.69	26.04	28.80	26.41	16.31	16.15	18.44	17.75	43.03	42.44	nd	nd	nd	nd	0.02
FeO	13.34	12.66	17.97	17.36	13.82	15.30	6.04	5.74	10.06	2.94	18.39	18.70	0.55	0.25	0.54	0.62	0.40
MnO	0.24	0.29	0.41	0.32	0.18	0.32	0.22	0.15	0.24	0.08	0.31	0.31	nd	nd	nd	0.05	0.00
Cr2O3	0.24	0.29	0.19	0.19	0.10	0.16	0.48	0.72	0.28	0.07	nd	nd	nd	nd	nd	nd	0.02
NiO	nd	nd	nd	nd	nd	nd	nd	nd	nd	0.03	0.32	0.30	0.02	nd	nd	nd	nd
K2O	nd	nd	nd	nd	0.00	0.00	nd	nd	nd	nd	nd	nd	0.09	0.19	0.06	0.09	0.20
CaO	1.19	1.43	0.91	0.36	0.70	2.72	22.88	23.42	17.06	25.60	0.05	0.06	16.98	11.61	17.55	16.34	14.75
TiO2	0.10	0.13	0.24	0.17	0.26	0.38	0.20	0.10	0.13	0.10	nd	nd	nd	nd	nd	nd	0.01
Total	97.54	98.64	99.13	99.05	99.48	100.12	98.63	99.86	99.04	102.09	99.90	100.49	97.81	98.12	99.15	100.63	102.28
Cations (based on 6 oxygen)							(6 oxygen)				(4 oxygen)		(32 oxygen)				
Si	1.91	1.93	1.96	1.94	1.95	1.94	1.89	1.89	1.92	1.96	0.97	0.99	8.57	9.70	8.52	8.77	8.87
Al	0.07	0.07	0.03	0.08	0.06	0.05	0.10	0.12	0.06	0.03	0.00	0.00	7.30	6.23	7.35	7.15	7.20
Na	0.00	0.00	0.00	0.00	0.00	0.01	0.02	0.02	0.01	0.00	0.00	0.00	0.73	1.78	0.64	0.86	1.13
Mg	1.60	1.57	1.41	1.43	1.55	1.43	0.92	0.90	1.03	0.95	1.65	1.61	0.00	0.00	0.01	0.00	0.00
Fe	0.41	0.38	0.56	0.53	0.42	0.47	0.19	0.18	0.32	0.09	0.40	0.40	0.09	0.04	0.09	0.10	0.06
Mn	0.01	0.01	0.01	0.01	0.01	0.01	0.01	0.01	0.01	0.00	0.01	0.01	0.00	0.00	0.00	0.01	0.00
Cr	0.01	0.01	0.01	0.01	0.00	0.01	0.01	0.02	0.01	0.00	0.00	0.00	0.00	0.00	0.00	0.00	0.00
Ni	0.00	0.00	0.00	0.00	0.00	0.00	0.00	0.00	0.00	0.00	0.01	0.01	0.00	0.00	0.00	0.00	0.00
K	0.00	0.00	0.00	0.00	0.00	0.00	0.00	0.00	0.00	0.00	0.00	0.00	0.02	0.05	0.01	0.02	0.05
Ca	0.05	0.06	0.04	0.01	0.03	0.11	0.92	0.93	0.69	0.98	0.00	0.00	3.44	2.30	3.51	3.20	2.83
Ti	0.00	0.00	0.01	0.01	0.01	0.01	0.01	0.00	0.00	0.00	0.00	0.00	0.00	0.00	0.00	0.00	0.00
Sum	4.05	4.03	4.02	4.01	4.02	4.03	4.07	4.05	4.04	4.02	3.03	3.01	20.15	20.10	20.13	20.10	20.12
Mg no.	79.57	80.39	71.81	72.81	78.79	75.45	82.84	83.41	76.58	91.51							
fo											80.4	79.9					
An													82	56	84	78	71

NB: UP = Upper Platreef, MP = Middle Platreef, LP = Lower Platreef

When plotted against depth, there is little systematic variation between the three Platreef layers in terms of Al_2O_3 and Mg# of orthopyroxene (Fig. 5.3). There appears to be a broad increase in Cr_2O_3 with height, i.e. from the Lower Platreef through the Middle Platreef to the Upper Platreef, and a decrease in TiO_2. NiO contents show considerable variation, but the Lower Platreef orthopyroxenes are particularly Ni-depleted (Fig. 5.3). In contrast, several other samples from the Upper and the Middle Platreef have NiO values similar to orthopyroxenes from the UCZ in the Western Bushveld Complex (Maier and Eales, 1997).

5.3. Clinopyroxene

Cumulus clinopyroxene occurs together with orthopyroxene in the Middle and Upper Platreef, but is absent in the Lower Platreef. The occurrence of cumulus clinopyroxene in the Platreef constitutes a notable difference to cumulates of the UCZ in the remainder of the Bushveld Complex where cumulus clinopyroxene is absent until some 500m into the Main Zone.

The clinopyroxene mostly plot in the diopside field of the pyroxene quadrilateral (Fig. 5.1) with a few falling in the augite field. Some clinopyroxene from the Middle Platreef plot above the Di-Hd joint.

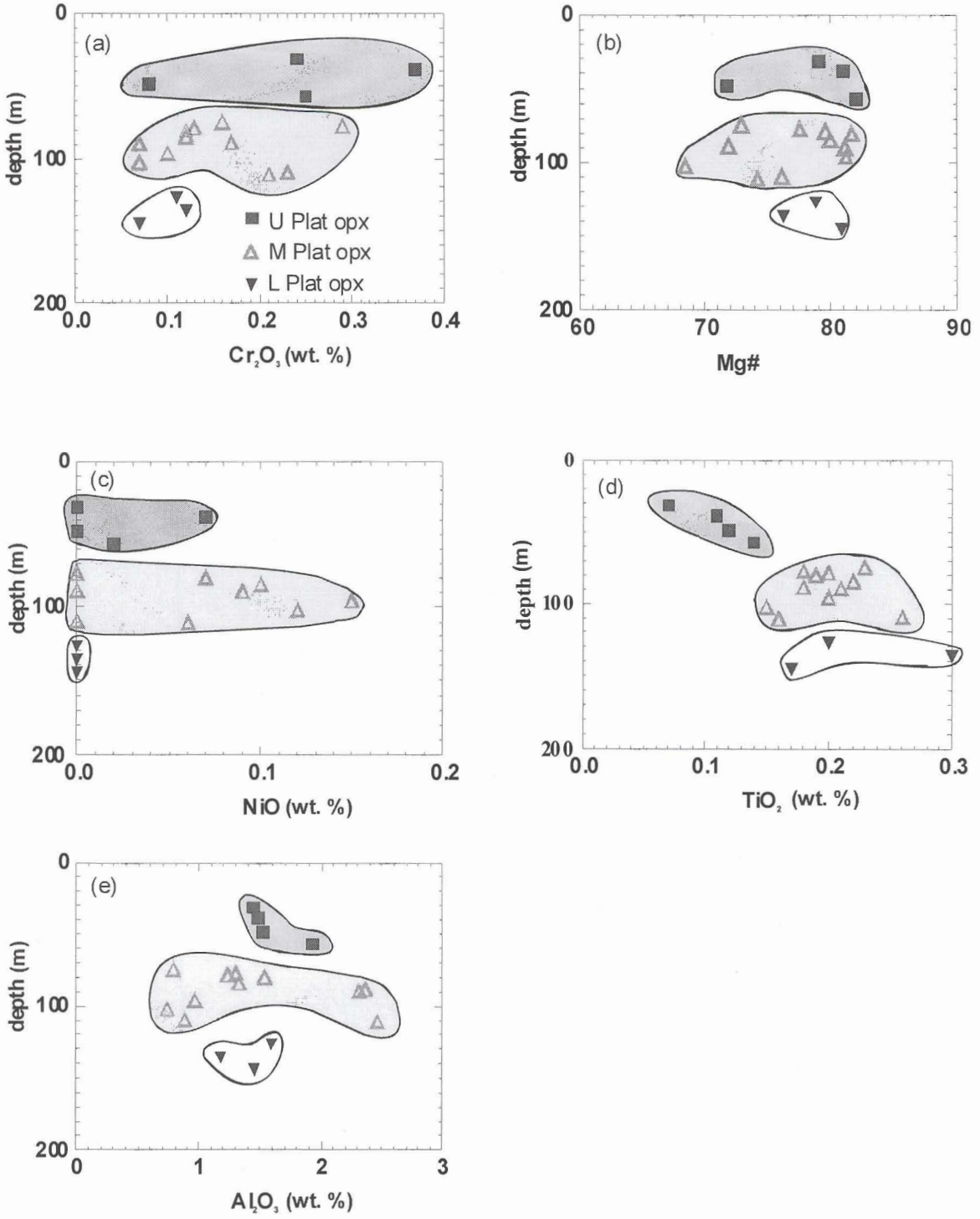

Fig. 5.3: Plot of depth versus Cr_2O_3, Mg#, NiO, TiO_2 and Al_2O_3 in orthopyroxene (opx). U Plat = Upper Platreef, M Plat = Middle Platreef and L Plat = Lower Platreef.

The Mg# of clinopyroxene from the Upper Platreef ranges from 82.3 to 83.41 while that from the Middle Platreef ranges from 76.58 to 91.51. Average Cr_2O_3 content of clinopyroxene is 0.53 wt. % in the Upper Platreef and 0.20 wt. % in the Middle Platreef, with the highest analysed value of 0.72 wt. % in the Upper Platreef. Thus there appears to be an analogous trend of Cr enrichment with height as observed for the orthopyroxenes. In comparison with the clinopyroxene from the Main Zone of the Bushveld Complex (0.45-0.77 wt. % Cr_2O_3), the average Cr contents of the Middle Platreef clinopyroxene is low (Table 5.1).

Clinopyroxene in samples TM 19, TM 22 and TM 26 of the Middle Platreef are notable for their high Al_2O_3 contents (generally above 5 wt. %, reaching 9.68 wt. % in sample TM 19). These clinopyroxene also have slightly higher CaO contents of about 24 wt. % compared to the other clinopyroxenes which have CaO mostly between 21-22 wt. %. In comparison, cumulus clinopyroxene from the Main Zone of the Bushveld Complex (Mitchell, 1990) has markedly lower Al_2O_3 (1-2 wt. %) and CaO contents (18-23 wt. %). Based on the combined textural and compositional evidence, I suggest that these pyroxenes are of metamorphic origin, probably related to reaction of calcsilicate xenoliths with silicate magma.

5.4 Olivine

Olivine is present in the Middle and Upper Platreef but is absent in the Lower Platreef. The olivine shows a restricted compositional range (Fig. 5.4). Analyses of core domains of olivine from the Upper Platreef display Fo contents between 80-83 (averaging Fo_{81}) and those from the Middle Platreef have Fo 78-83 (averaging Fo_{79}).

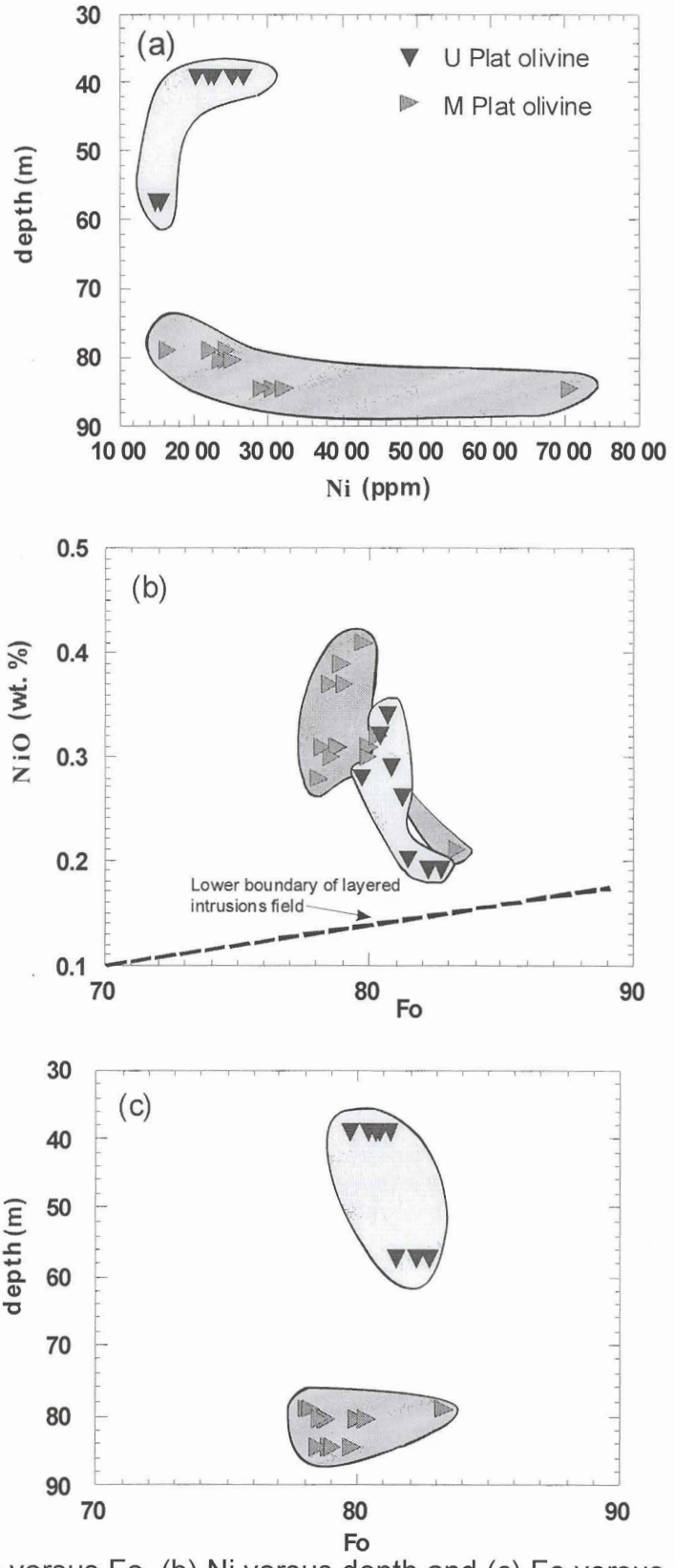

Fig. 5.4: (a) NiO versus Fo, (b) Ni versus depth and (c) Fo versus depth in Platreef olivine. . U Plat = Upper Platreef, M Plat = Middle Platreef and L Plat = Lower Platreef.

Thus the composition and distribution of olivine confirms the pattern of more primitive rock composition with height established by pyroxene compositions.

The analysed Platreef olivine has NiO contents varying from 0.19 to 0.39 wt. % (averaging 0.30 wt %), which is consistent with a magmatic origin of the olivine. There is considerable local variation in Ni content (Fig. 5.4a) possibly due to equilibration of olivine with sulphide. Such an interpretation is supported by the negative correlation between Fo and Ni (Fig. 5.4b). Alternatively, the negative correlation may be fortuitous and instead be related to distinct compositions of the magmas precipitating the Middle and Upper Platreef. Thus the Upper Platreef may have formed from a relatively more primitive magma (giving high Fo contents) that was relatively more Ni depleted (due to equilibration with sulphides) than the Middle Platreef.

Having said this, all analysed olivine in the Platreef studied are undepleted in Ni relative to Fo (Fig. 5.4b), when compared to the field of layered intrusions (Simpkin and Smith, 1970). This is notable as olivine from sulphide bearing ultramafic and mafic rocks are commonly depleted in Ni relative to Fo (e.g. Voisey's Bay, Li and Naldrett, 1999). In many of these examples, the Ni depletion is explained by scavenging of Ni from the magma by sulphide melt prior to olivine crystallisation. On the other hand, olivine within many of the sulphide-bearing intrusions at Noril'sk also shows little evidence for metal depletion (Arndt et al. 2003). The observation that olivine from the Platreef is undepleted in Ni, and that the Platreef sulphides are relatively metal-rich (as will be discussed in chapter 6) suggests that metal undepleted silicate magma was in equilibrium with Ni-rich sulphide.

5.5 Plagioclase

Plagioclase is mostly of intercumulus nature in the three Platreef layers and plots in the labradorite and bytownite field of the An-Ab-Or triangle, with the exception of two samples from TM 33 which plot in the oligoclase field. In all three Platreef layers, An contents range from 54 to 85.2 averaging 70.52. These values are broadly similar to those of plagioclase from the UCZ in the Western Bushveld Complex (Maier and Eales, 1997). Two samples show An values of 25.8 and 28.7. These represent intercumulus plagioclase and the variation may be largely due to zoning.

In contrast to the UCZ in the Western Bushveld (Maier and Eales, 1997), the composition of the plagioclase in the Platreef shows a positive correlation with Mg# of orthopyroxene (Fig. 5.5). The outliers may be due to zonation and/or the presence of phenocrysts.

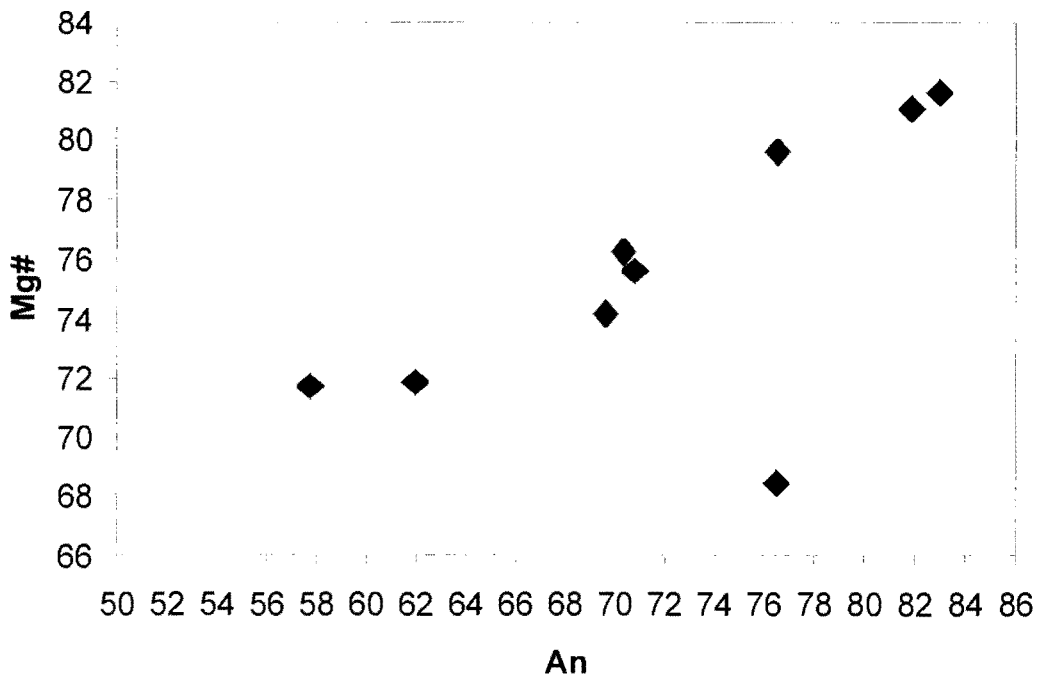

Fig. 5.5: Means of An content of plagioclase plotted versus Mg# of orthopyroxenes.

CHAPTER SIX: WHOLE-ROCK CHEMISTRY

6.1 Introduction

Thirty-two samples of gabbronorite/feldspathic pyroxenite, gabbro, hornfels and calcsilicate were analysed for whole rock major elements and lithophile trace elements using an ARL 9400XP+ wavelength dispersive XRF Spectrometer at the University of Pretoria. Twenty-seven of the samples were additionally analysed for platinum-group elements (PGE) by instrumental neutron activation analysis (INAA) at the University of Quebec at Chicoutimi, Canada. Analytical details are given in Appendix I and the analyses are tabulated in Appendix V.

6.2 Major Element Chemistry

Compositional ranges of major element oxides in the different Platreef layers are given in Table 6.1. The data are displayed as bivariate plots with MgO as the differentiation index in Fig. 6.1. Compositions of plagioclase, orthopyroxene, olivine and clinopyroxene determined by electron microprobe and B1 and B3 Bushveld parental magmas (Curl, 2001) were also plotted. This was done to determine whether the Platreef rocks are mixtures of the cumulus minerals and Bushveld trapped melt or whether there is an additional component present, possibly derived from the floor rocks.

When compared to the Merensky Reef in the Western Bushveld Complex (Barnes and Maier, 2002) it is clear that the Platreef on average has lower SiO_2, Al_2O_3 and Na_2O (with the

exception of the Lower Platreef) but markedly higher CaO and K_2O contents (Table 6.1). This pattern cannot be explained by variation in plagioclase or orthopyroxene content, but instead indicates addition of external CaO and K_2O to the Platreef magma or rocks.

wt. %	Lower Platreef	Middle Platreef	Upper Platreef	Pegmatoidal feldspathic pyroxenite of the Upper Platreef	Merensky Reef
SiO_2	47.4-49.92	39.11-49.58	42.82-51.38	41.64-46.68	51.09
MgO	13.76-16.64	19.06-26.18	18.32-20.91	16.32-21.4	18.89
Fe_2O_3	10.07-13.82	8.25-21.53	10.73-14.41	13.18-18.99	9.15
Al_2O_3	8.35-13.87	4.28-9.64	6.52-7.29	6.51-16.77	10.60
CaO	6.04-12.21	4.17-13.24	6.34-13.1	3.21-4.57	6.20
Na_2O	0.01-1.04	0.01	0.01-0.13	0.01-0.52	0.75
K_2O	0.31-0.76	0.12-0.44	0.26-0.46	0.34-0.48	0.20
Cr_2O_3	0.09-0.32	0.01-0.2	0.04-0.39	0.06-0.29	1.08

Table 6.1: Ranges of whole rock compositions for Platreef rocks compared to those from the Merensky Reef (Barnes and Maier, 2002)

The concentrations of the other major elements are broadly comparable in the Platreef and the Merensky Reef. Amongst the three Platreef layers, the Lower Platreef has the lowest MgO and Fe_2O_3 contents, but the highest Al_2O_3 contents. The Lower Platreef has higher contents of modal plagioclase than the other two Platreef layers, possibly explaining the high Al_2O_3 contents.

It is notable that there is little correlation between MgO and Fe_2O_3 (Fig. 6.1a), (and MnO, not shown in figure 6.1) similar to that observed in the mafic-ultramafic rocks of the UCZ (Maier and Eales, 1997). It is possible that this is partly due to the presence of sulphides and/or Fe-oxides. This interpretation is supported by the fact that several samples plot outside the compositional field defined by plagioclase, orthopyroxene, clinopyroxene and olivine (figure 6.1a). In terms of Al_2O_3, CaO and TiO_2, little evidence for the addition of components from the country rocks is evident (figures 6.1b, c and d). In contrast, the SiO_2 versus MgO diagram (Fig. 6.1e) may indicate an important role for calcsilicate. The alternative possibility, i.e. that the low SiO_2 contents are a function of significant amounts of modal olivine, is not supported by the Al_2O_3, Fe_2O_3, CaO or TiO_2 vs MgO diagrams.

Selected major elements are plotted against depth in figure 6.2. The data show a broad increase in MgO with height, and decreases in TiO_2 and Al_2O_3, confirming the trend shown by mineral chemistry data that indicated a reverse differentiation trend in the Platreef with height.

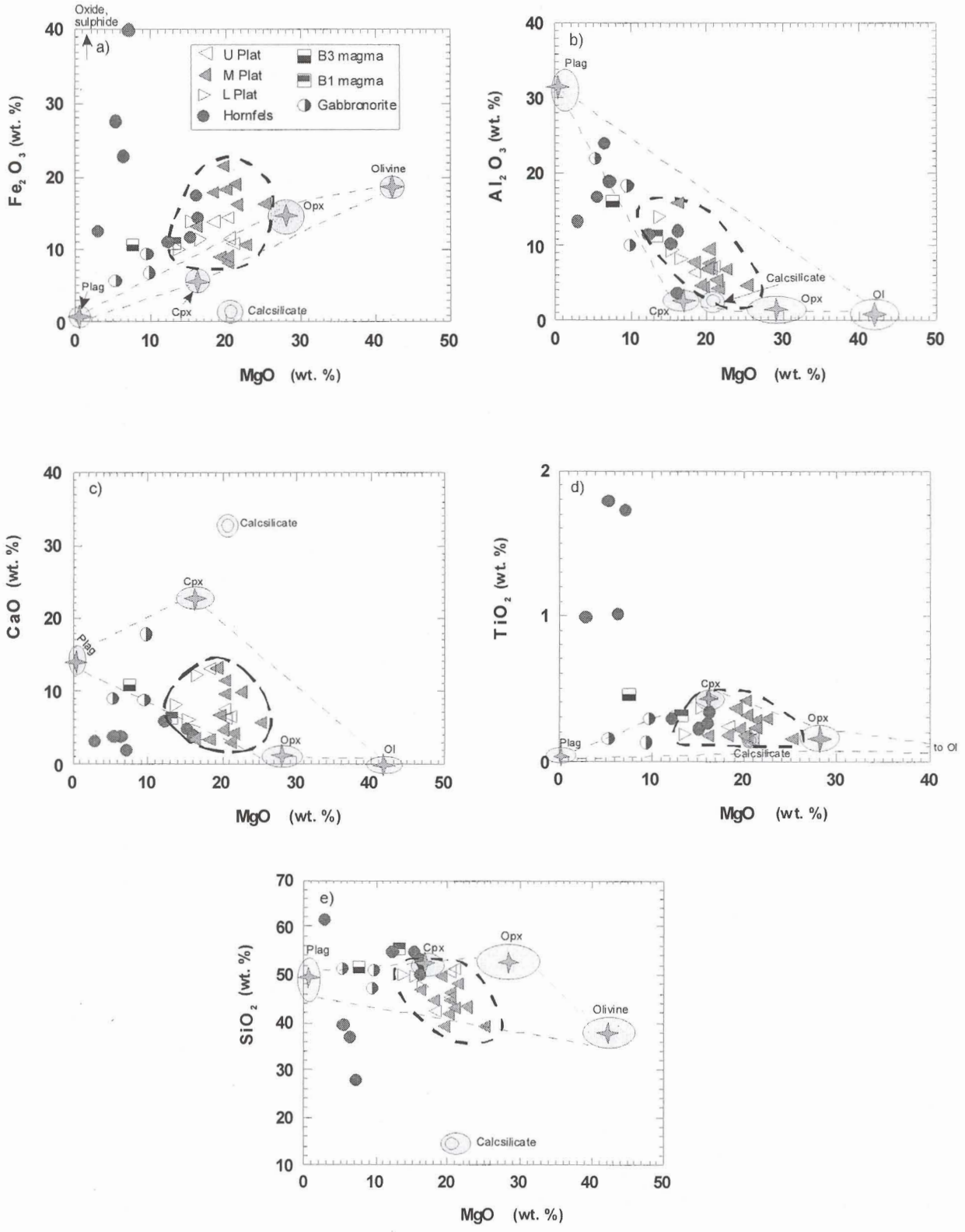

Fig. 6.1: a) Fe_2O_3, b) Al_2O_3, c) CaO, d) TiO_2 and d) SiO_2 versus MgO. Also plotted are B1 and B3 Bushveld parental magmas (Curl, 2001) and averaged microprobe mineral compositions for the Platreef. U Plat = upper Platreef, M Plat = middle Platreef, L Plat = lower Platreef. Stippled lines represent Platreef field.

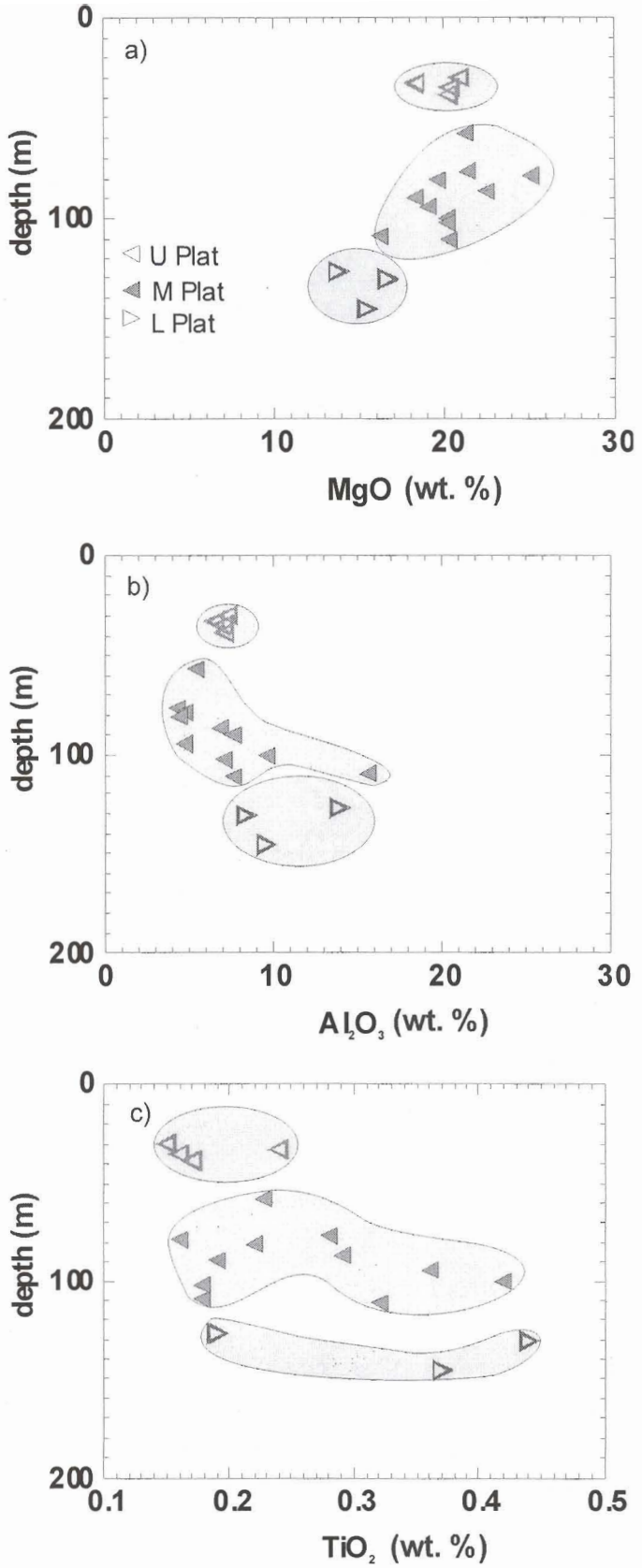

Fig. 6.2: Variation of a) MgO, b) Al_2O_3 and c) TiO_2 with depth. U Plat = Upper Platreef, M Plat = Middle Platreef and L Plat = Lower Platreef.

6.3 Trace Element Chemistry

Compositional ranges of the individual trace elements in the different Platreef layers are presented in Table 6.2 and plotted in Fig. 6.3.

Element	Lower Platreef	Middle Platreef	Upper Platreef	Pegmatoidal feldspathic pyroxenite	Merensky Reef (UCZ pyroxenite)
Sr	276-407	58-232	103-214	149-226	30-90
Rb	17-34	7-23	12-26	19-26	6-9
Zr	36-75	24-58	19-35	33-66	2-25
Y	13-19	7-22	6-13	8-11	0-15
Nb	3-4	2-5	2-3	2-5	<2
Zn	81-86	62-125	81-109	115-143	60-160
Cu	46-3519	17-3510	131-2463	2132-8239	700-800
Ni	336-1988	58-14072	572-3451	2188-7285	2300-3100
Co	66-112	45-292	87-124	123-305	106-143
Cr	683-2408	57-1560	251-3029	427-2063	6979-7390
V	69-132	66-119	78-112	59-66	60-100
Sc	13-21	5-19	12-21	8-17	24-31
Ga	12-14	7-13	8-9	9-17	
Pb	11-36	3-37	6-46	10-27	
Cl	257-585	413-1224	35	356-878	
F	1411-3727	1303-7130	905-2531	1174-6037	
S	16-11821	16-47608	554-13739	8796-37522	4000-5100

Table 6.2: Trace element distribution in the different Platreef layers compared to that from the Merensky Reef (Barnes and Maier, 2002)

It is evident that relative to the Merensky Reef, the Platreef has high contents of Sr, Rb, Zr, Y, Nb, V as well as Cu and Ni but low contents of Cr, Sc and Zn. The elevated Sr contents cannot be explained by a relatively high modal abundance of plagioclase, as the Platreef has approximately the same plagioclase content as the Merensky Reef

(Fig. 6.4). Thus, the relatively elevated concentration of the incompatible trace elements and Sr points either to a relatively larger proportion of trapped melt, or an enhanced component of crust.

The first proposition cannot explain the observed trace element variation. Bushveld B1 magma has 10 ppm Y, 66 ppm Zr and 29 ppm Rb (Curl, 2001). The Platreef rocks would require between 20 and 100 % trapped melt to satisfy the mass balance which seems unrealistic. Further, Y/Zr ratios of Platreef rocks are markedly higher than those in B1 Bushveld magma (Fig. 6.4a). This implies that the Platreef rocks contain a significantly larger component of crust than the B1 magma.

Plots of Cu versus Zr and Cu versus Y (Fig. 6.4b and c, respectively) do not show correlations among these trace elements. Zr, Cu and Y are highly incompatible elements in the absence of sulphides and should progressively increase in concentration with differentiation to show a positive correlation among themselves. The lack of correlation between Zr and Y with Cu and the high supracrustal Cu/Zr and Cu/Y ratios (up to 128.4 Cu/Zr and 757 Cu/Y) point to the presence of exsolved sulphides.

This model is supported by the S contents of the rocks in cases. Sulphur contents of the Platreef rocks range from 0.0016 to 4.76 % indicating ca. 0.004 to 13.5 % sulphide. Many basaltic magmas and the Bushveld B1 magma have ca. 1000 ppm S (~0.25 % sulphide) (Barnes and Maier, 2002). In the case of S-undersaturation during crystallisation, the Platreef cumulate would be expected to contain about 0.025 %

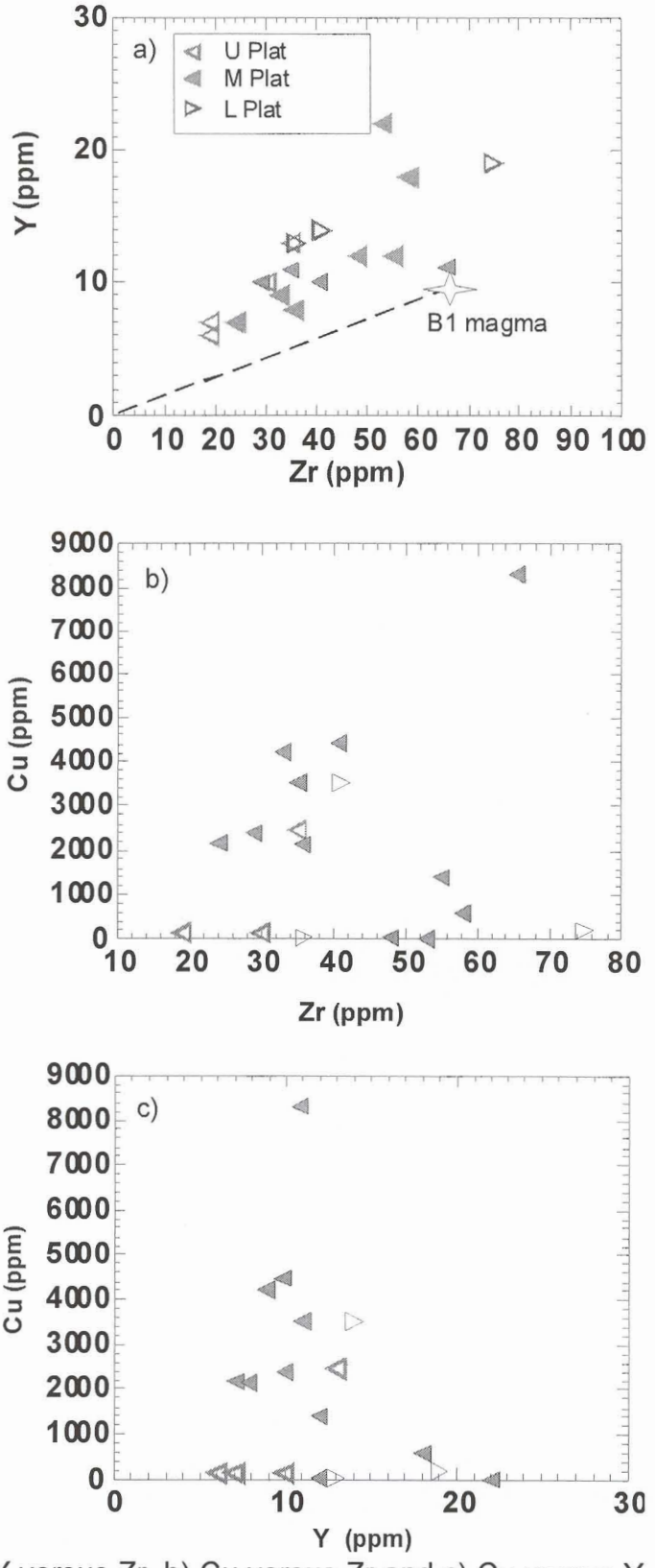

Fig. 6.3: Plot of a) Y versus Zr, b) Cu versus Zr and c) Cu versus Y. U Plat = Upper Platreef, M Plat = Middle Platreef and L Plat = Lower Platreef. Stippled line represents back projection of B1 Bushveld parental magma (Curl, 2001).

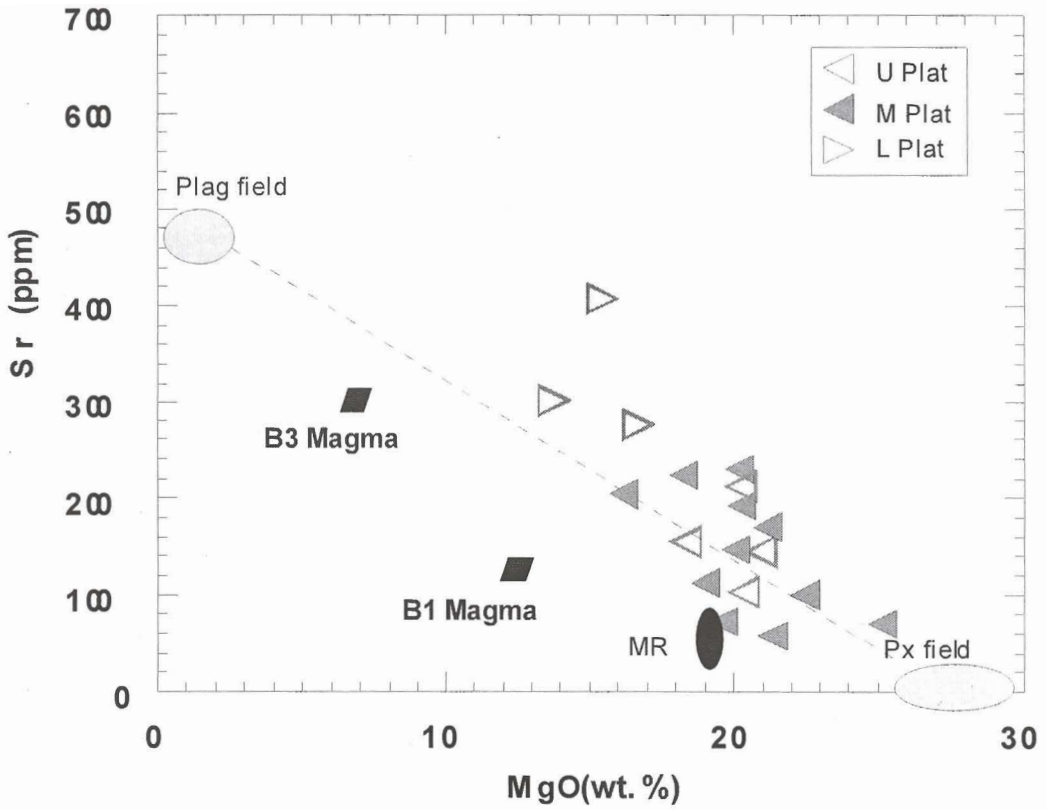

Fig. 6.4: Variation diagram of Sr versus MgO. U Plat = Upper Platreef, M Plat = Middle Platreef and L Plat = Lower Platreef, MR = Merensky Reef.

sulphide (100 ppm S), assuming 10 % trapped melt. If the magma was S-saturated, one could expect on the order of 1000 ppm S in the rocks. When S is plotted against height (Fig. 6.5d), it is clear that most of the rocks of the Platreef have S contents above 1000 ppm suggesting that the rocks contain a large amount of exsolved sulphides.

The bulk of the Ni content of the rocks is also controlled by sulphides. Ni concentrations range from 58 to 14072 ppm. The sample with the highest Ni concentration is from the Middle Platreef, where the average Ni concentration is 3650 ppm. Pegmatoidal feldspathic pyroxenite has the highest average Ni concentration of 5247 ppm. These Ni contents are far higher than those of pyroxenites and norites from the UG 2 - Merensky Reef interval of the western Bushveld Complex (Maier and Eales, 1997). The Lower and Upper Platreefs have average Ni concentrations of 1542 and 916 ppm, respectively, indicating much lower sulphide contents and/or lower metal tenors of the sulphides.

Cr shows a general increase in concentration towards the top of the Platreef, suggesting that the upper Platreef layers are relatively more primitive, as was suggested by the mineral chemistry data (Figure 5.3a).

When trace element data are plotted versus height, it is evident that the concentrations of the incompatible elements Y and Zr decrease with height (Figs. 6.5e and f respectively). This could suggest that the lowermost rocks (i.e. the Lower

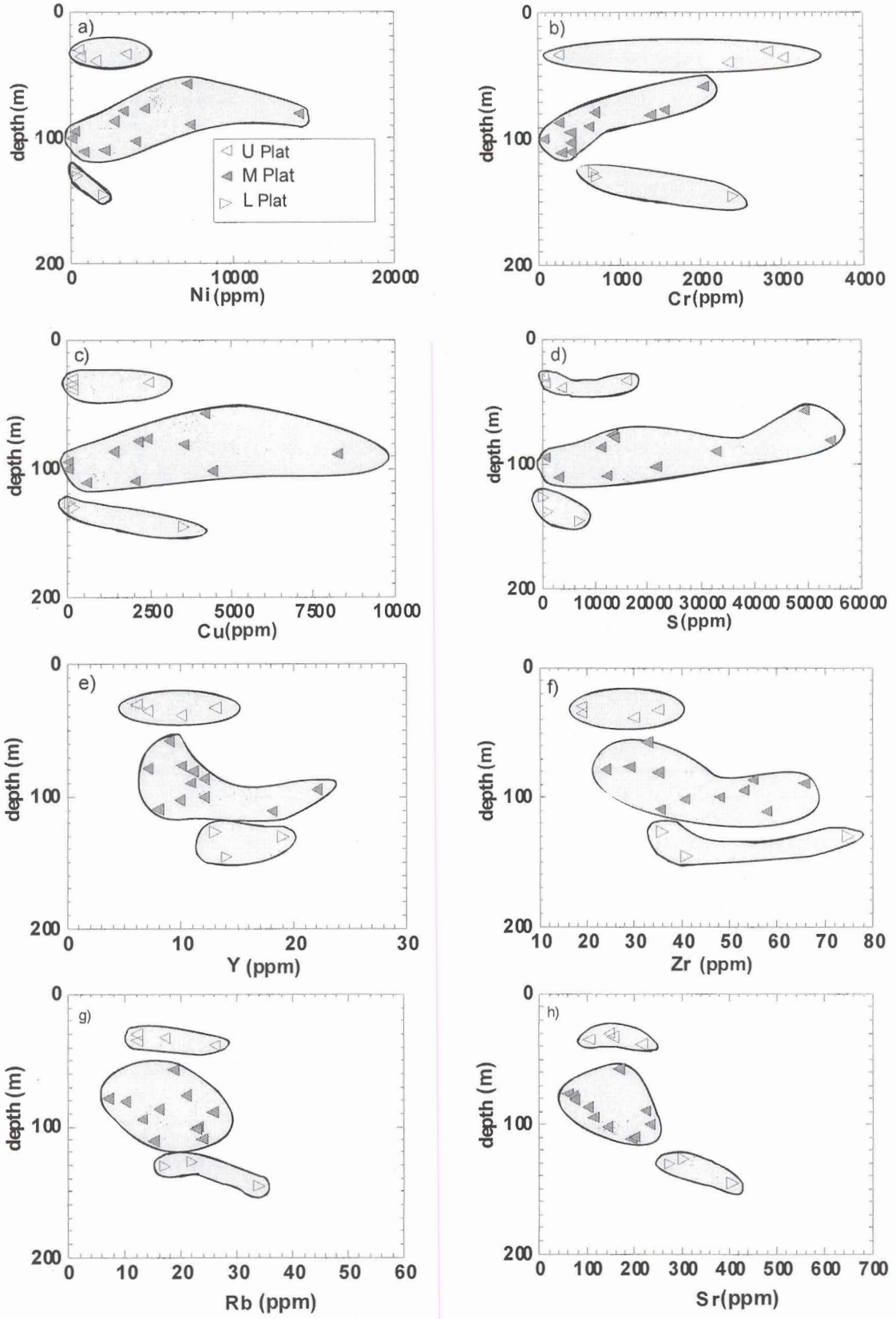

Fig. 6.5: Trace element variation with depth for the Platreef lithologies. U Plat = Upper Platreef, M Plat = Middle Platreef and L Plat = Lower Platreef.

Platreef) have assimilated more crust or that they contain a larger proportion of trapped melt.

6.4 Platinum-group elements

The noble metal concentrations are normalised to primitive mantle and plotted in order of decreasing melting temperature in Fig 6.6. Noble metal concentrations of the Merensky Reef, B1 and B3-type Bushveld parental magmas are shown for comparison. Ni is included in the plots to the left of Os, and Cu (as well as Au) to the right of Pd due to their broadly similar behaviour to Os and Pd, respectively, during fractionation. In general, the three Platreef layers on farm Townlands show a broadly similar noble metal pattern, with variation only seen in the metal contents. They are all PGE enriched when compared to the B1 and B3 parental magmas of the Bushveld Complex. The Middle Platreef and the associated pegmatoidal feldspathic pyroxenite, have the highest PGE contents followed by the Upper Platreef, with the Lower Platreef having the lowest PGE contents. The PGE content of the Middle Platreef is economic while those of the Lower Platreef and Upper Platreef are presently uneconomic and close to 'background'. The patterns are characterised by a broadly flat pattern from Ni to Ir, a progressive increase from Ir to Pd followed by a decrease from Pd to Cu. This is in marked contrast to the Merensky Reef pattern which shows an arch-shaped mantle-normalised pattern, reflecting a strong enrichment of all PGE relative to Ni and Cu. The lack of a strong PGE enrichment over Ni and Cu in most of the Platreef, may suggest that the sulphides segregated at a relatively low R factor (ratio of silicate melt to sulphide melt).

The metals are plotted versus stratigraphic height in Fig. 6.7. It is evident that the three platiniferous layers have different PGE concentrations. The Middle Platreef has

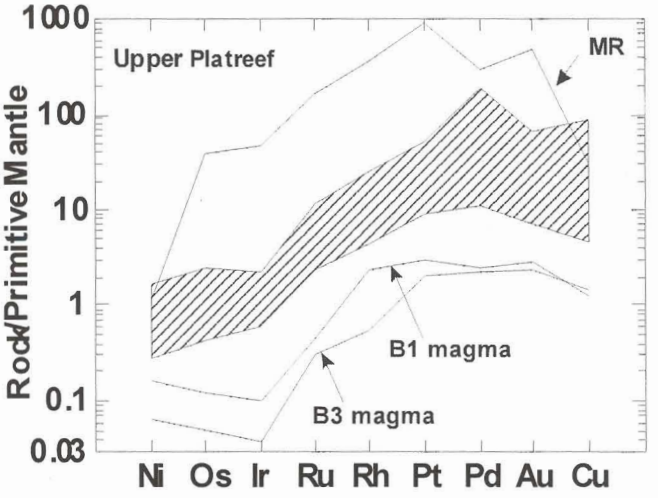

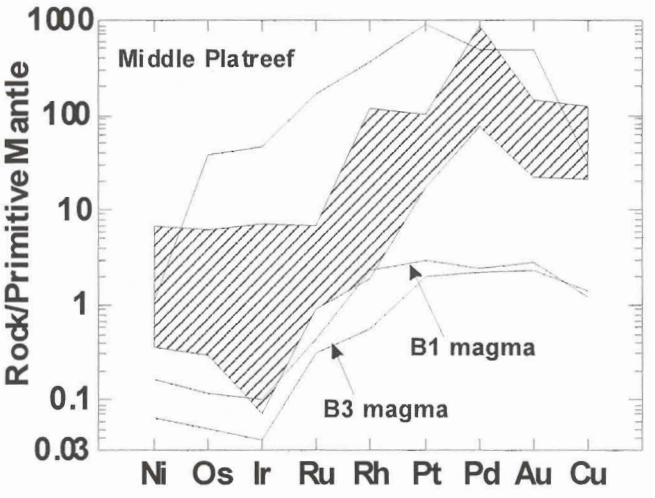

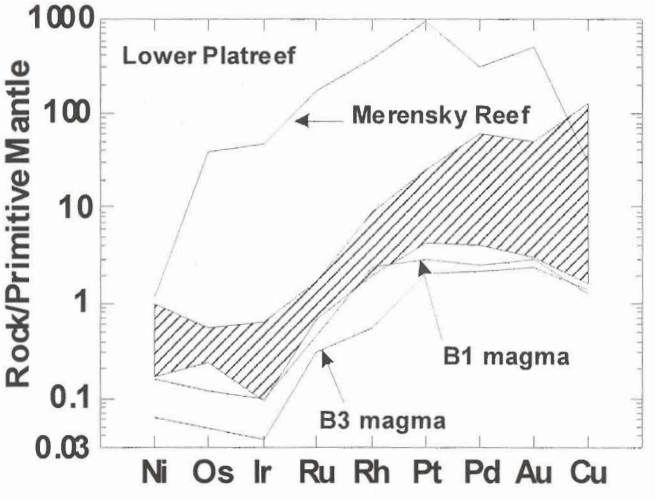

Fig. 6.6: Mantle-normalised PGE spider diagrams for rocks from the Platreef on the farm Townlands. Included are PGE concentrations for the B1 and B3 Bushveld parental magmas (Curl, 2001) and the Merensky Reef (Barnes and Maier, 2002). (Normalisation factors are from Barnes and Maier 1999).

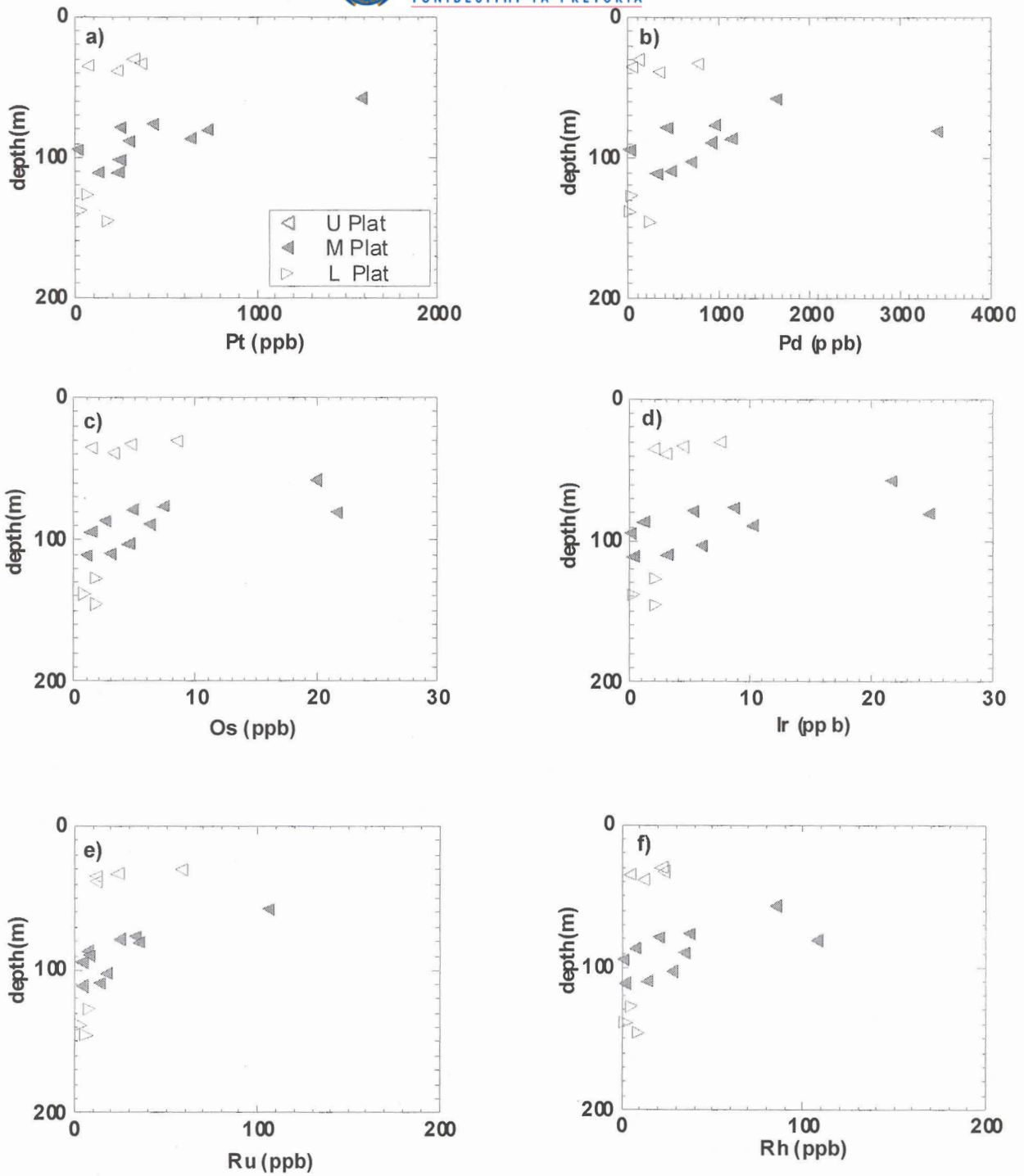

Fig. 6.7: Concentration of PGE plotted versus stratigraphic height. U Plat = Upper Platreef, M Plat = Middle Platreef and L Plat = Lower Platreef. MR = Merensky Reef.

the highest PGE concentrations, with the Lower Platreef having the lowest PGE concentrations. Pd/Ir and Pt/Pd ratios are plotted versus height in Fig. 6.8. It is evident that in each platiniferous layer, there is a trend of decreasing Pd/Ir ratio with height (Fig. 6.8a). The fact that Pd/Ir ratios change with height may suggest that Pd and Ir have different D values with respect to sulphide melt. Most authors found that PGE have broadly similar D values with respect to sulphide melt although the experimental data are understandably scattered (Barnes and Maier, 1999) and some authors (e.g. Bezmen et al., 1994) found considerable difference between D values. The change of the ratio may also suggest that other phases besides sulphides exerts some control on the PGE contents in the rocks (e.g. silicates, oxides, PGM or hydrothermal fluids). No clear trends are observed in the plot of Pt/Pd versus height (Fig. 6.8b).

To assess the nature of the phases controlling the PGE, the PGE are plotted against each other in Fig. 6.9. Pt shows a fairly good positive correlation with Pd and Ir, and Pd shows a good correlation with Ir, suggesting the PGE are essentially controlled by the same phase. The few outliers may be due to later remobilization of PGE. Pd and Pt (not shown) do not display a good correlation with Cu (Fig. 6.9f) suggesting remobilization of Cu, possibly due to hydrothermal processes.

Pt, Pd, Ir, Ru, Rh and Os show fairly good positive correlations with S (Fig. 6.10a-f, respectively). This suggests that sulphide was the primary metal collector. This is contrary to the situation at Sandsloot where Armitage et al. (2002) report that the PGE are mostly not hosted by sulphides, but by platinum-group minerals (PGM) that are enriched in low-temperature metals and semi-metals. They interpreted this to be a

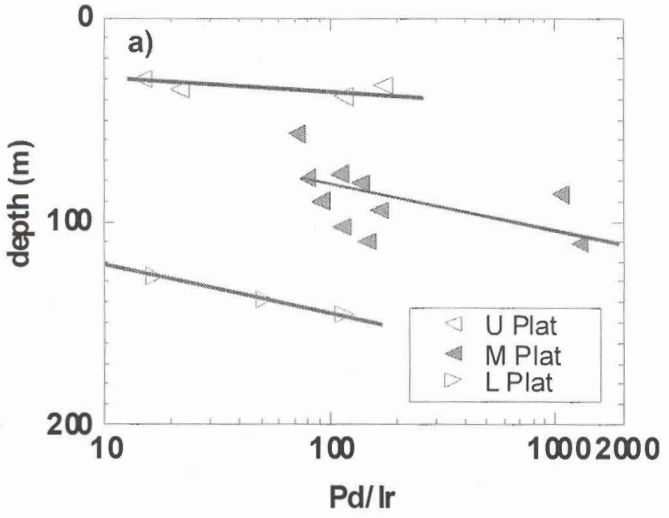

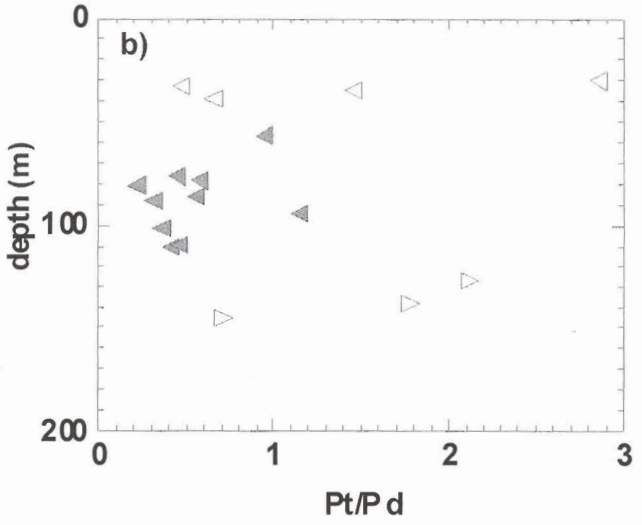

Fig. 6.8. Plots of a) Pt/Ir and b) Pd/Pd versus depth. Note that the Pd/Ir axis in 6.8(a) is in log-linear scale. U Plat = Upper Platreef, M Plat = Middle Platreef and L Plat = Lower Platreef. MR = Merensky Reef.

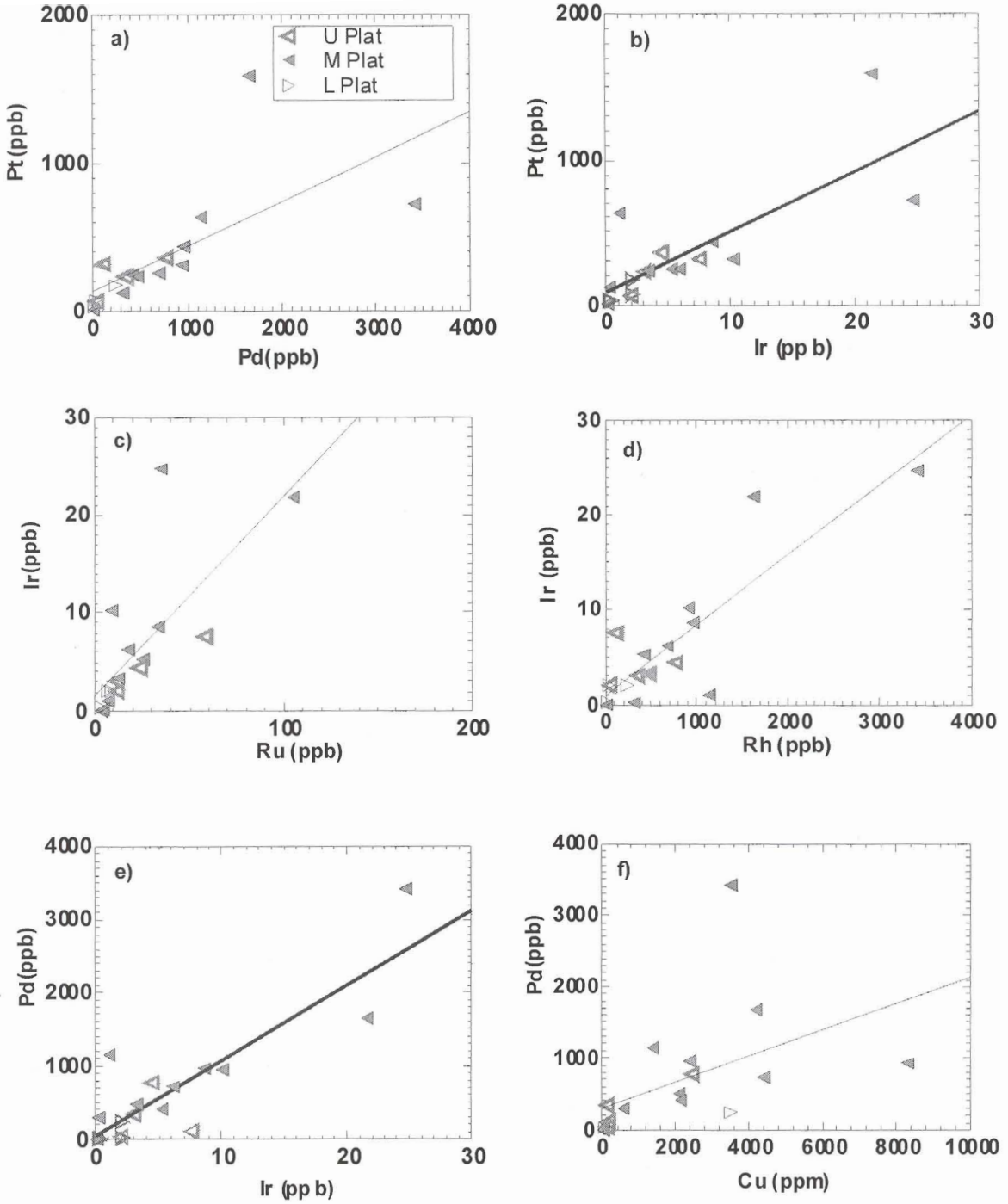

Fig. 6.9: PGE binary plots of the Platreef on the farm Townlands. U Plat = Upper Platreef, M Plat = Middle Platreef and L Plat = Lower Platreef. MR = Merensky Reef.

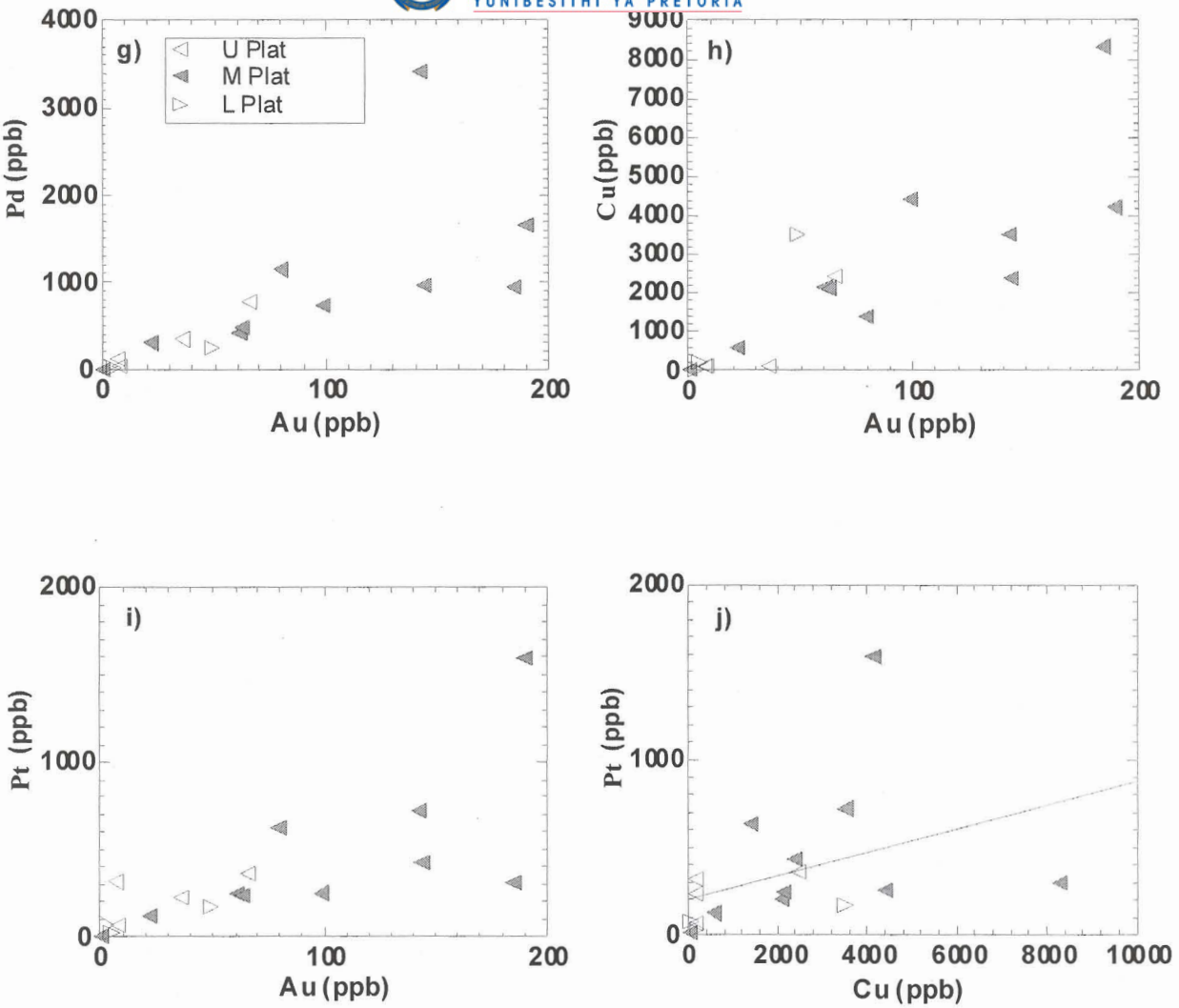

Fig. 6.9: (contd): PGE variation diagrams of the Platreef on the farm Townlands. U Plat = Upper Platreef, M Plat = Middle Platreef and L Plat = Lower Platreef. MR = Merensky Reef.

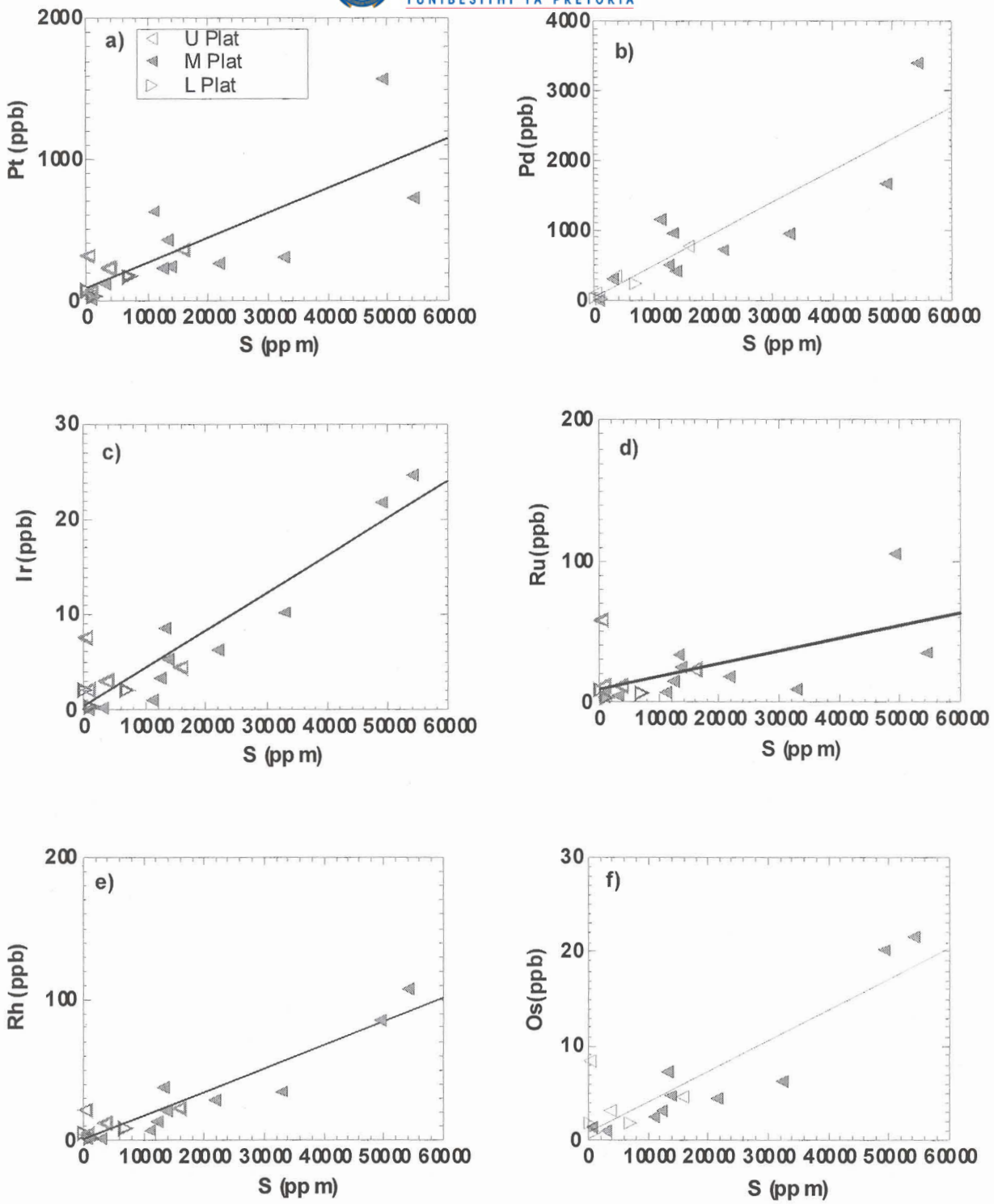

Fig. 6.10. Plots of PGE versus S with regression lines plotted. U Plat = Upper Platreef, M Plat = Middle Platreef and L Plat = Lower Platreef. MR = Merensky Reef.

Platreef rocks, ii) ^{18}O depletion in calcsilicate rocks within and just above the Platreef, which may have occurred during interaction with fluids, iii) the occurrence of sulphide mineralisation in the parapyroxenite suggesting the sulphides were at least in part, transported by fluids.

CHAPTER SEVEN: S-ISOTOPE GEOCHEMISTRY

Most magmatic sulphide ore (e.g. at Kambalda, Voisey's Bay, Noril'sk, Petchenga) are thought to have formed by assimilation of external S from the country rocks. A similar model has been proposed by Buchanan et al. (1981) for the Platreef on the farm Tweefontein. S-isotopic analyses may be used as tracers to detect the contamination. The mantle is taken to have a $\delta^{34}S$ value of ~0 ± 3 ‰ and any substantial deviation from these values is interpreted to be due to assimilation of country rock sulphur with $\delta^{34}S$ values that differ from the mantle values (Ripley, 1999).

Buchanan et al. (1981) carried out S-isotopic analyses on 9 samples of the Platreef on the farm Tweefontein, where the floor rocks are formed by calcsilicate, banded ironstone and argillaceous sediments. In the present study, I provide new S-isotopic data on 12 samples, covering the three Platreef layers and the floor rocks on the farm Townlands. This was done to i) make a comparison of the S-isotopic composition of the Platreef along strike ii) determine the role of crustal contamination in the formation of the Platreef, and iii) determine whether the different platiniferous layers of the Platreef underwent different degrees of contamination.

The samples were analysed at Indiana University, Bloomington, U.S.A. Analytical results are presented in Table 7.1 and analytical procedures are given in Appendix I. Sulphur isotopic compositions are reported in standard δ notation relative to VCDT (Vienna Cañon Diablo Troilite).

Sample	$\delta^{34}S$ ($^{0}/_{00}$VCDT)	Rock unit
P2	5.7	Upper Platreef
P3	10.1	Upper Platreef
P6	6.0	norite sill
P11	2.6	Middle Platreef
P15	5.3	Middle Platreef
P19	4.0	Middle Platreef
P25	7.3	Lower Platreef
P26	9.3	Lower Platreef
P28	16.9	hornfels
P30	14.2	calcsilicate
P31	15.2	hornfels
P32	15.3	hornfels

Table 7.1: S-isotopic analyses of samples from the Platreef and its floor rocks.

It is notable that all the samples have positive $\delta^{34}S$ values. The highest values are found in the hornfels and the calcsilicate, which have broadly similar S-isotopic signatures. The $\delta^{34}S$ signature of the Platreef is compared to other mafic/ultramafic intrusions around the world in Fig. 7.1. The Uitloop, Cape Smith, Kabanga, Mellon, Noril'sk and Muskox intrusions all contain a large contribution of sedimentary sulphide due to assimilation of country rock. It is also important to note that the Lower Platreef and the Upper Platreef have higher $\delta^{34}S$ (average 8 ‰) compared to the Middle Platreef (average 4 ‰), confirming the whole rock chemical data that showed high K_2O and CaO contents in the Lower and Upper Platreef which could not be explained by variation in pyroxene and plagioclase contents.

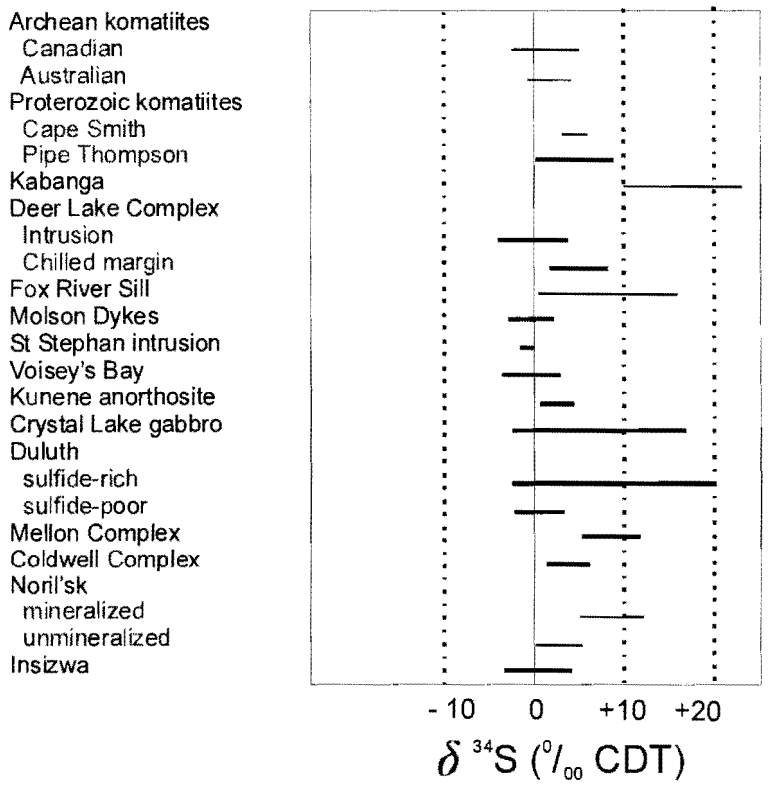

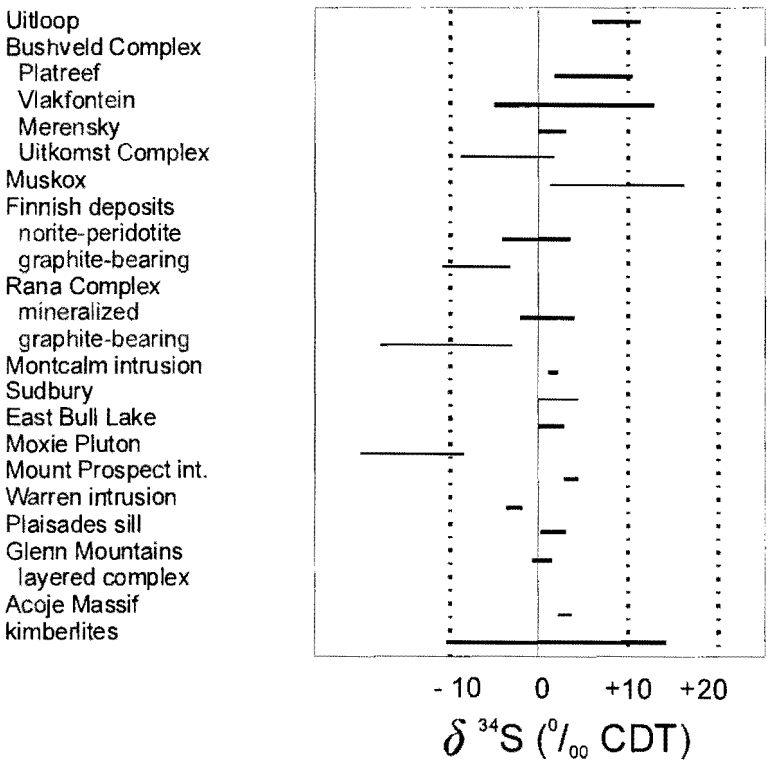

Fig. 7.1: $\delta^{34}S$ values of selected mafic/ultramafic intrusions in the world (modified from Ripley, 1999). Kabanga data from Maier (unpublished), and Uitloop data from Touvila, (personal communication).

Buchanan et al. (1981) reported $\delta^{34}S$ values of 6.3 to 9.2 per mil from the Platreef on the farm Tweefontein. These are comparable to the $\delta^{34}S$ isotopic signatures for the Platreef on the farm Townlands, suggesting the sulphides could have formed by assimilation of the same contaminant. Pyroxenite sills some 1 km in the floor rocks below the Platreef, and hosted by dolomite, also show a strong positive $\delta^{34}S$ isotopic signatures (Tuovila, personal communication).

In addition to variation between the different Platreef layers on Townlands, the data also suggest some systematic variation within the individual Platreef layers. There is a trend of an increase in the $\delta^{34}S$ values towards the base within the Middle and Lower Platreef, a phenomenon that can possibly be explained by enhanced assimilation of crustal sulphur towards the floor of each intrusion, perhaps by means of continued degassing of the floor rocks during crystallisation of the Platreef.

The high $\delta^{34}S$ values of the analysed hornfels are of note. Buchanan et al. (1981) report $\delta^{34}S$ values of -11.6 to +7.8 per mil for the Pretoria shales, and Cameron (1982) reports mostly significantly negative $\delta^{34}S$ values for the Transvaal metasediments south of Johannesburg. This could indicate significant localized variation in the S isotopic signatures of the Transvaal Supergroup, or it may reflect a change in the S-isotopic signature of the shales in the Northern limb due to the intrusion of the Platreef and associated devolatisation (notably loss of light S). Further work is clearly necessary to constrain this question. The analyses of calcsilicate interpreted to represent interlayers in the Pretoria Supergroup gave a $\delta^{34}S$ value of 14.2 per mil which is heavier than the Malmani dolomite analysed by Buchanan et al.,

1981, which has a $\delta^{34}S$ value of 7.1 per mil. The hornfels and calcsilicates of the Silverton formation probably formed in shallow water depths of between 30 and 100 m (Eriksson and Reczko, 1998) i.e. in slightly oxidizing conditions that could explain the elevated $\delta^{34}S$ values. Alternatively, the heavy S-isotopic signature may be the result of devolatisation of light S.

In summary, the S-isotopic data support a model whereby shale and dolomite were engulfed by the intruding Platreef magma and the xenoliths reacted with the hot magma releasing the contained sulphur. The released crustal sulphur caused S-supersaturation in the magma and segregation of an immiscible sulphide melt enriched in heavy S. This suggests that sulphidation is an important factor controlling sulphide precipitation in the Platreef on the farm Townlands and elsewhere.

Importantly, the data support the mineral and whole rock major and trace element chemical data indicating that the different layers of the Platreef may represent distinct magma injections, intruding as sill-like bodies.

CHAPTER EIGHT: DISCUSSION AND CONCLUSIONS

8.1. Nomenclature

The Platreef has in the past been subdivided into three reefs based on texture and composition (Buchanan, 1979; White, 1994). However, the classification was mainly based on the high grade portions of the Platreef notably at Sandsloot, where the floor rocks consist of calcsilicate. On the farm Townlands, the three distinct reef lithologies as defined at Sandsloot are not evident. Instead, there are three packages of medium-grained feldspathic pyroxenite/gabbronorite separated by interlayers of ferruginous hornfels. If the modal and textural classification applied at Sandsloot is to be followed, it follows that on the farm Townlands, the A and the C-reefs are not developed. It is possible that at Sandsloot, the A-reef is developed because of intense interaction between the intrusive rocks and calcsilicates of the floor rocks, as indicated by the development of 'parapyroxenite'. For the above reason, I refer to the three pyroxenite/gabbronorite units separated by hornfels interlayers on the farm Townlands as the Lower, Middle and Upper Platreef layers.

8.2. Major and Trace element data

The mineral- and whole rock data including the S-isotopic data, show distinct compositional breaks between the different Platreef layers. This suggests that the Platreef layers are separated by hornfels interlayers rather than xenoliths, and that the intrusives represent distinct sill-like bodies rather than a single body. The

interpretation is supported by the distinct S-isotopic signatures of the three Platreef layers.

The present data also reveal a reversed differentiation trend within the Platreef, with progressively more primitive layers being found towards the top. Orthopyroxene shows a broad increase in Cr_2O_3 with height, and a decrease in TiO_2. Clinopyroxene shows an analogous trend of Cr enrichment with height. Olivine from the Upper Platreef has Fo contents between 80-83 (averaging Fo_{81}) and those from the Middle Platreef have Fo from 78-83 (averaging Fo_{79}) confirming the pattern of more primitive rock composition with height established by the pyroxene compositions. Whole rock data also shows a broad increase with height in MgO, and decreases in TiO_2 and Al_2O_3, while incompatible element concentrations (e.g. Zr and Y) increase towards the base. Based on comparison to other intrusions where the basal rocks are relatively evolved and have elevated concentrations of incompatible trace elements (e.g. Muskox, Barnes and Francis, 1995), this may suggest enhanced contamination of the initial magma influxes. If this is indeed the case, it would indicate that the order of intrusion of the distinct Platreef sills was Lower Platreef, then Middle Platreef and lastly Upper Platreef. The reversed differentiation trend may also suggest the sequence is overturned, but this is not likely as there is no evidence of deformation on the farm Townlands.

8.3 Contamination

S-isotope data from the Platreef on the farm Townlands shows a strong crustal signature. The high $\delta^{34}S$ values indicate addition of ^{34}S-enriched crustal sulphur. This

suggests that the Platreef has assimilated country rock material which is thought to be important in the formation of magmatic sulphides (e.g. Gain and Mostert, 1982; Buchanan and Rouse, 1984; Barton et al. 1986; Buchanan, 1988). The possible source of the crustal sulphur is the hornfels and calcsilicate of the Silverton Formation that forms the floor rocks to the Platreef on the farm Townlands. Contamination of the magma by country rocks is supported by elevated Zr/Y ratio relative to B1 Bushveld magma and by high K and Ca contents of the rocks relative to other Critical Zone rocks elsewhere.

I envisage that during emplacement of the Platreef magma, hornfels and calcsilicate were engulfed and these reacted with the hot magma releasing heavy sulphur as well as other incompatible elements. The released heavy sulphur would cause S-supersaturation in the magma and segregation of an immiscible sulphide melt enriched in heavy S.

8.4 Platinum-Group Elements

The present study has established good positive correlation between the individual PGE, and between the PGE and S, suggesting that the PGE are largely controlled by sulphides. This result may have important implications for the origin of the PGE mineralisation at Sandsloot, where sulphide ores are less common and the PGE appear to be largely controlled by PGM (Armitage et al., 2002). Although at this stage, it is not yet known in which mineralogical form the PGE are present in the Townlands core, I suggest that the mineralisation at both localities (Townlands and Sandsloot) originally formed in a similar manner (sulphide segregation in response to assimilation

of external S), but that at Sandsloot, some of the S was lost due to interaction of the magma/rock with the floor rocks.

8.5 Sulphur Saturation and Magma Emplacement

The composition of olivine and the noble metal concentrations play a critical role in constraining the stage at which initial sulphide segregation took place and of what significance local crustal assimilation/contamination was to the ore forming process. The olivine from the Platreef is undepleted in Ni relative to Fo. Olivine from other sulphide-bearing ultramafic and mafic rocks elsewhere are commonly depleted in Ni relative to Fo (e.g. Voisey's Bay, Li and Naldrett, 1999). The Ni depletion is explained by scavenging of Ni from the magma by the sulphides prior to olivine crystallisation. Platreef sulphides are also relatively metal-rich when compared to many magmatic sulphide ores. The equilibration of Ni-rich olivines and metal-rich sulphides in the Platreef essentially implies that R-factors (mass ratio of silicate magma to sulphide melt) were very large. This is incompatible with the estimated silicate-sulphide ratio for the Platreef (1000 - 5000) and suggests that sulphides were entrained from elsewhere. The large proportion of ferromagnesian phases in the Platreef indicates that the rocks were deposited from a phenocryst-rich crystal mush, which would facilitate sulphide entrainment. This is in accord with the abundance of calcsilicate xenoliths in the present Platreef intersection, bearing in mind that calcsilicate is rare in the floor rocks at this locality.

ACKNOWLEDGEMETS

I would like to thank first and foremost my supervisors Prof. W.D. Maier and Prof. S.A. de Waal for guiding me through the research and for all the informative discussions. I thank P. Sibiya and M. Claassen (University of Pretoria) for thin section preparation, S. Bramdeo (Rhodes University) for her help during microprobe analysis and M. Loubscher (University of Pretoria) for assistance with XRF analysis. E.M. Ripley is greatly acknowledged for performing S-isotope analysis and Patrice Gingras for the PGE analyses.

This research was supported financially by the Centre for Research on Magmatic Ore Deposits (University of Pretoria). The PGE analyses were funded by a grant from the Ernest Oppenheimer Memorial Trust. Falconbridge Ventures of Africa and Thabex Exploration Company are thanked for providing the core material

I shall always be grateful and deeply indebted to my parents and the rest of the family, your strength and willpower was something I could always rely on. To my girlfriend Trish, thank you for bearing with me, on my every beg and call, thank you for having been there when I had no one to turn to and giving me moral strength and support to go through each day.

However my greatest strength lies in the Lord, who has faithfully been with me throughout the project. Thank you Lord for the gift of life you have bestowed upon me.

References

Armitage, P.E.B., McDonald, I., Edwards, J.S. and Manby, G.M. (2002). Platinum-group element mineralisation in the Platreef and calc-silicate footwall at Sandsloot, Potgietersrus District, South Africa. *Transactions of the Institute of Mining and Metallurgy* **111** (reprinted from Applied earth science, January-April 2002), B36-45.

Arndt, N.T., Czamanske, G.K., Walker, R.J., Chavel, C. and Fedorenko, V.A. (2003). Geochemistry and origin of the intrusive hosts of the Noril'sk-Talnakh Cu-Ni-PGE sulphide deposits. *Economic Geology* **98**. 495-515.

Barnes, S.-J. and Maier, W.D. (1999). Geological Association of Canada. *Short Course Notes* **13**, 69-106.

Barnes, S.-J. and Maier, W.D. (2002). Platinum-group Elements and Microstructures of Normal Merensky Reef from Impala Platinum Mines, Bushveld Complex. *Journal of Petrology* **43**, 103-128.

Barnes, S.-J. and Francis, D. (1995). The distribution of platinum-group elements, nickel, copper, and gold in the Muskox Layered Intrusion, northwest territories, Canada. *Economic Geology* **90**, 135-154.

Barton, J.M., Cawthorn, R.G. and White, J. (1986). The role of contamination in the evolution of the Platreef of the Bushveld Complex. *Economic Geology* **81**, 1096-1104.

Bennett, H. and Oliver, G. (1992). *XRF analysis of Ceramics, Minerals and Applied Materials*. John Wiley and Sons, 67-93.

Bezmen, N.S., Asif, M., Brugmann, G.E., Romanekno, I.M., and Naldrett, A.J., 1994. Experimental determinations of sulfide-silicate partitioning of PGE and Au. *Geochimica et Cosmochim Acta* **58**, 1251-1260.

Boudreau, A.E., Mathez, E.A. and McCallum, I. (1986). Halogen geochemistry of the Stillwater and Bushveld Complexes: Evidence for transport of the platinum-group elements by Cl-rich fluids. *Journal of Petrology* **27**, 967-986.

Buchanan, D.L. (1979). *Bureau for Mineral studies*: Report, *University of the Witwatersrand*, **4**.

Buchanan, D.L. (1988). *Platinum-group element exploration*. Elsevier: Amsterdam, 185p.

Buchanan, D.L. and Nolan, J. (1979). Solubility of sulphur and sulphide immiscibility in synthetic melts and their relevance to Bushveld-Complex rocks. *Canadian Mineralogist* **17**, 483-494.

Buchanan, D.L., Nolan, J., Suddaby., Rouse, M.J. and Davenport, J.W.J. (1981). The genesis of sulphide mineralisation in a portion of the Potgietersrus limb of the Bushveld Complex. *Economic Geology* **76**, 568-579.

Buchanan, D.L. and Rouse, J.E. (1984). Role of contamination in the precipitation of sulphides in the Platreef of the Bushveld Complex. *In*: Buchanan, D.L. and Jones M.J (editors) *Sulphide deposits in mafic and ultramafic rocks. Institute of Mining and Metallurgy, London*, 141-146.

Buick, I.S., Maas, R. and Gibson, R. (2001). Precise U-Pb titanite age constraints on the emplacement of the Bushveld Complex, South Africa. *Journal of the Geological Society* ***158****, London*, 3-6.

Cameron, E.N. (1980). Evolution of the Lower Critical Zone, central sector, Eastern Bushveld Complex and its economic deposits. *Economic Geology* **75**, 845-871.

Cameron, E.N. (1982). The Upper Critical Zone of the Eastern Bushveld Complex – Precursor of the Merensky Reef. *Economic Geology* **77**, 1307-1327.

Cameron, E.N. (1982). Sulphate and sulphate reduction in early Precambrian oceans. *Nature* **296**, 145-148.

Cawthorn, R.G. (2002). Magma mixing models for the Merensky-style mineralisation: the fallacy of binary diagrams: *Economic Geology* (submitted).

Cawthorn, R.G., Bartorn, J.M., Jr. and Viljoen, M.J. (1985). Interaction of floor rocks with the Platreef on Overysel, Potgietersrus, northern Transvaal: *Economic Geology* **80**, 988-1006.

Cawthorn, R.G., Lee, C.A., Schouwstra, R.P. and Mellowship, P. (2002). Relationship between PGE and PGM in the Bushveld Complex. *The Canadian Mineralogist* **40**, 311-328.

Cawthorn, R.G. and Webb, S.J. (2001). Connectivity between the western and eastern limbs of the Bushveld Complex. *Tectonophysics* **330,** Elsevier, 195-209.

Cheney, E.S. and Twist, D. (1992). The conformable emplacement of the Bushveld mafic rocks along a regional unconformity in the Transvaal succession of South Africa. *Precambrian Research* **52**, 115-132.

Coertze, F.J. (1974). The geology of the basic portion of the Western Bushveld Igneous Complex. *Geological Society of South Africa Memoir* **66**.

Cousins, C.A. (1959). The structure of the mafic portion of the Bushveld Igneous Complex. *Transactions of the Geological Society of South Africa* **62**, 174-189.

Cousins, C.A. and Feringa, G. (1964). The chromite deposits of the western belt of the Bushveld Complex. *In*: Haughton, S.H (editor) *The glossary of some ore deposits in Southern Africa* **2**, *Geological Society of South Africa*, 183-202.

Curl, E.A. (2001). *Parental magmas of the Bushveld Complex, South Africa*. PhD. thesis (unpublished), Department of Earth Sciences, Monash University, Australia, 140p.

de Waal, S.A. (1977). Carbon dioxide and water from metamorphic reactions as agents for sulphide and spinel precipitation in mafic magmas. *Transactions of the Geological Society of South Africa* **80**, 193-196.

Deer, W.A., Howie, R.A. and Zussman, J. (1978). *Rock-forming minerals: Single-chain silicates,* **2A** *second edition*. London: Longman Scientific and Technical, England, 61-62.

Eales, H.V., Marsh, J.S., Mitchell, A.A., De Klerk, W.J., Kruger, F.J. and Field, M. (1986). Some geochemical constraints upon models for the crystallisation of the Upper Critical zone – main zone interval, northwestern Bushveld Complex. *Mineralogical Magazine* **50**, 567-582.

Eales, H.V. and Cawthorn, R.G.C. (1996). The Bushveld Complex. *In*: Cawthorn R.G. (editor) *Layered Intrusion*: Elsevier, Amsterdam, 181-228.

Eriksson, P.G. and Reczko, F.F.F. (1998). Contourites associated with pelagic mudrocks and distal delta-fed turbidites in the Lower Proterozoic Timeball Hill

Formation epiric basin (Transvaal Supergroup), South Africa. *Sedimentary Geology* **120** (1-4), 319-335.

Eriksson, P.G., Schreiber, U.M. and Van der Neut, M. (1991). A review of the sedimentology of the early Proterozoic Pretoria Group, South Africa: Implications for tectonic setting. *Journal of African Earth Science* **13**, 107-119.

Gain, S.B. (1985). The geological setting of the Platiniferous UG2 chromitite layer on Maandagshoek, eastern Bushveld Complex. *Economic Geology* **80**, 925-943.

Gain, S.B. and Mostert, A.B. (1982). The geological setting of the platinoid and base metal sulphide mineralisation in the Platreef of the Bushveld Complex on Drenthe, north of Potgietersrus. *Economic Geology* **77**, 1395-1404.

Hall, A.L. (1932). The Bushveld Igneous Complex of the central Transvaal. *Memoir. Geological Survey of South Africa* **28**, 560.

Harris, C. and Chaumba, J.B. (2001). Crustal contamination and fluid-rock interaction during the formation of the Platreef, northern limb of the Bushveld Complex, South Africa. *Journal of Petrology* **42**, 1321-1347.

Hatton, C.H. and Von Gruenewaldt, G. (1987). The geological setting and petrogenesis of the Bushveld chromitite layers. *In*: Stowe, C.W. (editor) *Evolution of chromium ore fields*: Van Nostrand Reinhold, New York, 109-143.

Hiemstra, S.A. (1986). The distribution of chalcophile and platinum-group elements in the UG2 chromitite layer of the Bushveld Complex. *Economic Geology* **81**, 1080-1086.

Irvine, T.N. and Sharpe, M.R. (1986). Magma mixing and the origin of stratiform oxide ore zones in the Bushveld and Stillwater Complexes. *In*: *Metallogeny of Basic and Ultrabasic Rocks, Conference Proceedings, Edinburgh*, **1985**, 183-198.

Kinloch, E.D. (1982). Regional trends in platinum group mineralogy of the Critical Zone of the Bushveld Complex, South Africa. *Economic Geology* **85**, 1328-1347.

Klemm, D.D., Ketterer, S., Reichhardt, F., Steindl, J. and Weber-Diefenbach, K. (1985). Implications of vertical and lateral compositional variations across the Pyroxenite Marker and its associated rocks in the upper part of the Main Zone in the Eastern Bushveld Complex. *Economic Geology* **80**, 1075-1088.

Kruger, F.J. (1990). The stratigraphy of the Bushveld Complex: a reappraisal and relocation of the Main Zone boundaries. *South African Journal of Geology* **93**, 376-381.

Lee, C.A. (1983). Trace and platinum-group element chemistry and the development of the Merensky unit of the Western Bushveld Complex. *Mineralium Deposita* **18**, 173-190.

Lee, C.A. (1996). A review of mineralisation in the Bushveld Complex and some other layered mafic intrusions. *In*: Cawthorn, R.G. (editor) *Layered Intrusions.* Elsevier, Amsterdam, 103-145.

Lee, C.A. and Parry, S.J. (1988). Platinum-group element geochemistry of the Lower and Middle Group chromitites of the Eastern Bushveld Complex. *Economic Geology* **83**, 1127-1139.

Li, C. and Naldrett, A.J. (1999). Geology and petrology of the Voisey's Bay intrusion: reaction of olivine with sulphide and silicate liquids. *Lithos* **47**, 1-31.

Li, C., Maier, W.D. and de Waal, S.A. (2001a). The role of magma mixing in the genesis of PGE mineralisation of the Bushveld Complex: Thermodynamic calculation and new interpretations. *Economic Geology* **96**, 653-662.

Li, C., Maier, W.D. and de Waal, S.A. (2001b). The role of magma mixing in the genesis of PGE mineralisation of the Bushveld Complex: Thermodynamic calculation and new interpretations-erratum. *Economic Geology* **96**, 1487.

Maier, W.D. and Eales, H.V. (1997). Correlation within the UG2-Merensky Reef interval of the Western Bushveld Complex, based on geochemical, mineralogical and petrological data. *Council for Geosciences, Bulletin of the Geological Survey of South Africa* **120**, 56p.

Maier, W.D. (2003). Sulphide entrainment in the Bushveld Complex. *Mineralium Deposita* (submitted).

Mason, R. (1971). The chemistry and structure of the Sulitjelma gabbro. *Norges Geol. Unders*, **29**, 108-142.

Mitchell, A.A. (1990). The stratigraphy, petrology and mineralogy of the Main Zone of the northwestern Bushveld Complex. *South African Journal of Geology* **93**, 818-831.

Mitchell, A.A. and Scoon, R.N. (1991). Discussion on 'The stratigraphy of the Bushveld Complex: a reappraisal and the relocation of the Main Zone boundaries'. *South African Journal of Geology* **94**, 183-187.

Morrissey, C.J. (1988). Exploration for platinum. *In*: Prichard, H.M., Potts J., Bowles J.F.W. and Cribb, S.J (editors) *Geo-platinum* **87**. Elsevier, 1-12.

Naldrett, A.J., Gasparini, E.C., Barnes, S.J., Von Gruenewaldt, G. and Sharpe, M.R. (1986). The Upper Critical Zone of the Bushveld Complex and the origin of the Merensky-type ores. *Economic Geology* **81**, 1105-1117.

Naldrett, A.J. and Lehmann, J. (1988). Spinel non-stoichiometry as the explanation as the explanation for Ni-, Cu-, and PGE-enriched sulphides in chromitites. *In*:

Prichard, H.M., Potts, P.J., Bowles, J.F.W. and Cribb, S.J (editors) *Geo-Platinum* **87**. Amsterdam: Elsevier, 113-143.

Naldrett, A.J. and von Gruenewaldt, G. (1989). Association of platinum-group elements with chromitite in layered intrusions and ophiolite complexes. *Economic Geology* **84**, 180-187.

Nelson, D.R., Trendall, A.F. and Altermann, W. (1999). Chronological correlations between Pilbara and Kaapvaal Cratons. *Precambrian Research* **97**, 165-189.

Ripley, E.M. (1999). Systematics of sulphur and oxygen isotopes in mafic igneous rocks and related Cu-Ni-PGE mineralisation. *In*: Keays, R.R., Lesher, C.M., Lightfoot, P.C. and Farrow, C.E.G (editors) *Dynamic processes in magmatic ore deposits and their application in mineral exploration, Geological association of Canada, Short Course Volume* **13**, 133-158.

Rudnick, R.L. and Fountain, D.M. (1995). Nature and composition of the continental crust: A lower crustal perspective. *Reviews of Geophysics* **33**, **3**. 267-309.

SACS (South African Committee on Stratigraphy). (1980). Stratigraphy of South Africa. *Geological Survey of South Africa. Handbook* **8**, 690p.

Scoon, R.N. and Mitchell, A.A. (1994). Discordant iron-rich pegmatites in the Bushveld Complex and their relationship to iron-rich intercumulus residual liquids. *Journal of Petrology* **35**, 881-917.

Scoon, R.N. and Teigler, B. (1994). Platinum-group mineralisation in the Critical Zone of the Western Bushveld Complex: I. Sulfide poor chromitites below the UG2. *Economic Geology* **89**, 1094-1121.

Sharpe, M.R., Crouse, S.P., Gain, S.B., Chunnett, G.K. and Lee., C.A. (2002). Sheba's Ridge, An unconventional setting for Platreef, UG2 and Merensky-style PGE-BMS deposits in the Bushveld Complex. Edited by A. Boudreau. *9th International Platinum Symposium. Extended Abstracts*, 407-408.

Simpkin, T. and Smith, J.V. (1970). Minor-element distribution in olivines. *Journal of Geology* **78**, 304-325.

Stumpfl, E.F. (1993). Fluids: A prerequisite for Pt metals mineralisation. In: current Research in Geology Applied to Ore Deposits. Edited by Haeh-Alf, P.F., Torres-Ruiz, J. and Gervilla, F. *Proceedings, 2nd Biennial SGA Meeting*, 15-21.

Teigler, B. (1990a). *Mineralogy, petrology and geochemistry of the Lower and Lower Critical Zones, northwest Bushveld Complex*. Ph.D. thesis. *Rhodes University, Grahamstown, South Africa*.

Teigler, B. (1990b). Platinum group element distribution in the Lower and Middle chromitites in the Western Bushveld Complex. *Mineralogy and Petrology* **42**, 165-179.

Tredoux, M., Lindsay, N.M., Davies, G. and McDonald, I. (1995). The fractionation of platinum-group elements in magmatic systems, with the suggestion to a novel causal mechanism. *South African Journal of Geology* **98**, 157-167.

Van der Merwe, M.J. (1976). The layered sequence of the Potgietersrus limb of the Bushveld Complex. *Economic Geology* **71**, 1337-1351.

Vermaak, C.F. (1985). The UG2 layer – South Africa's slumbering chromitite giant. *Chromium Review* **5**, 9-22.

Vermaak, C.F. (1995). *The platinum-group metals. A global perspective. First edition. Mintek*, 19p.

Viljoen, M.J. and Schurmann, L.W. (1998). Platinum-group metals. *In*: Wilson, M.G.C. and Anhaeusser, C.R (editors) *The Mineral Resources of South Africa, Council for Geoscience, Pretoria*, 532-568.

Von Gruenewaldt, G. (1973). The Main and Upper Zones of the Bushveld Complex in the Roossenekal area, eastern Transvaal. *Transactions of the Geological Society of South Africa* **76**, 207-227.

Von Gruenewaldt, G. (1976). Sulphides in the Upper Zone of the Bushveld Complex. *Economic Geology* **71**, 1337-1351.

Von Gruenewaldt, G. (1977). The mineral resources of the Bushveld Complex. *Minerals Science and Engineering* **9**, no. 2, 83-95.

Von Gruenewaldt, G. (1989). A review of some recent concepts of the Bushveld Complex, with particular reference to sulphide mineralisation. *Canadian Mineralogist* **17**, 233-256.

Von Gruenewaldt, G., Sharpe, M.R. and Hatton C.J. (1985). The Bushveld Complex: Introduction and review. *Economic Geology* **80**, 803-812.

Von Gruenewaldt, G., Hatton, C.J., Merkle, R.K.W. and Gain, S.B. (1986). Platinum-group element – chromitite associations in the Bushveld Complex. *Mineral Petrology* **42**, 71-95.

Von Gruenewaldt, G., Hulbert, L.J. and Naldrett, A.J. (1989). Contrasting platinum-group concentration patterns in cumulates of the Bushveld Complex. *Mineralium Deposita* **24**, 219-229.

Wager, L.R. and Brown, G.M. (1968). *Layered igneous rocks.* Edinburgh and London. Oliver and Boyd, 58p.

Wagner, A. (1929). *The Platinum Deposits and Mines of South Afric.* Oliver and Boyd, 366p

Walraven, F., Armstrong, R.A. and Kruger, F.J. (1990). A chronostratigraphic framework for the north-central Kaapvaal craton, the Bushveld Complex and the Vredefort structure. *Tectonophysics* **171**, 23-48.

Watson, J. S. (1996). *Fast,* Simple Method of Powder Pellet Preparation for X-Ray Fluorescence Analysis. *X-Ray Spectrometry* **25**, 173-174.

White, J.A. (1994). The Potgietersrus project geology and exploration history: *Proceedings, 15th CMMI Congress, South African Institute of Mining and Metallurgy*, 173-182.

Appendix I

Analytical Methods

Appendix Ia: Sample preparation

Appendix Ib: X-Ray Fluorescence Analysis

Appendix Ic: PGE analysis

Appendix Id: Microprobe Analysis

Appendix Ie: S-Isotope analyses

Appendix Ia: Sample preparation

Quarter-core samples were crushed in a jaw crusher before being milled in a C-steel mill. The samples were milled to a particle size of <63 µm. To minimize possible cross contamination, the mill was cleaned after every sample by milling clean quartz, washing the mill pots, and drying with acetone.

Appendix Ib: X-Ray Fluorescence Analysis

APPARATUS: ARL 9400XP+ Wavelength dispersive XRF Spectrometer

SAMPLE PREPARATION: 3 grams of each sample powder were weighed and dried At 100^0C overnight before being roasted at 1000^0C overnight to determine the absorbed (H_2O^-) and the percentage loss on ignition, respectively.

Major elements were determined on fused beads, prepared following the standard method used in the XRD and XRF laboratory of the University of Pretoria, as adapted from Bennett and Oliver (1992). One gram of pre-roasted sample powder and 6 grams of flux (Lithium tetra borate) mixed in a Au crucible was fused at 1050^0C for 15 minutes in a muffle furnace with occasional swirling. The fusion mixture was poured into a pre-heated Pt/Au mould and left to cool at room temperature. The bottom surface of the glass disk was analysed by XRF.

Trace elements were determined on pressed powder briquettes prepared following the method of Watson (1996). Approximately 16-20ml of sample powder mixed with less than 1 volume % of a liquid binder (Mowiol: polyvinyl alcohol) was loaded into aluminum cups to increase the stability and strength before being pressed at ± 7 tons/in^2.

CALIBRATION: The XRF Spectrometer was calibrated with Certified reference materials. The NBSGSC fundamental parameter program was used for matrix correction of major elements

as well as Cl, Co, Cr, V, Sc and S. The Rh Compton peak ratio method was used for the other trace elements.

Standard deviations and detection limits are listed in Table

STANDARD DEVIATIONS AND LOWER LIMIT OF DETECTION OF THE XRF METHOD

	Std dev. (%)	LOD
SiO_2	0.4	0.02
TiO_2	0.03	0.0032
Al_2O_3	0.3	0.01
Fe_2O_3	0.3	0.0097
MnO	0.0065	0.0013
MgO	0.1	0.0118
CaO	0.07	0.01
Na_2O	0.11	0.0265
K2O	0.06	0.005
P_2O_5	0.08	0.01
Cr_2O_3	0.0053	0.0006
NiO	0.01	0.0013
V_2O_5	0.0018	0.0008
ZrO_2	0.005	0.0009
CuO	0.0037	0.0003

	Std dev. (ppm)	LOD
As*	10	3
Cu	3	2
Ga	2	2
Mo	1	1
Nb	3	2
Ni	6	3
Pb	3	3
Rb	4	2
Sr	4	3
Th	2	3
U	2	3
W*	10	6
Y	4	3
Zn	4	4
Zr	6	10
Ba	14	5
Ce	14	6
Cl*	100	11
Co	6	3
Cr	40	15
F*	500	400
S*	300	40
Sc	5	1
V	10	1

Values for elements indicated with an * should be considered semi-quantitative. LOD = Limit of Detection, std dev = standard deviation, ppm = parts per million.

Appendix Ic. PGE analysis

The platinum-group elements, Re and Au were determined by instrumental neutron activation analysis (INAA) at the University of Quebec at Chicoutimi (UQAC), after pre-concentration in a Ni-sulphide bead from 50g of rock powder. Sample irradiation was carried out at the Ecole Polytecnique in Montreal in a SLOWPOKE II reactor.

Five determinations of five different NiS beads of the CANMET standard WGB-1 (Table below) can be used to estimate the precision and accuracy of the analyses. For all the elements except Au the relative standard deviations are 9–17 %.

For Au, Pt and Pd the accuracy of the analyses may be assessed by comparing the results obtained at UQAC for standards UTM-1 and WGB-1 with the certified values. The results are in good agreement with both the high- and low-level standard. For Rh, Ru and Ir certified values are available only for UTM-1. The UQAC analysed results agree with CANMET results. For the low-level standard WGB-1 only informational values are available for Rh, Ru, Ir and Re. The results agree with these when the standard deviation on the CANMET informational value ic considered.

No noble metals were detected in the blank, except Ir and Au. These were present at 0.02 and 0.1 ppb, respectively. As both values are far lower than the levels present in the samples, no significant contamination is believed to have occurred in preparing the samples, and no blank correction was made on the samples.

Precision and accuracy of the PGE analyses

	UTM-1				WGB-1			
	UQAC*	s	CANMET^	error	UQAC*	s	CANMET	error
	ppb	+/-	ppb	+/-	ppb	+/-	ppb	+/-
Os ppb	7.1	0.57	8	2.1	0.48	0.08	n.v.	
Ir	10.0	0.40	8.8	0.6	0.25	0.04	0.33	0.27
Ru	10.9	0.98	10.9	1.5	<1.2	0.33	0.3	0.2
Rh	10.8	0.43	9.5	1.1	0.46	0.08	0.32	0.19
Pt	131	7.9	129	5	5.98	0.55	6.1	1.6
Pd	110	4.4	106	3	13.20	1.94	13.9	2.1
Au	47.9	4.3	48	2	1.34	0.59	2.9	1.1

* = average of five NiS beads all fused, dissolved and irradiated in the same batch,
s = 1 sigma of the five values, CANMET Certificate of Analysis (1996). Note that the figures in italics are informational values only, i.e. there are as yet no certified values for these elements in these standards, the error in these cases are the standard deviation of the values submitted in the round robin tests.
n.v. = no values

Appendix Id. Microprobe Analysis

APPARATUS: JEOL JXA – 733 Electron Microprobe.

The probe was operated at 20 kV accelerating voltage, 30nA beam current and the samples were analysed using a 10 µm beam diameter. K_α was used for all elements. Counting times were set at 10 seconds on peak and 5 seconds on either side of the peak on the background. To improve the detection limits for Ni, counting time was set at 50 seconds on peak and 25 seconds on either side of the peak on the background.

STANDARDS:
Orthoclase for K,Si
Jadeite for Al, Na
Plagioclase for Ca
Olivine for Mg
Nickel, magnetite for Ni, Fe
Willemite for Mn
Rutile for Ti
Chromite for Cr

ANALYSING CRYSTALS:
TAP crystals for Si, AL, Na, Mg
LIF crystals for Fe, Mn, Cr, Ni
PET crystals for K, Ca, Ti

DETECTION LIMITS at 99% confidence in elemental weight % (single line)

Si	Al	Na	Mg	Fe	Mn	Cr	Ni	K	Ca	Ti
0.028	0.029	0.045	0.028	0.036	0.037	0.037	0.018	0.033	0.036	0.055

Appendix Ie: S-Isotope analyses

APPARATUS: Finnigan MAT252 isotope ratio mass spectrometer

SAMPLE PREPARATION: Sulphide powders and small amount of V_2O_5 were loaded into tin capsules and analysed using Elemental Analyser-Continuous Flow Isotope Ratio Mass Spectrometry on a Finnigan MAT252 isotope ratio mass spectrometer.

ANALYTICAL PRECISION: better than ± 0.05 per mil.

SAMPLE REPRODUCIBILITY: ± 0.1 per mil.

Appendix II

THIN SECTION SAMPLE LIST

Sample number	Depth on the core(m)	PS/TS	Short description
TM1	30.50	PS	gabbronorite, with dissemited sulphides
TM2	31.78	PS	gabbronorite, with dissemited sulphides
TM3	35.12	PS	gabbronorite, with dissemited sulphides
TM4	38.94	PS	pyroxenite, medium-grained
TM5	40.44	PS	hornfels, with schlieren of gabbronorite
TM6	41.21	PS	hornfels, with schlieren of gabbronorite
TM7	41.53	PS	gabbro-sulphide free
TM8	44.78	PS	gabbro-sulphide free
TM9	48.87	PS	hybrid zone, gabbronorite-metasediment
TM10	55.89	PS	gabbro with disseminated sulphides
TM11	57.54	PS	melagabbro, with disseminated sulphides and calcsilicate schlieren
TM12	58.34	PS	melagabbro, with disseminated sulphides and calcsilicate schlieren
TM13	74.49	PS	gabbronorite, with numerous schlieren and xenoliths of calcsilicates.
TM14	77.09	PS	gabbronorite, with numerous schlieren and xenoliths of calcsilicates.
TM15	78.95	PS	gabbronorite, with numerous schlieren and xenoliths of calcsilicates.
TM16	80.61	PS	gabbronorite, with numerous schlieren and xenoliths of calcsilicates.
TM17	82.32	PS	gabbronorite, with numerous schlieren and xenoliths of calcsilicates.
TM18	84.69	PS	gabbronorite, with numerous schlieren and xenoliths of calcsilicates.
TM19	86.60	PS	gabbronorite, with numerous schlieren and xenoliths of calcsilicates.
TM20	88.65	PS	gabbronorite, with numerous schlieren and xenoliths of calcsilicates.
TM21	89.36	PS	gabbronorite, with numerous schlieren and xenoliths of calcsilicates.
TM22	91.13	PS	gabbronorite, with numerous schlieren and xenoliths of calcsilicates.
TM23	91.44	PS	gabbronorite, with numerous schlieren and xenoliths of calcsilicates.
TM24	94.40	PS	gabbronorite, with numerous schlieren and xenoliths of calcsilicates.
TM25	95.85	PS	gabbronorite, with numerous schlieren and xenoliths of calcsilicates.
TM26	99.86	PS	gabbronorite, with numerous schlieren and xenoliths of calcsilicates.
TM27	100.12	PS	gabbronorite, with numerous schlieren and xenoliths of calcsilicates.
TM28	101.86	PS	gabbronorite, with numerous schlieren and xenoliths of calcsilicates.
TM29	101.95	PS	gabbronorite, with numerous schlieren and xenoliths of calcsilicates.
TM30	102.45	PS	gabbronorite, with numerous schlieren and xenoliths of calcsilicates.
TM31	107.24	PS	gabbronorite, with numerous schlieren and xenoliths of calcsilicates.
TM32	109.39	PS	hybrid zone, gabbronorite with calcsilicate xenoliths
TM33	111.21	PS	hybrid zone, gabbronorite with calcsilicate xenoliths
TM34	111.25	PS	hornfels, with several fine grained gabbroic sills
TM35	116.72	PS	hornfels, with several fine grained gabbroic sills
TM36	127.15	PS	norite, with calcsilicate schlieren and xenoliths
TM37	136.39	PS	norite, with calcsilicate schlieren and xenoliths
TM38	144.47	PS	norite, with calcsilicate schlieren and xenoliths
TM39	197.97	PS	hornfels
TM40	200.50	PS	fine grained gabbroic sill

NB. The depth on core refers to the bottom measurement of the thin section position.

PS = Polished section.

Appendix III

XRF SAMPLE LIST

Sample	Depth(m)	Unit	S isotope	Rock type
P1	30.40	U- Platreef		gabbronorite
P2	32.69	U- Platreef	√	sulphide bearing gabbronorite
P3	34.91	U- Platreef	√	sulphide bearing gabbronorite
P4	38.85	U- Platreef		gabbronorite with minor disseminated sulphides
P5	44.77	Sill		gabbroic sill
P6	55.80	Sill	√	fine-med grained norite sill
P7	57.70	U- Platreef		sulphide bearing pegmatoidal gabbronorite
P8	62.55	Sill		fine-grained gabbro
P9	63.65	Shale interlayer		hornfels
P10	68.30	Shale interlayer		fine-grained hornfels
P11	76.99	M- Platreef	√	sulphide bearing gabbronorite
P12	78.74	M- Platreef		sulphide bearing gabbronorite
P13	80.75	M- Platreef		sulphide bearing gabbronorite
P14	86.42	M- Platreef		sulphide bearing gabbronorite
P15	89.55	M- Platreef	√	sulphide bearing pegmatoidal gabbronorite
P16	94.30	M- Platreef		non-sulphide bearing gabbronorite
P17	96.60	Xenolith		skarn (dolomite xenolith)
P18	100.05	M- Platreef		non-sulphide bearing gabbronorite
P19	102.35	M- Platreef	√	sulphide bearing pegmatoidal gabbronorite
P20	109.82	M- Platreef		sulphide bearing pegmatoidal gabbronorite
P21	110.95	M- Platreef		sulphide bearing gabbronorite
P22	112.75	Shale interlayer		hornfels
P23	118.95	Shale interlayer		hornfels
P24	126.90	L- Platreef		non-sulphide bearing norite
P25	138.38	L- Platreef	√	non-sulphide bearing norite
P26	145.60	L- Platreef	√	sulphide bearing norite
P28	170.40	Floor rock	√	sulphide bearing silica-rich hornfels
P29	174.95	Floor rock		hornfels
P30	189.95	Floor rock	√	calcsilicate
P31	197.37	Floor rock	√	hornfels
P32	205.18	Floor rock	√	hornfels
P33	213.00	Floor rock		sediment

U- Platreef = Upper Platreef

M- Platreef = Middle Platreef

L- Platreef = Lower Platreef

Appendix IV

MINERAL CHEMISTRY

Abbreviations used in the Tables

U-Plat = Upper Platreef

M-Plat = Middle Platreef

L-Plat = Lower Platreef

An = cationic ratio of 100 * Ca/(Ca + Na + K)

Fo = cationic ratio of 100 * Mg/(Mg + Fe^{2+}) in olivine

Mg no. = cationic ratio of 100 * Mg/(Mg + Fe^{2+})

nd = Not detected

Pl = Plagioclase

Ol = Olivine

Opx = Orthopyroxene

Cpx = clinopyroxene

Orthopyroxene Analyses

	TM2		TM4				TM9				TM11					TM13
Depth (m)	31.78		38.94				48.87				57.54					74.49
Unit	U-pyrox	U-pyrox	U-pyrox	U-pyrox	U-pyrox	U-pyrox	U-pyrox	U-pyrox	U-pyrox	U-pyrox	U-pyrox	U-pyrox	U-pyrox	U-pyrox	U-pyrox	M-pyrox
Sample	TM2 opx1	TM2 opx2	TM4 opx1	TM4 opx2	TM4 opx3	TM4 opx4	TM9 opx1	TM9 opx2	TM9 opx3	TM9 opx4	TM11 opx1	TM11 opx2	TM11 opx3	TM11 opx4	TM11 opx5	TM13 opx1
Wt %																
SiO2	53.22	51.73	53.34	52.87	53.11	54.59	50.43	51.78	50.92	51.51	54.18	52.87	52.94	54.11	53.63	53.07
Al2O3	1.30	1.57	1.55	1.55	1.62	1.19	1.34	1.12	1.52	2.10	1.91	2.08	1.90	1.88	1.90	0.65
Na2O	nd	nd	nd	nd	nd	nd	nd	nd	0.11	0.11	nd	nd	nd	0.05	nd	nd
MgO	28.86	29.12	29.48	29.58	29.09	29.50	26.42	25.47	25.58	25.84	30.66	30.72	30.52	29.89	30.33	25.69
FeO	13.91	13.34	11.68	12.64	12.66	12.26	17.86	18.34	18.31	17.98	11.57	11.84	12.30	11.91	11.86	17.97
MnO	0.28	0.24	0.27	0.24	0.29	0.22	0.26	0.33	0.34	0.29	0.26	0.30	0.23	0.31	0.24	0.41
Cr2O3	nd	0.24	0.41	0.41	0.29	0.39	0.08	nd	0.07	0.08	0.20	0.22	0.20	0.36	0.28	0.19
NiO	nd	nd	0.08	0.06	nd	nd	nd	nd	nd	nd	0.03	0.02	nd	nd	nd	nd
K2O	nd	nd	nd	nd	nd	nd	nd	nd	nd	nd	nd	nd	nd	nd	nd	nd
CaO	0.82	1.19	1.75	1.75	1.43	1.96	0.86	0.86	0.77	0.95	0.79	0.72	0.98	1.38	1.38	0.91
TiO2	0.05	0.10	0.16	0.05	0.13	nd	0.13	0.11	0.10	0.14	0.27	0.12	0.16	0.03	0.11	0.24
Total	98.47	97.54	98.75	99.17	98.64	100.12	97.39	98.02	97.71	98.99	99.85	98.91	99.22	99.92	99.73	99.13
Cations (based on 6 oxygens)																
Si	1.94	1.91	1.93	1.91	1.93	1.95	1.90	1.94	1.92	1.91	1.93	1.90	1.91	1.93	1.92	1.96
Al	0.06	0.07	0.07	0.07	0.07	0.05	0.06	0.05	0.07	0.09	0.08	0.09	0.08	0.08	0.08	0.03
Na	0.00	0.00	0.00	0.00	0.00	0.00	0.00	0.00	0.01	0.01	0.00	0.00	0.00	0.00	0.00	0.00
Mg	1.57	1.60	1.59	1.60	1.57	1.57	1.49	1.42	1.44	1.43	1.63	1.65	1.64	1.59	1.62	1.41
Fe	0.42	0.41	0.35	0.38	0.38	0.37	0.56	0.57	0.58	0.56	0.34	0.36	0.37	0.36	0.35	0.56
Mn	0.01	0.01	0.01	0.01	0.01	0.01	0.01	0.01	0.01	0.01	0.01	0.01	0.01	0.01	0.01	0.01
Cr	0.00	0.01	0.01	0.01	0.01	0.01	0.00	0.00	0.00	0.00	0.01	0.01	0.01	0.01	0.01	0.01
Ni	0.00	0.00	0.00	0.00	0.00	0.00	0.00	0.00	0.00	0.00	0.00	0.00	0.00	0.00	0.00	0.00
K	0.00	0.00	0.00	0.00	0.00	0.00	0.00	0.00	0.00	0.00	0.00	0.00	0.00	0.00	0.00	0.00
Ca	0.03	0.05	0.07	0.07	0.06	0.08	0.04	0.03	0.03	0.04	0.03	0.03	0.04	0.05	0.05	0.04
Ti	0.00	0.00	0.00	0.00	0.00	0.00	0.00	0.00	0.00	0.00	0.01	0.00	0.00	0.00	0.00	0.01
O	6.00	6.00	6.00	6.00	6.00	6.00	6.00	6.00	6.00	6.00	6.00	6.00	6.00	6.00	6.00	6.00
Total	10.03	10.05	10.03	10.05	10.03	10.02	10.06	10.03	10.05	10.05	10.03	10.04	10.05	10.03	10.04	10.02
Mg no.	78.71	79.57	81.81	80.81	80.39	81.12	72.50	71.24	71.36	71.93	82.53	82.20	81.56	81.73	82.02	71.81

Orthopyroxene Analyses

	TM13		TM14					TM15					TM16		
Depth (m)	74.49		77.09					78.95					80.61		
Unit	M-pyrox	M-pyrox	M-pyrox	M-pyrox	M-pyrox	M-pyrox	M-pyrox	M-pyrox	M-pyrox	M-pyrox	M-pyrox	M-pyrox	M-pyrox	M-pyrox	M-pyrox
Sample	TM13 opx2	TM13 opx3	TM14 opx1	TM14 opx2	TM14 opx3	TM14 opx4	TM14 opx5	TM15 opx1	TM15 opx2	TM15 opx3	TM15 opx4	TM15 opx5	TM16 opx1	TM16 opx2	TM18 opx1
Wt %															
SiO2	52.59	52.72	53.35	53.60	53.17	53.09	52.91	53.70	54.51	54.30	54.21	54.47	52.89	54.93	54.42
Al2O3	0.79	0.92	1.35	1.23	1.40	1.28	1.24	1.17	1.25	1.22	1.37	1.14	1.79	1.26	1.51
Na2O	0.03	nd	nd	nd	nd	nd	nd	0.09	nd	nd	0.06	0.06	nd	nd	nd
MgO	26.45	26.28	27.71	27.83	28.12	28.11	27.05	28.59	29.00	28.76	28.87	29.01	30.90	29.76	29.60
FeO	16.82	17.14	14.37	15.10	13.85	14.28	13.75	12.86	13.20	13.14	13.42	13.20	11.45	12.79	13.10
MnO	0.33	0.36	0.32	0.25	0.27	0.33	0.27	0.37	0.37	0.36	0.35	0.35	0.29	0.27	0.25
Cr2O3	0.15	0.15	0.36	0.26	0.27	0.22	0.34	0.14	0.09	0.18	0.14	0.09	0.16	0.08	0.08
NiO	nd	nd	nd	nd	nd	nd	nd	0.08	0.07	0.05	0.09	0.07	0.05	0.09	0.10
K2O	nd	nd	nd	nd	nd	nd	nd	nd	nd	nd	nd	nd	nd	nd	nd
CaO	1.31	1.24	1.86	1.50	1.41	1.26	2.95	1.82	1.40	2.02	1.20	1.84	0.93	1.17	1.08
TiO2	0.26	0.20	0.06	0.25	0.21	0.27	0.13	0.10	0.35	0.15	0.31	0.07	0.20	0.17	0.30
Total	98.73	99.03	99.42	100.05	98.72	98.84	98.65	98.92	100.28	100.19	100.01	100.30	98.71	100.53	100.44
Cations (based on 6 oxygens)															
Si	1.94	1.94	1.94	1.94	1.94	1.94	1.94	1.95	1.95	1.94	1.94	1.95	1.91	1.95	1.94
Al	0.04	0.04	0.06	0.05	0.06	0.06	0.05	0.05	0.05	0.05	0.06	0.05	0.08	0.05	0.06
Na	0.00	0.00	0.00	0.00	0.00	0.00	0.00	0.01	0.00	0.00	0.00	0.00	0.00	0.00	0.00
Mg	1.46	1.45	1.50	1.50	1.53	1.53	1.48	1.55	1.54	1.54	1.54	1.55	1.66	1.58	1.57
Fe	0.52	0.53	0.44	0.46	0.42	0.44	0.42	0.39	0.39	0.39	0.40	0.40	0.35	0.38	0.39
Mn	0.01	0.01	0.01	0.01	0.01	0.01	0.01	0.01	0.01	0.01	0.01	0.01	0.01	0.01	0.01
Cr	0.00	0.00	0.01	0.01	0.01	0.01	0.01	0.00	0.00	0.01	0.00	0.00	0.01	0.00	0.00
Ni	0.00	0.00	0.00	0.00	0.00	0.00	0.00	0.00	0.00	0.00	0.00	0.00	0.00	0.00	0.00
K	0.00	0.00	0.00	0.00	0.00	0.00	0.00	0.00	0.00	0.00	0.00	0.00	0.00	0.00	0.00
Ca	0.05	0.05	0.07	0.06	0.06	0.05	0.12	0.07	0.05	0.08	0.05	0.07	0.04	0.05	0.04
Ti	0.01	0.01	0.00	0.01	0.01	0.01	0.00	0.00	0.01	0.00	0.01	0.00	0.01	0.01	0.01
O	6.00	6.00	6.00	6.00	6.00	6.00	6.00	6.00	6.00	6.00	6.00	6.00	6.00	6.00	6.00
Total	10.03	10.03	10.03	10.03	10.03	10.03	10.03	10.03	10.02	10.02	10.02	10.03	10.05	10.02	10.02
Mg no.	73.70	73.20	77.48	76.68	78.35	77.84	77.82	79.84	79.66	79.62	79.32	79.65	82.80	80.60	80.11

Orthopyroxene Analyses

Sample	TM18					TM20						TM21			
Depth (m)	84.69					88.65						89.36			
Unit	M-pyrox TM18 opx2	M-pyrox TM18 opx3	M-pyrox TM18 opx4	M-pyrox TM18 opx5	M-pyrox TM18 opx6	M-pyrox TM20 opx1	M-pyrox TM20 opx2	M-pyrox TM20 opx3	M-pyrox TM20 opx4	M-pyrox TM20 opx5	M-pyrox TM20 opx6	M-pyrox TM21 opx1	M-pyrox TM21 opx2	M-pyrox TM21 opx3	M-pyrox TM21 opx4
Wt %															
SiO2	54.50	53.83	53.89	53.27	54.37	51.82	51.89	52.19	51.77	52.82	52.85	54.71	55.09	53.79	54.03
Al2O3	1.34	1.12	1.30	1.34	1.34	2.44	3.00	3.00	2.01	1.79	1.92	2.27	1.68	2.53	2.74
Na2O	nd	nd	nd	nd	nd	nd	nd	nd	nd	nd	0.08	nd	nd	nd	nd
MgO	29.74	28.99	29.17	28.90	29.92	25.38	25.32	25.46	25.15	26.04	26.09	30.58	29.87	29.66	29.73
FeO	12.56	13.80	13.46	13.62	12.47	17.83	18.18	17.70	18.32	17.36	17.61	12.18	12.34	12.51	12.68
MnO	0.27	0.28	0.24	0.31	0.31	0.27	0.29	0.23	0.30	0.32	0.30	0.24	0.27	0.18	0.22
Cr2O3	0.14	0.14	0.06	0.21	0.09	0.24	0.15	0.24	0.11	0.19	0.12	0.11	0.08	0.04	0.04
NiO	0.09	0.10	0.09	0.11	0.09	nd	nd	nd	nd	nd	nd	0.06	0.09	0.09	0.10
K2O	nd	nd	nd	nd	nd	nd	nd	nd	nd	nd	nd	nd	nd	nd	nd
CaO	1.70	1.58	1.65	1.56	1.65	0.22	0.27	0.33	0.28	0.36	0.26	1.15	1.21	0.91	0.66
TiO2	0.15	0.15	0.19	0.23	0.28	0.18	0.17	0.23	0.18	0.17	0.13	0.10	0.23	0.22	0.29
Total	100.49	100.00	100.05	99.55	100.51	98.42	99.27	99.39	98.15	99.05	99.37	101.43	100.87	99.93	100.50
Cations (based on 6 oxygens)															
Si	1.94	1.94	1.93	1.93	1.93	1.92	1.91	1.91	1.93	1.94	1.94	1.92	1.94	1.92	1.92
Al	0.06	0.05	0.06	0.06	0.06	0.11	0.13	0.13	0.09	0.08	0.08	0.09	0.07	0.11	0.11
Na	0.00	0.00	0.00	0.00	0.00	0.00	0.00	0.00	0.00	0.00	0.01	0.00	0.00	0.00	0.00
Mg	1.58	1.55	1.56	1.56	1.59	1.40	1.39	1.39	1.40	1.43	1.43	1.60	1.57	1.58	1.57
Fe	0.37	0.42	0.40	0.41	0.37	0.55	0.56	0.54	0.57	0.53	0.54	0.36	0.36	0.37	0.38
Mn	0.01	0.01	0.01	0.01	0.01	0.01	0.01	0.01	0.01	0.01	0.01	0.01	0.01	0.01	0.01
Cr	0.00	0.00	0.00	0.01	0.00	0.01	0.00	0.01	0.00	0.01	0.00	0.00	0.00	0.00	0.00
Ni	0.00	0.00	0.00	0.00	0.00	0.00	0.00	0.00	0.00	0.00	0.00	0.00	0.00	0.00	0.00
K	0.00	0.00	0.00	0.00	0.00	0.00	0.00	0.00	0.00	0.00	0.00	0.00	0.00	0.00	0.00
Ca	0.07	0.06	0.06	0.06	0.06	0.01	0.01	0.01	0.01	0.01	0.01	0.04	0.05	0.04	0.03
Ti	0.00	0.00	0.01	0.01	0.01	0.01	0.01	0.01	0.01	0.01	0.00	0.00	0.01	0.01	0.01
O	6.00	6.00	6.00	6.00	6.00	6.00	6.00	6.00	6.00	6.00	6.00	6.00	6.00	6.00	6.00
Total	10.03	10.03	10.03	10.04	10.03	10.02	10.02	10.01	10.02	10.01	10.02	10.03	10.02	10.02	10.02
Mg no.	80.87	78.92	79.43	79.08	81.04	71.74	71.27	71.94	71.00	72.81	72.53	81.75	81.19	80.86	80.69

Orthopyroxene Analyses

	TM25					TM30				TM32				
Depth (m)	95.85					102.45				109.39				
Unit	M-pyrox	M-pyrox	M-pyrox	M-pyrox	M-Plat	M-Plat	M-Plat	M-Plat	M-Plat	M-Plat	M-Plat	M-Plat	M-Plat	M-Plat
Sample	TM25 opx1	TM25 opx2	TM25 opx3	TM25 opx4	TM25 opx5	TM30 opx1	TM30 opx2	TM30 opx3	TM30 opx4	TM32 opx1	TM32 opx2	TM32 opx3	TM32 opx4	TM32 opx5
Wt %														
SiO2	53.96	54.65	55.09	53.91	54.29	52.89	53.36	53.47	53.63	54.27	55.46	54.86	53.61	53.89
Al2O3	0.89	0.90	0.87	1.45	0.70	0.63	0.91	0.68	0.73	0.55	0.49	0.65	1.60	1.12
Na2O	nd	nd	nd	nd	nd	nd	nd	nd	nd	nd	nd	nd	nd	nd
MgO	28.45	30.64	30.74	29.77	28.67	23.98	24.31	24.08	25.32	27.42	26.98	27.39	27.41	27.27
FeO	11.62	11.82	11.52	12.34	13.76	20.33	19.81	20.64	19.49	15.10	15.51	15.39	15.03	15.22
MnO	0.23	0.18	0.23	0.24	0.27	0.43	0.38	0.38	0.39	0.40	0.40	0.36	0.45	0.50
Cr2O3	0.07	nd	0.08	0.16	0.10	nd	0.07	0.05	0.08	0.07	0.18	0.19	0.32	0.40
NiO	nd	nd	0.13	0.12	0.19	0.08	0.22	nd	0.05	nd	nd	nd	nd	nd
K2O	nd	nd	nd	nd	nd	nd	nd	nd	nd	nd	nd	nd	nd	nd
CaO	1.33	1.04	1.07	0.89	1.26	1.14	1.44	1.09	0.98	0.99	1.25	0.95	0.56	0.77
TiO2	0.18	0.20	0.23	0.16	0.22	0.14	0.20	0.12	0.15	0.25	0.28	0.28	0.24	0.26
Total	96.75	99.45	99.96	99.04	99.46	99.64	100.73	100.51	100.86	99.04	100.57	100.09	99.24	99.46
Cations (based on 6 oxygens)														
Si	1.98	1.95	1.96	1.94	1.96	1.97	1.96	1.97	1.96	1.98	1.99	1.98	1.95	1.96
Al	0.04	0.04	0.04	0.06	0.03	0.03	0.04	0.03	0.03	0.02	0.02	0.03	0.07	0.05
Na	0.00	0.00	0.00	0.00	0.00	0.00	0.00	0.00	0.00	0.00	0.00	0.00	0.00	0.00
Mg	1.56	1.63	1.63	1.60	1.54	1.33	1.33	1.32	1.38	1.49	1.44	1.47	1.48	1.48
Fe	0.36	0.35	0.34	0.37	0.42	0.63	0.61	0.64	0.60	0.46	0.47	0.46	0.46	0.46
Mn	0.01	0.01	0.01	0.01	0.01	0.01	0.01	0.01	0.01	0.01	0.01	0.01	0.01	0.02
Cr	0.00	0.00	0.00	0.01	0.00	0.00	0.00	0.00	0.00	0.00	0.01	0.01	0.01	0.01
Ni	0.00	0.00	0.00	0.00	0.01	0.00	0.01	0.00	0.00	0.00	0.00	0.00	0.00	0.00
K	0.00	0.00	0.00	0.00	0.00	0.00	0.00	0.00	0.00	0.00	0.00	0.00	0.00	0.00
Ca	0.05	0.04	0.04	0.03	0.05	0.05	0.06	0.04	0.04	0.04	0.05	0.04	0.02	0.03
Ti	0.01	0.01	0.01	0.00	0.01	0.00	0.01	0.00	0.00	0.01	0.01	0.01	0.01	0.01
O	6.00	6.00	6.00	6.00	6.00	6.00	6.00	6.00	6.00	6.00	6.00	6.00	6.00	6.00
Total	10.00	10.02	10.02	10.02	10.02	10.02	10.02	10.01	10.02	10.01	9.99	10.00	10.01	10.01
Mg no.	81.37	82.21	82.62	81.15	78.79	67.76	68.61	67.54	69.84	76.43	75.63	76.02	76.49	76.16

Orthopyroxene Analyses

	TM33					TM36				TM37				TM38		
Depth (m)	111.21					127.15				136.39				144.47		
Unit	M-Plat	M-Plat	M-Plat	M-Plat	M-Plat	L-Plat	L-Plat	L-Plat	L-Plat	L-Plat	L-Plat	L-Plat	L-Plat	L-Plat	L-Plat	L-Plat
Sample	TM33 opx1	TM33 opx2	TM33 opx3	TM33 opx4	TM33 opx5	TM36 opx1	TM36 opx2	TM36 opx3	TM36 opx4	TM37 opx1	TM37 opx2	TM37 opx3	TM37 opx4	TM38 opx1	TM38 opx2	TM38 opx3
Wt %																
SiO2	53.96	54.21	52.81	53.95	53.30	53.932	53.185	53.931	54.114	54.145	53.905	53.446	54.09	54.493	55.22	54.421
Al2O3	1.80	2.88	2.51	2.42	2.72	1.395	1.711	1.763	1.487	1.113	1.404	1.193	0.97	1.596	1.158	1.599
Na2O	0.06	nd	nd	nd	nd	0.032	0.013	0	0.121	0	0	0.189	0.064	0	0	0
MgO	25.72	26.70	26.64	26.93	26.49	28.802	28.413	28.366	28.321	26.582	28.577	26.409	27.298	30.453	30.682	28.745
FeO	16.74	16.43	16.15	16.29	16.52	13.815	13.461	13.813	13.431	16.083	13.87	15.304	15.202	12.014	11.958	13.853
MnO	0.32	0.26	0.27	0.32	0.29	0.178	0.194	0.253	0.294	0.283	0.263	0.319	0.221	0.267	0.291	0.247
Cr2O3	0.12	nd	nd	nd	0.30	0.103	0.123	0.088	0.116	0.193	0	0.158	0.129	0.094	0.031	0.077
NiO	nd	nd	nd	0.06	nd	nd	nd	nd	nd	nd	nd	nd	nd	nd	nd	nd
K2O	nd	nd	nd	nd	nd	0	0	0	0	0	0	0	0	0	0	0
CaO	1.36	0.21	0.18	0.08	0.11	0.699	1.079	1.055	1.045	1.645	1.365	2.722	0.777	0.802	0.6	0.779
TiO2	0.20	0.10	0.16	0.23	0.13	0.263	0.104	0.228	0.215	0.386	0.284	0.38	0.138	0.09	0.132	0.284
Total	100.28	100.80	98.72	100.29	99.86	99.48	98.282	99.498	99.144	100.43	99.669	100.12	98.89	99.809	100.073	100.004
Cations (based on 6 oxygens)																
Si	1.95	1.94	1.93	1.94	1.93	1.946	1.938	1.942	1.953	1.955	1.941	1.94	1.97	1.939	1.956	1.947
Al	0.08	0.12	0.11	0.10	0.12	0.059	0.073	0.075	0.063	0.047	0.06	0.051	0.042	0.067	0.048	0.067
Na	0.00	0.00	0.00	0.00	0.00	0.002	0.001	0	0.008	0	0	0.013	0.005	0	0	0
Mg	1.39	1.43	1.45	1.45	1.43	1.549	1.544	1.523	1.524	1.431	1.534	1.429	1.482	1.616	1.621	1.533
Fe	0.51	0.49	0.49	0.49	0.50	0.417	0.41	0.416	0.405	0.486	0.418	0.465	0.463	0.358	0.354	0.415
Mn	0.01	0.01	0.01	0.01	0.01	0.005	0.006	0.008	0.009	0.009	0.008	0.01	0.007	0.008	0.009	0.007
Cr	0.00	0.00	0.00	0.00	0.01	0.003	0.004	0.003	0.003	0.006	0	0.005	0.004	0.003	0.001	0.002
Ni	0.00	0.00	0.00	0.00	0.00	0.00	0.00	0.00	0.00	0.00	0.00	0.00	0.00	0.00	0.00	0.00
K	0.00	0.00	0.00	0.00	0.00	0	0	0	0	0	0	0	0	0	0	0
Ca	0.05	0.01	0.01	0.00	0.00	0.027	0.042	0.041	0.04	0.064	0.053	0.106	0.03	0.031	0.023	0.03
Ti	0.01	0.00	0.00	0.01	0.00	0.007	0.003	0.006	0.006	0.01	0.008	0.01	0.004	0.002	0.004	0.008
O	6.00	6.00	6.00	6.00	6.00	6.00	6.00	6.00	6.00	6.00	6.00	6.00	6.00	6.00	6.00	6.00
Total	10.00	10.00	10.01	10.00	10.00	10.02	10.02	10.01	10.01	10.01	10.02	10.03	10.01	10.02	10.02	10.01
Mg no.	73.26	74.33	74.64	74.68	74.05	78.79	79.02	78.55	79.00	74.65	78.59	75.45	76.20	81.86	82.08	78.70

Clinopyroxene Analyses

	TM2			TM4	TM13						TM14			TM16	TM18
Depth (m)	31.78			38.94	74.49						77.09			80.61	84.69
Unit	U-Plat	U-Plat	U-Plat	U-Plat	M-Plat	M-Plat	M-Plat	M-Plat	M-Plat	M-Plat	M-Plat	M-Plat	M-Plat	M-Plat	M-Plat
sample	TM2cpx1	TM2cpx1	TM2cpx1	TM4cpx1	TM13cpx1	TM13cpx2	TM13cpx3	TM13cpx4	TM13cpx5	TM13cpx6	TM14cpx1	TM14cpx2	TM14cpx3	TM16cpx1	TM18cpx1
Wt %															
SiO2	49.98	51.54	50.25	50.70	51.33	50.89	51.35	50.41	50.86	51.86	51.32	51.20	50.39	51.62	52.55
Al2O3	2.21	2.55	2.26	2.65	1.40	1.37	1.53	1.30	1.40	1.55	2.10	1.97	2.27	2.03	2.08
Na2O	0.31	0.18	0.21	0.24	0.10	0.18	0.21	0.19	0.14	0.31	0.25	0.21	0.17	0.23	0.23
MgO	16.31	16.20	16.11	16.15	18.44	16.13	15.73	15.68	15.54	15.46	15.84	16.37	18.26	17.36	16.21
FeO	6.04	5.99	6.16	5.74	10.06	7.56	7.04	7.10	6.97	6.80	6.24	6.64	7.90	5.95	6.28
MnO	0.22	0.10	0.15	0.15	0.24	0.20	0.17	0.17	0.18	0.19	0.16	0.20	0.16	0.13	0.11
Cr2O3	0.48	0.54	0.37	0.72	0.28	0.24	0.25	0.35	0.29	0.26	0.64	0.36	0.60	0.42	0.34
NiO	nd	nd	nd	nd	nd	nd	nd	nd	nd	nd	nd	nd	nd	0.05	0.07
K2O	nd	nd	nd	nd	nd	nd	nd	nd	nd	nd	nd	nd	nd	nd	nd
CaO	22.88	22.76	23.18	23.42	17.06	22.24	22.89	22.92	22.91	22.83	22.88	21.37	18.34	22.06	22.92
TiO2	0.20	0.19	0.28	0.10	0.13	0.30	0.30	0.44	0.36	0.40	0.40	0.56	0.22	0.20	0.32
Total	98.63	100.05	98.98	99.86	99.04	99.12	99.46	98.56	98.65	99.67	99.83	98.87	98.30	100.04	101.10
Cations (based on 6 oxygens)															
Si	1.89	1.91	1.89	1.89	1.92	1.92	1.92	1.91	1.92	1.93	1.91	1.92	1.89	1.91	1.92
Al	0.10	0.11	0.10	0.12	0.06	0.06	0.07	0.06	0.06	0.07	0.09	0.09	0.10	0.09	0.09
Na	0.02	0.01	0.02	0.02	0.01	0.01	0.02	0.01	0.01	0.02	0.02	0.02	0.01	0.02	0.02
Mg	0.92	0.89	0.90	0.90	1.03	0.91	0.88	0.89	0.88	0.86	0.88	0.91	1.02	0.96	0.88
Fe	0.19	0.19	0.19	0.18	0.32	0.24	0.22	0.23	0.22	0.21	0.19	0.21	0.25	0.18	0.19
Mn	0.01	0.00	0.01	0.01	0.01	0.01	0.01	0.01	0.01	0.01	0.01	0.01	0.01	0.00	0.00
Cr	0.01	0.02	0.01	0.02	0.01	0.01	0.01	0.01	0.01	0.01	0.02	0.01	0.02	0.01	0.01
Ni	0.00	0.00	0.00	0.00	0.00	0.00	0.00	0.00	0.00	0.00	0.00	0.00	0.00	0.00	0.00
K	0.00	0.00	0.00	0.00	0.00	0.00	0.00	0.00	0.00	0.00	0.00	0.00	0.00	0.00	0.00
Ca	0.92	0.90	0.93	0.93	0.69	0.90	0.92	0.93	0.93	0.91	0.91	0.86	0.74	0.87	0.90
Ti	0.01	0.01	0.01	0.00	0.00	0.01	0.01	0.01	0.01	0.01	0.01	0.02	0.01	0.01	0.01
O	6.00	6.00	6.00	6.00	6.00	6.00	6.00	6.00	6.00	6.00	6.00	6.00	6.00	6.00	6.00
Total	10.07	10.03	10.06	10.05	10.04	10.05	10.04	10.05	10.04	10.03	10.04	10.03	10.05	10.05	10.03
Mg no.	82.84	82.84	82.30	83.41	76.58	79.18	79.96	79.73	79.91	80.21	81.90	81.45	80.49	83.86	82.16

Clinopyroxene Analyses

	TM19			TM22							TM24					
Depth (m)	86.6			91.13							94.4					
Unit	M-Plat	M-Plat	M-Plat	M-Plat	M-Plat	M-Plat	M-Plat	M-Plat	M-Plat	M-Plat	M-Plat	M-Plat	M-Plat	M-Plat	M-Plat	M-Plat
sample	TM19cpx1	TM19cpx2	TM19cpx3	TM22cpx1	TM22cpx2	TM22cpx3	TM22cpx4	TM22cpx5	TM22cpx6	TM22cpx7	TM24cpx1	TM24cpx2	TM24cpx3	TM24cpx4	TM24cpx5	TM24cpx6
Wt %																
SiO2	48.49	46.23	46.90	50.01	53.98	54.73	47.68	49.89	51.73	51.66	53.05	53.39	52.85	51.77	51.99	52.36
Al2O3	7.68	9.68	9.66	5.07	1.16	0.76	6.33	5.59	2.44	3.29	0.66	1.15	2.27	3.17	2.28	1.73
Na2O	0.10	0.14	0.19	0.16	0.06	nd	0.15	0.07	0.08	0.17	0.19	0.20	0.21	0.17	0.22	0.17
MgO	14.37	13.58	13.57	16.44	17.54	17.75	15.53	15.49	16.96	17.21	16.48	17.09	17.65	16.83	17.28	16.72
FeO	3.67	4.13	4.00	3.84	3.40	2.94	3.68	3.58	3.65	3.37	4.84	4.63	4.23	4.26	5.28	5.22
MnO	0.06	0.05	0.06	0.06	0.10	0.08	0.06	0.05	0.09	nd	0.16	0.12	0.11	0.06	0.13	0.14
Cr2O3	nd	0.06	0.05	0.05	0.05	0.07	0.10	0.08	0.05	0.07	0.06	0.09	0.06	0.10	0.09	nd
NiO	nd	nd	nd	0.03	0.02	0.03	nd	0.02	0.03	nd	nd	nd	0.16	nd	nd	nd
K2O	nd	nd	nd	nd	nd	nd	nd	nd	nd	nd	nd	nd	nd	nd	0.01	nd
CaO	25.31	24.97	24.97	24.43	25.05	25.60	24.95	24.98	24.61	24.32	24.04	23.64	23.06	23.59	22.44	23.28
TiO2	0.76	1.01	0.89	0.37	0.22	0.10	0.41	0.35	0.58	0.18	0.10	0.40	0.20	0.25	0.83	0.38
Total	100.46	99.86	100.30	100.45	101.58	102.09	98.90	100.10	100.20	100.30	99.57	100.70	100.77	100.21	100.55	100.04
Cations (based on 6 oxygens)																
Si	1.78	1.71	1.73	1.83	1.95	1.96	1.78	1.83	1.90	1.89	1.96	1.95	1.92	1.90	1.90	1.93
Al	0.33	0.42	0.42	0.22	0.05	0.03	0.28	0.24	0.11	0.14	0.03	0.05	0.10	0.14	0.10	0.08
Na	0.01	0.01	0.01	0.01	0.00	0.00	0.01	0.01	0.01	0.01	0.01	0.01	0.01	0.01	0.02	0.01
Mg	0.79	0.75	0.75	0.90	0.94	0.95	0.87	0.85	0.93	0.94	0.91	0.93	0.96	0.92	0.94	0.92
Fe	0.11	0.13	0.12	0.12	0.10	0.09	0.12	0.11	0.11	0.10	0.15	0.14	0.13	0.13	0.16	0.16
Mn	0.00	0.00	0.00	0.00	0.00	0.00	0.00	0.00	0.00	0.00	0.01	0.00	0.00	0.00	0.00	0.00
Cr	0.00	0.00	0.00	0.00	0.00	0.00	0.00	0.00	0.00	0.00	0.00	0.00	0.00	0.00	0.00	0.00
Ni	0.00	0.00	0.00	0.00	0.00	0.00	0.00	0.00	0.00	0.00	0.00	0.00	0.01	0.00	0.00	0.00
K	0.00	0.00	0.00	0.00	0.00	0.00	0.00	0.00	0.00	0.00	0.00	0.00	0.00	0.00	0.00	0.00
Ca	1.00	0.99	0.99	0.96	0.97	0.98	1.00	0.98	0.97	0.95	0.95	0.92	0.90	0.93	0.88	0.92
Ti	0.02	0.03	0.03	0.01	0.01	0.00	0.01	0.01	0.02	0.01	0.00	0.01	0.01	0.01	0.02	0.01
O	6.00	6.00	6.00	6.00	6.00	6.00	6.00	6.00	6.00	6.00	6.00	6.00	6.00	6.00	6.00	6.00
Total	10.04	10.05	10.04	10.05	10.02	10.02	10.07	10.04	10.04	10.04	10.03	10.02	10.03	10.03	10.03	10.03
Mg no.	87.53	85.44	85.83	88.39	90.15	91.51	88.28	88.53	89.23	90.10	85.84	86.82	88.11	87.52	85.34	85.08

Clinopyroxene Analyses

				TM25				TM26					TM31				
Depth(m)	94.4			95.85				99.86					107.24				
Unit	M-Plat	M-Plat	M-Plat	M-Plat	M-Plat	M-Plat	M-Plat	M-Plat	M-Plat	M-Plat	M-Plat	M-Plat	M-Plat	M-Plat	M-Plat	M-Plat	M-Plat
sample	TM24cpx7	TM24cpx8	TM24cpx9	TM25cpx1	TM25cpx2	TM25cpx3	TM25cpx4	TM26cpx1	TM26cpx2	TM26cpx3	TM26cpx4	TM26cpx5	TM31cpx1	TM31cpx2	TM31cpx3	TM31cpx4	TM31cpx5
Wt %																	
SiO2	52.76	53.02	52.36	52.09	52.48	52.52	51.86	47.47	48.97	50.33	48.16	51.65	54.65	58.30	55.01	53.07	52.12
Al2O3	1.72	2.06	2.03	2.35	1.75	1.52	1.86	6.68	5.58	4.33	6.55	2.63	1.23	0.00	0.61	1.34	2.02
Na2O	0.21	0.22	0.12	0.19	0.20	0.19	0.15	0.11	0.16	nd	0.20	0.10	0.21	nd	0.06	0.20	0.32
MgO	16.65	17.70	16.83	16.29	18.18	17.63	16.72	14.35	15.01	15.27	15.05	16.58	16.47	19.68	16.59	16.46	16.01
FeO	5.05	4.82	5.06	5.62	6.04	4.47	4.96	5.00	5.15	4.76	4.41	4.61	4.63	7.09	4.22	4.62	5.13
MnO	0.07	0.12	0.10	0.13	0.14	0.07	0.14	0.09	0.10	0.13	0.06	0.09	0.14	nd	0.10	0.13	0.15
Cr2O3	0.05	nd	nd	0.54	0.18	0.46	0.21	0.06	0.09	0.06	nd	0.05	0.21	nd	0.10	0.13	0.39
NiO	nd	nd	nd	nd	nd	nd	nd	nd	nd	nd	nd	nd	nd	nd	nd	nd	nd
K2O	nd	nd	nd	nd	nd	nd	0.03	nd	nd	nd	nd	nd	nd	nd	nd	nd	nd
CaO	23.46	22.15	23.66	21.03	20.45	22.85	23.54	23.86	24.23	24.33	24.34	23.46	22.96	13.33	24.37	22.88	21.63
TiO2	0.49	0.39	0.53	0.30	0.49	0.17	0.50	0.86	1.19	0.98	0.77	0.79	0.33	nd	0.06	0.36	0.39
Total	100.46	100.50	100.71	98.54	99.90	99.87	99.96	98.47	100.49	100.21	99.54	99.95	100.81	98.41	101.12	99.19	98.15
Cations (based on 6 oxygens)																	
Si	1.93	1.93	1.92	1.94	1.93	1.93	1.91	1.79	1.81	1.86	1.79	1.90	1.98	2.11	1.99	1.96	1.95
Al	0.07	0.09	0.09	0.10	0.08	0.07	0.08	0.30	0.24	0.19	0.29	0.11	0.05	0.00	0.03	0.06	0.09
Na	0.02	0.02	0.01	0.01	0.01	0.01	0.01	0.01	0.01	0.00	0.02	0.01	0.01	0.00	0.00	0.01	0.02
Mg	0.91	0.96	0.92	0.90	1.00	0.97	0.92	0.81	0.83	0.84	0.83	0.91	0.89	1.06	0.90	0.91	0.89
Fe	0.16	0.15	0.16	0.18	0.19	0.14	0.15	0.16	0.16	0.15	0.14	0.14	0.14	0.21	0.13	0.14	0.16
Mn	0.00	0.00	0.00	0.00	0.00	0.00	0.00	0.00	0.00	0.00	0.00	0.00	0.00	0.00	0.00	0.00	0.01
Cr	0.00	0.00	0.00	0.02	0.01	0.01	0.01	0.00	0.00	0.00	0.00	0.00	0.01	0.00	0.00	0.00	0.01
Ni	0.00	0.00	0.00	0.00	0.00	0.00	0.00	0.00	0.00	0.00	0.00	0.00	0.00	0.00	0.00	0.00	0.00
K	0.00	0.00	0.00	0.00	0.00	0.00	0.00	0.00	0.00	0.00	0.00	0.00	0.00	0.00	0.00	0.00	0.00
Ca	0.92	0.86	0.93	0.84	0.81	0.90	0.93	0.96	0.96	0.96	0.97	0.93	0.89	0.52	0.95	0.91	0.87
Ti	0.01	0.01	0.02	0.01	0.01	0.01	0.01	0.02	0.03	0.03	0.02	0.02	0.01	0.00	0.00	0.01	0.01
O	6.00	6.00	6.00	6.00	6.00	6.00	6.00	6.00	6.00	6.00	6.00	6.00	6.00	6.00	6.00	6.00	6.00
Total	10.02	10.02	10.03	10.00	10.03	10.03	10.04	10.04	10.04	10.03	10.05	10.02	9.99	9.90	10.00	10.01	10.00
Mg no.	85.43	86.73	85.55	83.78	84.25	87.58	85.74	83.68	83.86	85.09	85.88	86.50	86.41	83.19	87.49	86.37	84.79

Plagioclase Analyses

	TM4		TM9			TM15				TM16			TM 20		
Depth (m)	38.94		48.87			78.95				80.61			88.65		
Unit	U-Plat	U-Plat	U-Plat	U-Plat	U-Plat	M-Plat	M-Plat	M-Plat	M-Plat	M-Plat	M-Plat	M-Plat	M-Plat	M-Plat	M-Plat
Sample	TM4 pl1	TM4 pl2	TM9 pl1	TM9 pl2	TM9 pl3	TM15 pl1	TM15 pl2	TM15 pl3	TM15 pl4	TM16 pl1	TM16 pl2	TM16 pl3	TM 20 pl1	TM 20 pl2	TM 20 pl3
Wt %.															
SiO2	45.39	46.43	52.47	51.35	51.19	44.67	48.71	48.06	46.74	46.09	45.72	46.26	52.18	53.49	50.49
Al2O3	32.77	32.95	28.60	28.66	28.85	32.71	30.57	31.39	31.59	32.13	33.46	33.34	29.37	28.18	30.25
Na2O	1.99	2.02	4.98	4.69	4.47	2.07	2.91	3.21	2.14	2.02	1.78	1.88	4.59	4.96	4.01
MgO	nd	0.06	nd	nd	nd	nd	0.16	nd	1.89	0.89	nd	0.12	0.05	nd	nd
FeO	0.55	0.54	0.25	0.32	0.31	0.41	1.09	0.55	0.71	1.86	0.54	0.74	0.16	0.18	0.17
MnO	nd	nd	nd	nd	nd	nd	0.04	0.04	0.06	0.05	nd	0.02	nd	nd	nd
Cr2O3	nd	nd	nd	nd	0.04	nd	nd	nd	nd	nd	nd	nd	nd	nd	nd
NiO	0.02	nd	nd	nd	nd	nd	nd	nd	nd	nd	nd	nd	nd	nd	0.12
K2O	0.09	0.10	0.19	0.25	0.20	0.05	0.18	0.13	0.06	0.03	0.06	0.06	0.28	0.32	0.24
CaO	16.98	16.85	11.61	12.11	12.16	17.35	14.90	15.22	15.30	15.88	17.55	16.92	11.96	11.20	13.66
TiO2	nd	nd	nd	nd	nd	nd	nd	nd	nd	nd	nd	nd	0.06	nd	nd
Total	97.81	98.96	98.12	97.39	97.25	97.28	98.56	98.62	98.51	98.96	99.15	99.37	98.64	98.34	98.97
Cations (based on 32 oxygens)															
Si	8.57	8.65	9.70	9.59	9.57	8.50	9.09	8.96	8.73	8.63	8.52	8.59	9.60	9.84	9.32
Al	7.30	7.24	6.23	6.31	6.36	7.34	6.72	6.90	6.95	7.09	7.35	7.30	6.37	6.11	6.58
Na	0.73	0.73	1.78	1.70	1.62	0.76	1.05	1.16	0.78	0.73	0.64	0.68	1.64	1.77	1.44
Mg	0.00	0.02	0.00	0.00	0.00	0.01	0.05	0.01	0.53	0.25	0.01	0.03	0.01	0.00	0.00
Fe	0.09	0.09	0.04	0.05	0.05	0.07	0.17	0.09	0.11	0.29	0.09	0.12	0.02	0.03	0.03
Mn	0.00	0.00	0.00	0.00	0.00	0.00	0.01	0.01	0.01	0.01	0.00	0.00	0.00	0.00	0.00
Cr	0.00	0.00	0.00	0.00	0.01	0.00	0.00	0.00	0.00	0.00	0.00	0.00	0.00	0.00	0.00
Ni	0.00	0.00	0.00	0.00	0.00	0.00	0.00	0.00	0.00	0.00	0.00	0.00	0.00	0.00	0.02
K	0.02	0.03	0.05	0.06	0.05	0.01	0.04	0.03	0.02	0.01	0.01	0.01	0.07	0.08	0.06
Ca	3.44	3.36	2.30	2.42	2.43	3.54	2.98	3.04	3.06	3.19	3.51	3.37	2.36	2.21	2.70
Ti	0.00	0.00	0.00	0.00	0.00	0.00	0.00	0.00	0.00	0.00	0.00	0.00	0.01	0.00	0.00
O	32.00	32.00	32.00	32.00	32.00	32.00	32.00	32.00	32.00	32.00	32.00	32.00	32.00	32.00	32.00
Total	52.15	52.11	52.10	52.13	52.09	52.22	52.10	52.19	52.19	52.20	52.13	52.10	52.06	52.03	52.14
An	82.1	81.7	55.7	58.0	59.4	82.0	73.1	71.9	79.5	81.1	84.2	83.0	58.1	54.5	64.4

Plagioclase Analyses

				TM 24	TM 30				TM 32				
Depth (m)	88.65			94.4	102.45				109.39				
Unit	M-Plat	M-Plat	M-Plat	M-Plat	M-Plat	M-Plat	M-Plat	M-Plat	M-Plat	M-Plat	M-Plat	M-Plat	M-Plat
Sample	TM 20 pl4	TM 20 pl5	TM 20 pl6	TM 24 pl1	TM 30 pl1	TM 30 pl2	TM 30 pl3	TM 30 pl4	TM 32 pl1	TM 32 pl2	TM 32 pl3	TM 32 pl8	TM 32 pl10
Wt %.													
SiO2	48.99	51.03	50.82	46.86	46.92	47.93	49.19	49.24	49.09	51.91	49.99	49.03	48.88
Al2O3	31.30	30.03	30.55	32.78	33.17	33.15	31.85	32.12	32.68	30.57	32.72	32.63	32.42
Na2O	3.32	4.42	3.78	2.34	2.04	2.43	3.01	3.11	2.99	4.35	3.01	2.78	3.10
MgO	nd	0.04	0.04	0.05	nd	nd	nd	0.05	nd	nd	nd	nd	nd
FeO	0.23	0.21	0.19	0.38	0.56	0.62	0.44	0.40	0.22	0.17	0.20	0.17	0.08
MnO	nd	nd	nd	nd	nd	0.05	nd	nd	nd	nd	nd	nd	nd
Cr2O3	nd	nd	nd	0.04	nd	nd	nd	nd	nd	nd	nd	nd	0.04
NiO	nd	nd	nd	nd	nd	nd	nd	nd	nd	nd	nd	nd	nd
K2O	0.19	0.30	0.22	0.10	0.08	0.09	0.16	0.10	0.06	0.13	0.10	0.07	0.05
CaO	14.06	12.37	13.38	16.17	17.09	16.34	15.07	15.38	14.81	12.45	14.59	14.71	14.43
TiO2	nd	nd	nd	nd	nd	nd	nd	nd	nd	nd	nd	nd	0.06
Total	98.12	98.45	99.02	98.71	99.92	100.63	99.78	100.41	99.86	99.60	100.66	99.41	99.06
Cations (based on 32 oxygens)													
Si	9.12	9.43	9.34	8.73	8.66	8.77	9.03	8.99	8.98	9.46	9.06	9.00	9.00
Al	6.87	6.54	6.62	7.20	7.22	7.15	6.89	6.91	7.04	6.56	6.99	7.06	7.04
Na	1.20	1.58	1.35	0.85	0.73	0.86	1.07	1.10	1.06	1.54	1.06	0.99	1.11
Mg	0.00	0.01	0.01	0.01	0.01	0.00	0.01	0.02	0.00	0.00	0.00	0.00	0.00
Fe	0.04	0.03	0.03	0.06	0.09	0.10	0.07	0.06	0.03	0.03	0.03	0.03	0.01
Mn	0.00	0.00	0.00	0.00	0.00	0.01	0.00	0.00	0.00	0.00	0.00	0.00	0.00
Cr	0.00	0.00	0.00	0.01	0.00	0.00	0.00	0.00	0.00	0.00	0.00	0.00	0.01
Ni	0.00	0.00	0.00	0.00	0.00	0.00	0.00	0.00	0.00	0.00	0.00	0.00	0.00
K	0.05	0.07	0.05	0.02	0.02	0.02	0.04	0.02	0.01	0.03	0.02	0.02	0.01
Ca	2.80	2.45	2.64	3.23	3.38	3.20	2.96	3.01	2.90	2.43	2.83	2.89	2.85
Ti	0.00	0.00	0.00	0.00	0.00	0.00	0.00	0.00	0.00	0.00	0.00	0.00	0.01
O	32.00	32.00	32.00	32.00	32.00	32.00	32.00	32.00	32.00	32.00	32.00	32.00	32.00
Total	52.07	52.12	52.04	52.10	52.11	52.10	52.08	52.12	52.04	52.04	51.99	51.98	52.03
An	69.3	59.7	65.3	78.8	81.9	78.4	72.8	72.8	73.0	60.8	72.3	74.2	71.8

Plagioclase Analyses

	TM 33					TM37
Depth (m)	111.21					136.39
Unit	M-Plat	M-Plat	M-Plat	M-Plat	M-Plat	L-Plat
Sample	TM 33 pl1	TM 33 pl2	TM 33 pl8	TM 33 pl9	TM 33 pl10	TM37pl1
Wt %.						
SiO2	60.40	60.51	53.28	52.01	49.14	49.52
Al2O3	24.82	24.19	29.74	30.17	33.35	34.12
Na2O	7.68	7.93	4.97	4.64	2.61	3.24
MgO	nd	nd	nd	nd	nd	0.02
FeO	0.06	0.10	0.15	0.24	0.19	0.40
MnO	nd	nd	nd	nd	nd	0.00
Cr2O3	nd	0.04	nd	nd	0.05	0.02
NiO	nd	nd	nd	nd	nd	nd
K2O	0.72	0.60	0.30	0.28	0.09	0.20
CaO	5.95	5.25	10.99	11.40	15.25	14.75
TiO2	nd	0.05	nd	nd	nd	0.01
Total	99.63	98.66	99.50	98.77	100.70	102.28
Cations (based on 32 oxygens)						
Si	10.80	10.90	9.68	9.54	8.91	8.87
Al	5.23	5.13	6.37	6.52	7.13	7.20
Na	2.66	2.77	1.75	1.65	0.92	1.13
Mg	0.00	0.00	0.00	0.00	0.00	0.00
Fe	0.01	0.02	0.02	0.04	0.03	0.06
Mn	0.00	0.00	0.00	0.00	0.00	0.00
Cr	0.00	0.01	0.00	0.00	0.01	0.00
Ni	0.00	0.00	0.00	0.00	0.00	0.00
K	0.16	0.14	0.07	0.07	0.02	0.05
Ca	1.14	1.01	2.14	2.24	2.96	2.83
Ti	0.00	0.01	0.01	0.00	0.00	0.00
O	32.00	32.00	32.00	32.00	32.00	32.00
Total	52.00	51.98	52.04	52.06	51.99	52.12
An	28.7	25.8	54.1	56.6	75.9	70.7

Olivine Analyses

	TM4					TM11			TM15			TM16			
Depth (m)	38.94					57.54			78.95			80.61			
Unit	U-Plat	U-Plat	U-Plat	U-Plat	U-Plat	U-Plat	U-Plat	U-Plat	M-Plat	M-Plat	M-Plat	M-Plat	M-Plat	M-Plat	M-Plat
sample	TM4 ol1	TM4 ol2	TM4 ol3	TM4 ol4	TM4 ol5	TM11 ol1	TM11 ol2	TM11 ol3	TM15 ol1	TM15 ol2	TM15 ol3	TM16 ol1	TM16 ol2	TM16 o3	TM16 ol4
Wt %															
SiO2	37.68	38.47	37.63	37.79	37.32	38.61	38.47	38.74	37.81	38.33	40.05	37.71	38.70	38.68	38.79
Al2O3	0.00	0.00	0.00	0.00	0.00	nd	nd	nd	0.00	0.00	0.00	0.00	0.00	0.00	0.00
Na2O	nd	nd	nd	nd	nd	nd	nd	0.05	0.08	0.05	nd	nd	nd	nd	nd
MgO	43.55	43.05	41.62	43.03	43.10	44.03	43.36	44.61	41.45	41.17	42.41	42.45	40.92	42.44	41.09
FeO	17.67	17.92	18.62	18.39	18.09	16.67	17.41	16.37	20.21	20.24	14.91	18.63	19.35	18.70	19.70
MnO	0.26	0.25	0.28	0.31	0.31	0.30	0.21	0.24	0.36	0.36	0.27	0.28	0.32	0.31	0.31
Cr2O3	nd	nd	nd	nd	nd	nd	nd	nd	nd	nd	nd	0.03	nd	nd	nd
NiO	0.26	0.29	0.28	0.32	0.34	0.19	0.20	0.19	0.31	0.28	0.21	0.31	0.31	0.30	0.30
K2O	nd	nd	nd	nd	nd	nd	nd	nd	nd	nd	nd	nd	nd	nd	nd
CaO	0.05	0.06	0.03	0.05	nd	nd	nd	nd	nd	0.04	nd	nd	nd	0.06	0.05
TiO2	nd	nd	nd	nd	nd	nd	nd	nd	nd	nd	nd	nd	nd	nd	nd
Total	99.47	100.06	98.46	99.90	99.22	99.83	99.68	100.24	100.22	100.46	97.87	99.42	99.62	100.49	100.29
Cations (based on 4 oxygens)															
Si	0.97	0.98	0.98	0.97	0.97	0.98	0.98	0.98	0.98	0.99	1.03	0.97	1.00	0.99	1.00
Al	0.00	0.00	0.00	0.00	0.00	0.00	0.00	0.00	0.00	0.00	0.00	0.00	0.00	0.00	0.00
Na	0.00	0.00	0.00	0.00	0.00	0.00	0.00	0.00	0.00	0.00	0.00	0.00	0.00	0.00	0.00
Mg	1.67	1.64	1.62	1.65	1.66	1.67	1.65	1.68	1.60	1.58	1.62	1.64	1.57	1.61	1.57
Fe	0.38	0.38	0.41	0.40	0.39	0.36	0.37	0.35	0.44	0.44	0.32	0.40	0.42	0.40	0.42
Mn	0.01	0.01	0.01	0.01	0.01	0.01	0.00	0.01	0.01	0.01	0.01	0.01	0.01	0.01	0.01
Cr	0.00	0.00	0.00	0.00	0.00	0.00	0.00	0.00	0.00	0.00	0.00	0.00	0.00	0.00	0.00
Ni	0.01	0.01	0.01	0.01	0.01	0.00	0.00	0.00	0.01	0.01	0.00	0.01	0.01	0.01	0.01
K	0.00	0.00	0.00	0.00	0.00	0.00	0.00	0.00	0.00	0.00	0.00	0.00	0.00	0.00	0.00
Ca	0.00	0.00	0.00	0.00	0.00	0.00	0.00	0.00	0.00	0.00	0.00	0.00	0.00	0.00	0.00
Ti	0.00	0.00	0.00	0.00	0.00	0.00	0.00	0.00	0.00	0.00	0.00	0.00	0.00	0.00	0.00
O	4.00	4.00	4.00	4.00	4.00	4.00	4.00	4.00	4.00	4.00	4.00	4.00	4.00	4.00	4.00
Total	7.03	7.02	7.02	7.03	7.04	7.02	7.02	7.02	7.03	7.02	6.97	7.03	7.00	7.01	7.01
fo	81.24	80.86	79.70	80.40	80.68	82.22	81.44	82.72	78.22	78.08	83.28	80.01	78.76	79.92	78.54

Olivine Analyses

			TM18				
Depth (m)	80.61		84.69				
Unit	M-Plat	M-Plat	M-Plat	M-Plat	M-Plat	M-Plat	M-Plat
sample	TM16 ol5	TM16 ol6	TM18 ol1	TM18 ol2	TM18 ol2	TM18 ol3	TM18 ol4
Wt %							
SiO2	38.67	38.45	38.64	38.68	36.87	38.64	39.06
Al2O3	0.00	0.00	0.00	0.00	0.00	0.00	0.00
Na2O	nd	nd	nd	0.05	nd	nd	nd
MgO	42.72	41.47	41.46	41.28	43.11	42.24	41.82
FeO	18.37	19.60	19.48	19.90	19.22	19.69	19.68
MnO	0.30	0.25	0.25	0.26	0.28	0.26	0.25
Cr2O3	nd	nd	nd	nd	nd	nd	nd
NiO	0.32	0.31	0.39	0.37	0.41	0.37	0.39
K2O	nd	nd	nd	nd	nd	nd	nd
CaO	nd	nd	0.06	0.06	0.06	0.03	0.08
TiO2	nd	nd	nd	nd	nd	nd	nd
Total	100.39	100.10	100.28	100.60	99.95	101.26	101.30
Cations (based on 4 oxygens)							
Si	0.99	0.99	0.99	0.99	0.95	0.98	0.99
Al	0.00	0.00	0.00	0.00	0.00	0.00	0.00
Na	0.00	0.00	0.00	0.00	0.00	0.00	0.00
Mg	1.62	1.59	1.59	1.58	1.66	1.60	1.58
Fe	0.39	0.42	0.42	0.43	0.42	0.42	0.42
Mn	0.01	0.01	0.01	0.01	0.01	0.01	0.01
Cr	0.00	0.00	0.00	0.00	0.00	0.00	0.00
Ni	0.01	0.01	0.01	0.01	0.01	0.01	0.01
K	0.00	0.00	0.00	0.00	0.00	0.00	0.00
Ca	0.00	0.00	0.00	0.00	0.00	0.00	0.00
Ti	0.00	0.00	0.00	0.00	0.00	0.00	0.00
O	4.00	4.00	4.00	4.00	4.00	4.00	4.00
Total	7.01	7.01	7.01	7.01	7.05	7.02	7.01
fo	80.31	78.83	78.93	78.49	79.76	79.05	78.91

Appendix V

MAJOR ELEMENT, TRACE ELEMENT AND PGE

WHOLE ROCK XRF ANALYSES

sample	P1	P3	P5	P7	P8	P10	P13	P14	P15	P19	P21	P22	P23	P24	P26	P28	P30	P31	P33
depth (m)	30.4	34.91	44.77	57.7	62.65	68.3	80.75	86.42	89.55	102.35	110.95	112.75	118.95	126.9	145.6	170.4	189.95	197.37	213
SiO2	52.37	52.19	52.03	43.18	52.65	50.35	39.37	45.26	45.55	43.49	48.11	38.01	56.16	50.97	50.97	63.09	35.55	39.90	20.02
TiO2	0.15	0.16	0.30	0.23	0.16	0.34	0.22	0.30	0.19	0.19	0.33	1.04	0.30	0.19	0.38	1.01	0.18	1.81	0.21
Al2O3	7.43	7.20	10.38	5.56	22.57	12.23	4.43	7.24	7.88	7.52	7.97	24.67	11.92	14.16	9.76	13.59	7.96	16.74	3.75
Fe2O3	10.94	11.77	6.93	19.15	5.70	14.52	21.67	11.10	18.17	19.00	9.44	23.41	11.36	10.28	14.17	12.72	4.55	27.74	2.12
MnO	0.21	0.24	0.14	0.21	0.09	0.23	0.18	0.14	0.18	0.18	0.17	0.16	0.20	0.18	0.21	0.09	0.17	0.13	0.07
MgO	21.31	20.97	10.05	21.58	5.48	16.39	19.71	23.59	18.83	21.14	21.15	6.52	12.59	14.05	15.81	2.97	42.66	5.45	28.43
CaO	6.65	6.52	18.24	3.24	9.21	3.83	6.82	10.35	3.60	4.77	11.96	3.85	5.99	8.15	6.19	3.26	7.88	3.80	45.31
Na2O	0.13	0.04	1.07	0.01	3.41	1.65	0.01	0.01	0.01	0.01	0.01	1.55	0.07	1.06	0.01	2.36	0.01	3.27	0.00
K2O	0.27	0.29	0.68	0.34	0.47	0.15	0.14	0.35	0.49	0.43	0.35	0.34	1.15	0.58	0.78	0.31	0.02	0.62	0.01
P2O5	0.01	0.01	0.04	0.05	0.03	0.02	0.02	0.03	0.03	0.03	0.03	0.03	0.05	0.20	0.06	0.05	0.01	0.03	0.08
Cr2O3	0.42	0.46	0.04	0.30	0.07	0.23	0.20	0.04	0.10	0.07	0.04	0.07	0.18	0.10	0.36	0.03	0.01	0.10	0.00
Ni	0.06	0.06	0.03	0.73	0.01	0.03	1.42	0.28	0.76	0.43	0.08	0.01	0.02	0.03	0.20	0.01	0.00	0.02	0.00
S	0.04	0.07	0.08	4.98	0.13	0.01	5.45	1.16	3.37	2.29	0.30	0.33	0.01	0.02	0.72	0.50	0.98	0.37	0.00
Cu	0.02	0.01	0.00	0.43	0.00	0.00	0.35	0.15	0.85	0.46	0.06	0.00	0.00	0.00	0.36	0.00	0.00	0.01	0.00
TOTAL	100.00	100.00	100.00	100.00	100.00	100.00	100.00	100.00	100.00	100.00	100.00	100.00	100.00	100.00	100.00	100.00	100.00	100.00	100.00
LOI	0.43	1.13	1.58	4.27	1.44	*	4.78	5.60	3.35	4.88	2.80	1.31	1.07	1.16	1.83	1.69	13.85	*	37.41
Trace elements (ppm)																			
As	3	3	3	10	3	3	6	6	3	9	3	3	4	3	6	6	3	6	4
Cu	153	135	14	4274	9	4	3533	1471	8510	4648	609	39	5	47	3609	6	5	125	3
Ga	8	8	12	9	22	14	8	8	11	10	10	43	11	14	12	22	11	40	7
Mo	1	1	1	3	1	1	1	1	2	1	2	1	2	2	2	1	1	2	3
Nb	3	2	4	5	2	3	2	4	3	2	5	3	3	3	3	7	6	4	7
Ni	583	629	281	7346	120	302	14166	2818	7568	4292	775	122	237	343	2039	63	27	241	15
Pb	6	13	17	31	16	9	37	34	28	10	22	16	5	37	11	9	3	13	6
Rb	12	12	32	19	16	3	10	17	27	24	16	20	42	22	35	11	6	21	4
Sr	149	106	170	174	650	355	74	107	231	156	201	755	344	308	417	439	15	640	158
Th	3	3	3	5	3	3	6	3	3	3	3	6	6	7	4	4	12	7	6
U	3	3	3	3	3	3	3	3	3	3	3	3	3	3	3	3	3	3	4
W	6	6	6	6	6	6	6	6	6	6	6	6	6	6	6	6	7	6	8
Y	6	7	31	9	7	11	11	13	11	10	19	7	11	13	14	21	7	8	14
Zn	83	112	70	144	56	128	111	78	144	120	71	186	196	88	83	74	75	200	26
Zr	19	20	54	33	21	31	35	58	67	43	60	56	36	37	42	212	22	39	80
Cl	165	343	784	359	326	180	710	1034	781	917	828	177	195	597	264	349	2771	262	2500
Co	89	93	41	308	25	90	294	96	174	177	68	96	72	67	115	53	19	112	3
Cr	2876	3116	257	2080	463	1576	1391	261	660	446	294	454	1210	697	2470	238	71	701	18
F	922	1914	2596	1184	2109	692	5110	6355	2103	6316	4109	242	1564	2960	1447	1661	6190	153	7783
Sc	19	22	41	12	2	40	7	7	11	8	8	7	33	16	22	11	2	18	1
V	100	102	80	66	33	108	83	80	66	62	92	213	148	70	116	151	7	377	17
ppb																			
Rh	21.6	4.2	0.3	86.4	0.4	1.4	107.7	7.1	34.9	28.6	1.8	0.9	1.6	5.3	8.6	<0.6	na	0.7	na
Pd	112	44	4	1665	<6	<6	3409	1142	953	724	307	4	5	34	247	<6.8	na	5	na
Re	0.3	<0.3	<0.1	13.3	<0.4	<0.4	28.2	4.2	<0.6	5.0	<0.3	0.1	0.1	0.3	0.8	<0.23	na	<0.2	na
Au	7.0	7.7	0.5	191.0	0.5	0.6	142.6	79.1	186.0	99.4	21.7	1.3	1.0	3.0	49.1	0.4	na	1.0	na
Os	8.4	1.5	<1.1	20.1	<1.5	0.9	21.6	2.5	6.3	4.4	1.0	<1.1	0.7	1.9	1.9	<1.0	na	<0.9	na
Ir	7.49	2.01	0.14	21.85	0.14	0.58	24.75	1.07	10.22	6.21	0.24	0.48	0.60	2.05	2.11	0.15	na	0.17	na
Ru	58	12	<4	106	<5.9	2	35	<7.3	<9.3	18	<4.6	<4.0	4	8	7	<3.2	na	3	na
Pt	319	64	8	1592	8	21	727	633	311	253	125	5	23	72	177	3	na	6	na

* = not detected, < = below detection limit

Appendix VI

BOREHOLE LOG (PROVIDED BY FALCONBRIDGE VENTURES OF AFRICA)

Hole ID: TL01-3

From	To	DESCREPTION
31.55	32.20	Medium-grained, slightly felspathic pyroxenite, slightly magnetic. 2-5% interstitial pyrrhotite>chalcopyrite.
32.20	33.15	Medium-grained pyroxenite. 3 mm carbonate vein. Fine to medium-grained zones. Slightly magnetic. 2-5% fine to coarse interstitial - blebby pyrrhotite>chalcopyrite.
33.15	33.70	Medium to coarse-grained altered/contaminated magnetic metasediment. Epidotized with narrow pyroxenite zones. 1-2% interstitial pyrrhotite>chalcopyrite.
33.70	34.68	Medium-grained, slightly felspathic pyroxenite. 1-2% pyrrhotite>=chalcopyrite. at upper contact, chloritized veins. Slightly magnetic.
34.68	35.43	Medium-grained, slightly felspathic pyroxenite, slightly magnetic. 2% pyrrhotite>chalcopyrite. over a 6cm zone at 35.10 m. Variable texture.
35.43	36.54	Medium-grained, slightly felspathic pyroxenite, coarser grained zone. Slightly magnetic. 1-2% pyrrhotite= chalcopyrite., finely disseminated.
36.54	37.45	Medium-grained, slightly felspathic pyroxenite, coarser grained zones. Moderately - strongly magnetic. Coarse magnetite. Trace pyrrhotite.
37.45	38.59	Medium-grained, slightly felspathic pyroxenite, coarser grained zones. Moderately - strongly magnetic. Coarse magnetite. Trace pyrrhotite.
38.59	39.47	Medium-grained, slightly felspathic pyroxenite. Slightly magnetic. 2% interstitial pyrrhotite>chalcopyrite.
39.47	39.95	Medium-grained, slightly felspathic pyroxenite with coarser grained zones. Slightly magnetic. Trace pyrrhotite.
39.95	40.75	Fine to medium-grained, highly magnetic meta-sediment with massive magnetite. Strongly magnetic. Trace pyrite.
40.75	41.44	Fine to medium-grained, highly magnetic meta-sediment with massive magnetite. Strongly magnetic. Trace pyrite.
41.44	42.56	Medium-grained, feldspathic pyroxenite, weakly magnetic. Trace, fine interstitial pyrrhotite.
42.56	43.52	Medium-grained, feldspathic pyroxenite, weakly magnetic. Trace, fine interstitial pyrrhotite.
43.52	44.52	Medium-grained, feldspathic pyroxenite, weakly magnetic. Trace, fine interstitial pyrrhotite.
44.52	45.60	Medium-grained, feldspathic pyroxenite, weakly magnetic. Trace, fine interstitial pyrrhotite.
45.60	46.35	Medium-grained, feldspathic pyroxenite weakly magnetic. Trace, fine interstitial pyrrhotite.
46.35	47.05	Medium-grained, feldspathic pyroxenite weakly magnetic. Trace, fine interstitial pyrrhotite.
47.05	48.01	Fine to medium-grained, altered/contaminated meta-sediment and minor felspathic pyroxenite. Highly magnetic. 6cm wide epidote zone. Trace fine pyrrhotite.
48.01	48.92	Fine to medium-grained, altered/contaminated meta-sediment and minor felspathic pyroxenite. Highly magnetic. Trace fine pyrrhotite.
48.92	50.00	Medium-grained, feldspathic pyroxenite, weakly magnetic. Trace, fine interstitial pyrrhotite.
50.00	51.00	Medium-grained, feldspathic pyroxenite, weakly magnetic. Trace, fine interstitial pyrrhotite.
51.00	52.00	Medium-grained, feldspathic pyroxenite, weakly magnetic. Trace, fine interstitial pyrrhotite.
52.00	53.05	Medium-grained, feldspathic pyroxenite, weakly magnetic. Trace, fine interstitial pyrrhotite.
53.05	53.61	Medium-grained, feldspathic pyroxenite, granite appearance. Moderately magnetic. Trace pyrrhotite.
53.61	54.62	Medium-grained, feldspathic pyroxenite, weakly magnetic. Trace, fine interstitial pyrrhotite.
54.62	55.63	Medium-grained, feldspathic pyroxenite, weakly magnetic. Trace, fine interstitial pyrrhotite.
55.63	56.15	Medium-grained, feldspathic pyroxenite, weakly magnetic. Up to 2% fine to blebby interstitial pyrrhotite.
56.15	56.61	Medium-grained, meta-sediment (quartzite), highly magnetic in places with massive magnetite. Narrow pyroxenite zone.
56.61	57.06	Medium-grained, feldspathic pyroxenite, moderately magnetic. Finer grained towards lower contact. Trace pyrrhotite.
57.06	57.96	Medium-grained, slightly felspathic pyroxenite. Slightly magnetic. Fine to blebby interstitial pyrrhotite>chalcopyrite up to 2%. 10cm wide 10-20%pyrrhotite>chalcopyrite (57.63 - 57.73 m).
57.96	58.75	Medium-grained, slightly felspathic pyroxenite. Slightly magnetic. Trace pyrrhotite. Small xenolith of magnetic meta-sediment.
58.75	59.55	Medium-grained meta-sediment. Narrow felspathic zones, highly magnetic.
59.55	60.64	Medium-grained, feldspathic pyroxenite. Weakly magnetic with trace pyrrhotite.
60.64	61.78	Medium-grained, feldspathic pyroxenite. Weakly magnetic with trace pyrrhotite.
61.78	62.83	Medium-grained, feldspathic pyroxenite. Weakly magnetic with trace pyrrhotite. Magnetic meta-sediment xenolith 61.78 - 61.84 m.
62.83	63.84	Fine to medium-grained highly magnetic meta-sediment xenolith with fine interstitial magnetite throughout and in places massive.
63.84	64.85	Fine to medium-grained highly magnetic meta-sediment xenolith with fine interstitial magnetite throughout and in places massive.
64.85	65.90	Fine to medium-grained highly magnetic meta-sediment xenolith with fine interstitial magnetite throughout and in places massive. Narrow pyroxenite zone.
65.90	66.95	Fine to medium-grained highly magnetic sedimentary xenolith. Massive magnetite and trace pyrite. Narrow carbonate vein and fine grained mudstone layer? 67.54 - 67.64 m (75° contacts)
67.75	68.40	Fine to medium-grained moderately magnetic mudstone layer.
68.40	69.50	Medium-grained highly magnetic sedimentary xenolith. Massive magnetite in narrow (<2cm wide) zones and as blebs. Carbonate filled vugs (Zeolite). Trace pyrite.
69.50	70.39	Medium-grained highly magnetic sedimentary xenolith. Massive magnetite in narrow (<2cm wide) zones and as blebs. Carbonate filled vugs (Zeolite). Trace pyrite.
70.39	71.28	Medium-grained highly magnetic sedimentary xenolith. Massive magnetite in narrow (<2cm wide) zones and as blebs, becoming mottled more contaminated and chloritized. Trace pyrite.
71.28	72.50	Medium-grained highly magnetic sedimentary xenolith. Massive magnetite in narrow (<2cm wide) zones and as blebs, becoming mottled more contaminated and chloritized. Trace pyrite.
72.50	73.60	Medium-grained highly magnetic sedimentary xenolith. Massive magnetite in narrow (<2cm wide) zones and as blebs, becoming mottled more contaminated and chloritized. Trace pyrite. 5 mm carbonate filled vein (zeolite).
73.60	74.10	Medium-grained pyroxenite, slightly felspathic to 73.75 m. Weakly magnetic. 2 - 5% interstitial pyrrhotite=chalcopyrite
74.10	74.47	Fine-grained pyroxenite, zone, fine interstitial pyrrhotite to 2%. Weakly magnetic.
74.47	75.43	Medium-grained pyroxenite, slightly felspathic. Interstitial to blebby pyrrhotite>chalcopyrite to 10%. Minor pyrrhotite along fractures. Fine-grained pyroxenite between 74.97 - 75.05 m. Weakly magnetic.
75.43	76.25	Medium-grained pyroxenite, minor felspar. Moderately magnetic. Fine interstitial to blebby pyrrhotite>chalcopyrite to 5 - 10%.
76.25	77.04	Medium-grained pyroxenite, minor felspar. Moderately magnetic. Fine interstitial to blebby pyrrhotite>chalcopyrite to 5 - 10%.
77.04	78.02	Medium-grained pyroxenite, with olivine content variable from here down. Interstitial pyrrhotite>chalcopyrite, 5 - 10%. Minor felspar and moderately magnetic.
78.02	78.95	Medium-grained pyroxenite with olivine content variable from here down. Interstitial pyrrhotite>chalcopyrite, 5 - 10%. Minor felspar and moderately magnetic.
78.95	79.93	Medium-grained pyroxenite with olivine content variable from here down. Interstitial pyrrhotite>chalcopyrite, 5 - 10%. Minor felspar and moderately magnetic.
79.93	81.08	Medium-grained pyroxenite with olivine content variable from here down. Interstitial pyrrhotite>chalcopyrite, 5 - 10%. Minor felspar and moderately magnetic.
81.08	82.06	Medium-grained pyroxenite with olivine content variable from here down. Interstitial pyrrhotite>chalcopyrite, 5 - 10%. Moderately magnetic becoming more felspathic.
82.06	83.02	Medium-grained pyroxenite with some coarser felspar, narrow F-gr olivine / shaly zones. Fine interstitial - blebby pyrrhotite>=chalcopyrite to 5%. Narrow coarse-grained zone with biotite.

From	To	DESCREPTION
83.02	83.83	Medium-grained feldspathic pyroxenite. Fine interstitial - blebby pyrrhotite>chalcopyrite up to 5%. Moderately magnetic.
83.83	84.75	Medium-grained, in places medium to coarse-grained feldspathic pyroxenite. Fine interstitial - disseminated pyrrhotite>chalcopyrite 2-5%. Moderately magnetic.
84.75	85.80	Medium-grained pyroxenite, slightly felspathic with narrow olivine / shaly zones (magnetic). Interstitial - blebby pyrrhotite>chalcopyrite 5 - 10%. Moderately magnetic.
85.80	86.86	Medium-grained pyroxenite, slightly felspathic with narrow olivine / shaly zones (magnetic). Interstitial - blebby pyrrhotite>chalcopyrite 10 - 20% locally concentrated (86.52 - 86.65 m) but 2 - 5% average. Moderately magnetic.
86.86	87.90	Medium-grained pyroxenite becoming fespathic (87.60 m) Sediment xenolith (87.16 - 87.26 m) and quartz felspar vein (87.30 - 87.40 m). Interstitial pyrrhotite>chalcopyrite up to 5%.
87.90	88.87	Medium-grained pyroxenite in places slightly felspathic with narrow finer graind zones. Moderately magnetic. Interstitial - disseminated pyrrhotite>chalcopyrite to 2%.
88.87	89.60	Medium-grained pyroxenite, in places coarser grained and felspathic. Up to 10% pyrrhotite>chalcopyrite, blebby and finer interstitial.
89.60	90.59	Medium-grained pyroxenite, minor felspar. Moderately magnetic. Fine interstitial to blebby pyrrhotite>chalcopyrite 2 - 5%. One 10 mm pyrrhotite bleb.
90.59	91.60	Medium-grained pyroxenite, minor felspar with finer grained zones. Interstitial fine pyrrhotite=chalcopyrite to 10% and coarse blebby pyrrhotite/chalcopyrite (12 mm ea). Moderately magnetic.
91.60	92.52	Medium-grained pyroxenite, minor felspar with finer grained olivine / shaly zones. Interstitial fine Po=chalcopyrite to 10% and coarse blebby pyrrhotite/chalcopyrite (12 mm ea). Moderately magnetic.
92.52	93.40	Medium-grainedr pyroxenite, narrow felspathic zone (12 cm) and 6 cm wide F-gr zone. Moderately magnetic with interstitial - blebby pyrrhotite - chalcopyrite up to 5%.
93.40	94.23	Medium-grained pyroxenite, slightly felspathic. Moderately magnetic in finer grained olivine/shaly zones. Disseminated - blebby 1 - 2% pyrrhotite>chalcopyrite.
94.23	95.23	Medium-grained pyroxenite, slightly felspathic. Moderately magnetic in finer grained olivine/shaly zones. Trace pyrrhotite/chalcopyrite. Biotite.
95.23	95.62	Coarse- grained feldspathic pyroxenite, biotite.
95.62	96.65	Medium-grained pyroxenite, slightly felspathic. Moderately magnetic in olivine/shaly zones. Interstitial - blebby pyrrhotite=chalcopyrite to 2%. Massive granular magnetite in finer grained zones.
96.65	97.33	Medium-grained pyroxenite, slightly felspathic. Moderately magnetic in olivine/shaly zones. Fine interstitial - blebby pyrrhotite=chalcopyrite to 2%.
97.33	98.23	Medium-grained pyroxenite, slightly felspathic. Moderately magnetic. Fine interstitial pyrrhotite - trace and blebby pyrrhotite=chalcopyrite in top 5cm.
98.23	99.09	Medium-grained pyroxenite slightly felspathic. Moderately magnetic. Interstitial - blebby pyrrhotite>>chalcopyrite to 5%
99.09	99.81	Medium-grained pyroxenite, slightly felspathic. Moderately magnetic with interstitial pyrrhotite>chalcopyrite to 1%
99.81	100.54	Medium-grained pyroxenite, slightly felspathic, moderately magnetic. Trace pyrrhotite / chalcopyrite
100.54	101.25	Medium-grained pyroxenite, with coarse fespathic zone. Trace - 5% (locally concentrated) pyrrhotite>chalcopyrite. Moderately
101.25	101.58	Medium-grained pyroxenite, slightly coarser below sulphide zone. Interstitial pyrrhotite > chalcopyrite with semi - massive to massive F-gr pyrrhotite>>chalcopyrite zone (101.43 - 101.49 m). In places net-textured.
101.58	102.20	Medium-grained pyroxenite, with finer grained olivine / shaly zone and coarse blebby / interstitial pyrrhotite>chalcopyrite (101.71 - 101.76 m) up to 20%. Moderately magnetic.
102.20	103.14	Medium-grained pyroxenite, slightly felspathic. Interstitial to coarse blebby pyrrhotite>>chalcopyrite, net-textured in places. Ex-solution network evident in coarse pyrrhotite. 20 - 50% locally concentrated in semi-massive zones (102.46 - 102.51 m, 102.67 - 102.72 m). Moderately magnetic.
103.14	103.80	Medium-grained pyroxenite, variable with fine-grained pyroxenite and felspathic zones. Interstitial to blebby pyrrhotite=chalcopyrite between 2-5%. Weakly to moderately magnetic.
103.80	104.66	Medium-grained pyroxenite, variable with fine-grained pyroxenite and felspathic zones. 1-2% pyrrhotite=chalcopyrite interstitial to blebby. Weakly to moderately magnetic.
104.66	105.33	Medium-grained pyroxenite, variable with fine-grained pyroxenite, fine-grainedr magnetic, olivine / shaly zones. Interstitial to blebby pyrrhotite=chalcopyrite up to 2% in upper 34 cm.
105.33	106.26	Medium-grained pyroxenite, variable with magnetic olivine? rich zone. Interstitial to blebby pyrrhotite=chalcopyrite to 2%. Moderately magnetic.
106.26	106.94	Medium-grained pyroxenite, variable with magnetic olivine? rich zone. Interstitial to blebby pyrrhotite=chalcopyrite to 2% in places net-textured. Moderately magnetic.
106.94	107.38	Medium-grained pyroxenite, Semi-massive pyrrhotite>chalcopyrite (50%) from 106.94 - 106.97 m. Variable to fine-grained pyroxenite, pyrrhotite>chalcopyrite to 20% locally concentrated (107.15 - 107.25 m). Fine interstitial elsewhere to 2%. Moderately magnetic.
107.38	108.33	Medium-grained, well layered pyroxenite with layers of concentrated opx 12 cm wide (108.22 - 108.34 m). Interstitial 1-2% pyrrhotite>chalcopyrite. Moderately magnetic.
108.33	109.20	Medium-grained, well layered pyroxenite with layers of concentrated opx 5 cm wide (108.58 - 108.63 m). Fine interstitial pyrrhotite=chalcopyrite up to 5%. Moderately magnetic. Mottled appearance (felspar).
109.20	110.28	Medium-grained pyroxenite, slightly felspathic, variable with narrow, magnetic sediment xenolith (109.92 - 110.03 m). Interstitial pyrrhotite=chalcopyrite up to 2%. Moderately magnetic.
110.28	111.25	Medium-grained pyroxenite, variable, well layered. Interstitial to blebby pyrrhotite=chalcopyrite to 5% locally concentrated. Moderately magnetic.
111.25	112.03	Fine to medium-grained quartzite / sediment. Highly magnetic with disseminated to granular magnetite and fine interstitial Py.
139.05	140.05	Medium-grained, feldspathic pyroxenite (hybrid?), weakly magnetic
140.05	140.53	Medium-grained, highly serpentinized calcsilicate. Weakly magnetic
140.53	141.46	Medium-grained, serpentinized calcsilicate, Trace pyrite. Weakly magnetic
141.46	142.26	Medium-grained, chloritized feldspathic pyroxenite. Trace pyrrhotite. Weakly magnetic.
142.26	143.18	Medium-grained, chloritized feldspathic pyroxenite. Up to 5% pyrrhotite=chalcopyrite, locally concentrated. Narrow fine- grained shaly zones (Highly magnetic). Weakly - moderately magnetic throughout.
143.18	144.32	Medium-grained, chloritized feldspathic pyroxenite. Narrow, fine- grained shaly zone. Trace disseminated pyrrhotite. Minor carbonate veining. Weakly magnetic.
144.32	145.30	Medium-grained, chloritized feldspathic pyroxenite, narrow calcsilicate zone between 144.54 - 144.84 m. Up to 2% chalcopyrite>pyrrhotite. Weakly magnetic.
145.30	146.08	Medium-grained feldspathic pyroxenite, weakly - moderately magnetic. 1-2% fine pyrrhotite=chalcopyrite.
146.08	147.04	Medium-grained feldspathic pyroxenite with slightly coarser zone. Weakly - moderately magnetic. Trace fine pyrrhotite.
147.04	148.27	Medium-grained, in places finer grained. Highly magnetic, epidotized meta-sediment / calcsilicate. Occassional pyrite blebs.
148.27	148.79	Fine-grained, highly magnetic quartzite
169.04	170.10	Fine-grained, dolomite intrusive. Moderately - highly magnetic

From	To	DESCREPTION
170.10	170.83	Medium-grained, meta-pyroxenite, HY. Felspathic, moderately magnetic with Trace pyrrhotite.
170.83	171.98	Medium-grained, meta-pyroxenite, HY. Felspathic, moderately magnetic with Trace pyrrhotite. Occassional quartzite xenoliths / clasts.
171.98	172.63	Medium-grained meta-pyroxenite, HY. Felspathic, moderately magnetic with Trace pyrrhotite. Occassional quartzite xenoliths / clasts.
172.63	173.42	Medium-grained, meta-pyroxenite, HY. Felspathic, moderately magnetic with Trace pyrrhotite. Occassional quartzite xenoliths / clasts.
173.42	173.82	Fine-grained meta-sedimentary / quartzite xenolith, moderately magnetic.
173.82	174.38	Medium-grained, meta-pyroxenite, HY. Felspathic, moderately magnetic with Trace pyrrhotite.
174.38	175.14	Fine-grained dolomite intrusive with 5 cm wide quartz / felspar vein. Chloritized
175.14	176.01	Medium-grained, meta-pyroxenite, HY. Felspathic with quartzite xenolith / clasts. Trace - % pyrrhotite=chalcopyrite, fine to blebby and locally concentrated in narrow accumulations at 175.55 m and 175.90 m.
176.01	177.12	Medium-grained felspathic meta-pyroxenite, HY with finer grained shaly zones. 2 - 5% pyrrhotite.>chalcopyrite but concentrated up to 20% in narrow zones <1 cm wide at 176.30 m, 176.85 m, 176.87 m and 176.98 m.
177.12	178.23	Medium-grained felspathic meta-pyroxenite, HY with finer grained zones and quartzite. xenoliths / clasts. Trace pyrrhotite.
178.23	178.80	Medium-grained quartzite. Moderately to strongly magnetic.
192.36	192.90	Medium-grained serpentinized calcsilicate.
192.90	193.95	Medium-grained, highly magnetic, biotitic, felspathic in places meta-sedimentary (quartzite). Semi-massive magnetite bleb and 1-2% finely disseminated pyrite.
193.95	195.05	Medium-grained, highly magnetic biotitic, felspathic meta-sedimentary (quartzite). Narrow, irregular carbonate veining. 1-2% disseminated pyrite and a 6 cm wide coarse grained vein.
195.05	196.07	Medium-grained, highly magnetic, biotitic, felspathic meta-sedimentary (quartzite). Trace - % finely disseminated pyrite and a 4 cm wide coarse-grained quartz / felspar vein.
196.07	197.04	Medium-grained, highly magnetic, biotitic, felspathic meta-sedimentary (quartzite). Trace finely disseminated pyrite and a 4 cm wide coarse-grained quartz / felspar vein and narrow, irregular carbonate veining.